

Distribution Agreement

In presenting this thesis or dissertation as a partial fulfillment of the requirements for an advanced degree from Emory University, I hereby grant to Emory University and its agents the non-exclusive license to archive, make accessible, and display my thesis or dissertation in whole or in part in all forms of media, now or hereafter known, including display on the world wide web. I understand that I may select some access restrictions as part of the online submission of this thesis or dissertation. I retain all ownership rights to the copyright of the thesis or dissertation. I also retain the right to use in future works (such as articles or books) all or part of this thesis or dissertation.

Signature:

Date

The role of Arl13b in the maintenance of neural tube patterning and oligodendrocyte development

By

Chen-Ying Su

Doctor of Philosophy

Graduate Division of Biological and Biomedical Science
Genetics and Molecular Biology

Tamara Caspary, Ph.D.
Advisor

Anthony Chan, Ph.D.
Committee Member

Ping Chen, Ph.D.
Committee Member

Xiao-Jiang Li, Ph.D.
Committee Member

Peter Wenner, Ph.D.
Committee Member

Accepted:

Lisa A. Tedesco, Ph.D.
Dean of the Graduate School

Date

The role of Arl13b in the maintenance of neural tube patterning and oligodendrocyte development

By

Chen-Ying Su

B.Sc National Taiwan University, 2001

M.S University of Birmingham, 2003

Advisor: Tamara Caspary, Ph.D.

An abstract of

A dissertation submitted to the Faculty of the
James T. Laney School of Graduate Studies of Emory University
in partial fulfillment of the requirements for the degree of
Doctor of Philosophy

in Graduate Division of Biological and Biomedical Science
Genetics and Molecular Biology

2011

Abstract

The role of Arl13b in the maintenance of neural tube patterning and oligodendrocyte development

By Chen-Ying Su

Both motor neurons (MNs) and oligodendrocytes are essential for establishing neural circuits in the central nervous system (CNS). They are distinct cell types, yet derived from the same progenitor population, progenitors of motor neurons (pMN). In mouse, pMN cells are specified at E8.5 in response to a low level of sonic hedgehog (Shh) activity and differentiate as MNs at E9.5. *Arl13b^{hmn}* is a mouse mutant that disrupts a ciliary small GTPase. Primary cilia are required for Shh signaling, and *Arl13b^{hmn}* disrupts cilium architecture and Shh signaling. There is a constitutive low level of Shh activation resulting in an expansion of pMN cells and MNs. The expansion persists to E12.5 leading us to investigate whether Shh activity gradient is needed for the maintenance of neural tube patterning over time, thus we induced a constitutive low level of Shh activity by temporally deleting Arl13b. We defined a specific window when cells are sensitive to changes in Shh activity. Surprisingly, cells that change their fate upon loss of Arl13b are restored to normal over time suggesting that graded Shh response is not needed for maintaining neural tube patterning. Our data suggest that Shh initially is an instructive signal for specification, and then becomes a permissive signal for normal neural pattern.

At E12.5, pMN cells switch to become oligodendrocyte precursors (OLPs), and platelet-derived growth factor receptor α (PDGFR α) signaling is important for OLP specification. In *Arl13b^{hmn}*, there are no OLPs at E13.5 before the embryos die. Primary cilia are also implicated to be important for PDGFR α signaling, thus it is possible that defective cilia result in impaired PDGFR α signaling in *Arl13b^{hmn}*. We deleted Arl13b at E8.5 specifically in the pMN population, as well as at E10.5 in the CNS to target progenitors before they become OLPs. We found that OLP specification is normal, but oligodendrocyte differentiation and myelination are affected suggesting that Arl13b is involved in the later steps of oligodendrocyte development. Taken together, our results provide a better understanding of the maintenance of neural tube patterning, and of the potential relationship between cilia and oligodendrocyte development.

The role of Arl13b in the maintenance of neural tube patterning and oligodendrocyte development

By

Chen-Ying Su

B.Sc National Taiwan University, 2001

M.S University of Birmingham, 2003

Advisor: Tamara Caspary, Ph.D.

A dissertation submitted to the Faculty of the
James T. Laney School of Graduate Studies of Emory University
in partial fulfillment of the requirements for the degree of

Doctor of Philosophy

in Graduate Division of Biological and Biomedical Science
Genetics and Molecular Biology

2011

Table of Contents

Chapters

Chapter 1 Signaling, cilia, neural tube patterning, and oligodendrocyte

development.....	1
1.1 Introduction.....	2
1.2 The introduction of Arl13b protein and <i>Arl13b^{hmn}</i> mouse mutant	4
1.3 Neural tube patterning.....	5
1.4 Shh signaling and cilia	9
1.5 Oligodendrocyte specification	12
1.6 Signaling in oligodendrocyte development	14
1.7 Preview	17

Chapter 2 Materials and methods.....23

2.1 Generation of a conditional <i>Arl13b</i> allele.....	24
2.2 Genotyping for mouse strains	26
2.3 Preparation of genomic DNA from mouse tails	28
2.4 Southern blotting.....	29
2.5 Immunofluorescence.....	30
2.6 Western blotting.....	31
2.7 RNA <i>in situ</i> hybridization.....	32
2.8 X-gal staining.....	35
2.9 Tamoxifen injection	35

2.10 Quantitative analysis.....	35
2.11 Generation of mouse embryonic fibroblasts (MEFs).....	36
2.12 Arl13b deletion in MEFs	37

Chapter 3 Shh acts first as an instructive morphogen and then as a permissive

signal in mammalian neural tube patterning	43
3.1 Summary	44
3.2 Introduction.....	45
3.3 Results.....	47
3.4 Discussion.....	55

Chapter 4 The role of Arl13b in oligodendrocyte development

4.1 Summary.....	84
4.2 Introduction.....	84
4.3 Results.....	86
4.4 Discussion.....	88
4.5 In the course of analysis of the <i>Arl13b</i> ^{<i>AOlig1-Cre</i>} , we found minority of mutants is identical to the null.....	91

Chapter 5 The prospective views of Arl13b in neural tube development and the

significance of Shh being a permissive role	105
5.1 Summary of chapter 3.....	106
5.2 The significance of Shh being an instructive and a permissive signal	106

5.3 Summary of chapter 4.....	108
5.4 The potential roles of Arl13b in oligodendrocyte development	108
5.5 The potential role of Arl13b in neuroepithelial stem cells (NSCs)	110
5.6 Perspective and conclusion.....	111
Bibliography	114

List of Figures

Figures

1.1	Cell signaling and neural tube patterning	18
1.2	Motile and primary cilia.....	20
1.3	Cilia are required for Shh signaling	21
1.4	Two models of how pMN cells become motor neurons and oligodendrocyte precursors (OLPs)	22
2.1	Cloning sites of 5' arm, exon 2 of <i>Arl13b</i> , and 3' arm on pFlexible	38
2.2	The construct of a conditional <i>Arl13b</i> allele.....	39
2.3	The generation of a <i>Arl13b^{floxed}</i> allele	40
2.4	Exon two of <i>Arl13b</i> can be deleted upon <i>Cre</i> recombination	41
3.1	The generation of a conditional <i>Arl13b</i> allele.....	61
3.2	The rate of <i>Arl13b</i> protein turnover <i>in vivo</i>	63
3.3	Temporal deletion of <i>Arl13b</i> results in different neural tube patterning ...	64
3.4	The kinetics of <i>Arl13b</i> protein deletion in conditional <i>Arl13b</i> knockout MEFs is similar to <i>in vivo</i>	66
3.5	The localization of Smo in MEFs	68
3.6	The pMN expansion is restored over time when <i>Arl13b</i> is deleted by E9.25 and E9.5	70
3.7	Rescue of patterning at E12.5 is not due to reactivation of Shh activity or incomplete deletion of <i>Arl13b</i>	72

3.8	The expression of the floor plate and p3 progenitors in different conditional <i>Arl13b</i> knockout caudal neural tubes.....	73
3.9	Abnormal Shh activity gradient results in distinct patterning in the <i>Arl13b^{hmn}</i> rostral and caudal neural tube	75
3.10	Rostral neural tube displays normal patterning in all conditional <i>Arl13b</i> knockout mutants	77
3.11	Summary of phenotypic analyses	79
3.12	The timeframe for the role of Shh in neural tube patterning	81
4.1	There are no OLPs in <i>Arl13b^{hmn}</i> at E13.5.....	94
4.2	Oligodendrocyte specification and differentiation is normal when <i>Arl13b</i> is deleted in the pMN lineage	95
4.3	MBP and LINGO-1 expression is abnormal in <i>Arl13b^{ΔBrn4-Cre}</i>	96
4.4	An expansion of pMN cells and MNs in the minority of <i>Arl13b^{ΔOlig1-Cre}</i> ..	98
4.5	Leaky <i>Olig1-Cre</i> expression.....	100
4.6	Predictions of two models.....	101
4.7	The expansion of pMN cells is resulted from <i>Arl13b</i> deletion regardless of the number of <i>Arl13b</i> -lacking cells	102
4.8	Working model for the specification of distinct progenitors in the neural tube.....	103
5.1	The potential role of <i>Arl13b</i> in neuroepithelial stem cells (NSCs)	113

CHAPTER 1
SIGNALING, CILIA, NEURAL TUBE PATTERNING, AND OLIGODENDROCYTE
DEVELOPMENT

1.1 Introduction

In order to respond internal and external environmental stimuli that are transmitted to the central nervous system (CNS), motor neurons (MNs) project their axons to connect muscles or glands to the CNS. Oligodendrocytes myelinate axons in the CNS to provide insulation for proper transmission of electrical signals. By morphology and functions, MNs and oligodendrocytes are very distinct cell types, but yet they are derived from the same progenitors – progenitors of motor neurons (pMNs). In mouse, pMN cells differentiate as MNs at embryonic day 9.5 (E9.5) and switch to become oligodendrocyte precursors (OLPs) at E12.5 (Rowitch, 2004). Sonic Hedgehog (Shh) signaling is required for specifying distinct ventral progenitors, and pMN cells are specified in response to a low level of Shh activity (Briscoe et al., 2000; Chiang et al., 1996). Cilia are required for Shh signaling, and ventral progenitors cannot be specified properly when there are defects in cilia or ciliary proteins (Caspary et al., 2007; Cortellino et al., 2009; Eggenschwiler et al., 2001; Houde et al., 2006; Huangfu and Anderson, 2005; Huangfu et al., 2003; Liu et al., 2005; Qin et al., 2011; Tran et al., 2008). *Arl13b^{hennin(hmn)}* is a mouse mutant that disrupts a ciliary small GTPase (Caspary et al., 2007). In *Arl13b^{hmn}* embryos, the architecture of cilia is abnormal and Shh signaling is disrupted: there is a constitutive low level of Shh activation in *Arl13b^{hmn}* resulting in an expansion of pMN cells and MNs.

Shh is a morphogen that acts in a concentration-dependent manner to specify distinct progenitors in the ventral neural tube (Briscoe et al., 2000; Briscoe et al., 1999; Ericson et al., 1997b). Gli proteins mediate the transcriptional response to Shh signaling, and are processed to become either activator (GliA) or repressor (GliR) forms (Aza-Blanc

et al., 2000; Ruiz i Altaba, 1998). The extracellular Shh concentration is thus mediated by intracellular GliA/R responses resulting in a graded Shh activity, and cells are specified to become distinct progenitors depending on their distance from the source of Shh morphogen. Once progenitors are specified, Shh is needed again for progenitors to differentiate as MNs and interneurons (Ericson et al., 1996). In order to maintain neural tube patterning over time, continuous Shh signaling is required (Dessaud et al., 2010). Therefore, different levels of Shh activity are critical for specifying distinct progenitors initially. However, it is unknown whether Shh activity gradient still needs to be maintained for differentiation of interneurons and MNs, and for the maintenance of neural tube patterning. Therefore, we generated a conditional *Arl13b* allele to induce a constitutive low level of Shh activation to manipulate Shh activity at different time points, and observed neural tube patterning over time. This conditional deletion allows us to test whether Shh activity gradient is needed after the initial specification in the neural tube.

In *Arl13b^{hmn}*, OLPs cannot be detected before the embryos die. Platelet-derived growth factor receptor α (PDGFR α) signaling is important for oligodendrocyte specification (Fruttiger et al., 1999; Klinghoffer et al., 2002). Cilia have also been implicated to be important for PDGFR α signaling (Schneider et al., 2005). To circumvent the embryonic lethality and understand whether *Arl13b* plays a role in oligodendrocyte development, we used our conditional *Arl13b* allele to delete *Arl13b* specifically in pMN cells. This conditional deletion allows us to investigate whether disrupting *Arl13b* in the oligodendrocyte lineage has effects on oligodendrocyte development. We also deleted *Arl13b* at E10.5, right before OLP specification, to examine whether deleting *Arl13b* on progenitors as they become OLPs affects specification of oligodendrocytes.

1.2 The introduction of Arl13b protein and *Arl13b^{hnn}* mouse mutant

I have been studying a unique cilium mutant, *Arl13b^{hnn}*, whose neural tube displays an expansion of pMN cells and MNs (Casparly et al., 2007). Arl13b was first identified through N-ethyl-N-nitrosourea (ENU)-induced mutagenesis for mutants that have defects in neural tube patterning (Garcia-Garcia et al., 2005). Arl13b is a member of ADP-ribosylation factor (ARF) like family of small GTPases., and the *hnn* mutation is in the splice site of exon two of Arl13b resulting in a protein null mutation (Casparly et al., 2007). *Arl13b^{hnn}* embryos have exencephaly and sometimes spina bifida, and they display polydactaly, left-right axis defects, abnormal eyes before dying around E13.5. Arl13b is localized to cilia and the length of cilia is shorter in *Arl13b^{hnn}* than in wild-type, and there is a defect in axoneme architecture (Casparly et al., 2007).

The Arl13b protein is composed of two parts: a conserved Arf domain and a novel vertebrate-specific C-terminus. Several members of Arf/Arl family are involved in vesicle trafficking, microtubule dynamics, or lipid metabolism, but many of them still have unknown functions (D'Souza-Schorey and Chavrier, 2006; Kahn et al., 2005). In Arf domain of all Arf/Arl proteins, there is a GTP consensus binding site - DXGGQ. But in Arl13b, this consensus sequence becomes DXGGG suggesting that GTP cannot be hydrolyzed so Arl13b is a constitutively active GTPase (Casparly, unpublished). Arl13b is a membrane-associated protein, and it may interact with components of the exocyst complex that are important for vesicle trafficking (Larkins et al., under revision).

In mouse mutants that do not have cilia, ventral progenitors fail to be specified due to the absence of Shh signaling (Houde et al., 2006; Huangfu et al., 2003; Liu et al.,

2005). In contrast, there is a constitutive low level of Shh activation in *Arl13b^{hmn}* resulting in an expansion of pMN cells and MNs (Casparly et al., 2007). The expansion of pMN cells and MNs persists to E12.5, predicting excessive OLPs. However, no PDGFR α -expressing OLPs are detected at E13.5 in *Arl13b^{hmn}* as the embryos die. Therefore, it is unknown whether there is a delay in OLP specification or a complete block of oligodendrocyte development since *Arl13b^{hmn}* mutation is embryonic lethal. *Arl13b^{hmn}* disrupts two important developmental processes: neural tube specification and oligodendrocyte development. In order to understand why disrupting the ciliary protein affects these two processes, we first need to understand how neural tube is normally patterned and the relationship between cilia and cell signaling.

1.3 Neural tube patterning

The ability of sensing and responding environmental stimuli is relied on neurons that are involved in sensation and movement. Neurons that are involved in sensation are derived from progenitors in the dorsal half of neural tube, while neurons that are responsible for motor outputs are differentiated from progenitors in the ventral half. This dorsal-ventral organization is established during development, and distinct progenitors are specified in order to differentiate as neurons and MNs. Each type of progenitors is defined by combinations of transcription factors that are summarized in figure 1.1. In general, dorsal progenitors are mainly defined by Olig3, Pax6 and Pax7 expression (Ericson et al., 1997b; Muller et al., 2005; Timmer et al., 2002). Although all the ventral progenitors express Nkx6.1, pMN and p3 cells can be more specifically defined by Olig2

and Nkx2.2, respectively (Briscoe et al., 2000; Briscoe et al., 1999; Lu et al., 2000; Zhou et al., 2000).

The specification of these transcription factors is initially triggered by dorsal signals from the ectoderm surface, and by ventral signals from the notochord that is underlined the ventral midline of the neural tube. Subsequently, the roof plate and the floor plate become secondary sources of signals to continue specifying cells in the neural tube into distinct progenitors. Wnts and bone morphogenetic proteins (BMPs) are generated in the roof plate, and they are required for specifying cells in the dorsal neural tube (Chesnutt et al., 2004; Lee et al., 1998; Liem et al., 1997; Liem et al., 1995; Muroyama et al., 2002; Parr et al., 1993; Timmer et al., 2002; Wine-Lee et al., 2004; Zechner et al., 2007). Shh signaling, on the other hand, is needed for ventral neural tube specification (Chiang et al., 1996). The fourth signal, retinoic acid (RA), is produced in mesoderm adjacent to the neural tube and is important for intermediate neural tube patterning (Pierani et al., 1999) (Figure 1.1).

BMP signaling

Several members of transforming growth factor β (TGF β) family are expressed in the roof plate, including BMP4, BMP7, and growth differentiation factor 7 (GDF7) (Lee et al., 2000; Lee et al., 1998; Liem et al., 1997; Liem et al., 1995). *In vitro* experiments show that addition of BMPs promote naïve neural plate cells to become progenitors of dorsal interneurons (pdIs) suggesting that BMPs are needed for specifying cells to become dorsal cell fates (Liem et al., 1997; Liem et al., 1995). Indeed, activating receptors of BMPs ectopically results in an expansion of dorsal progenitors to the ventral neural tube *in vivo* suggesting that BMP signaling is sufficient to transform ventral cells

into dorsal cell fates (Timmer et al., 2002). When BMP signaling is eliminated by over-expressing BMP antagonists in the dorsal neural tube or deleting BMP receptors *in vivo*, dorsal progenitors (pdI1-pdI4) are not specified indicating BMP signaling is required for dorsal neural tube patterning (Chesnutt et al., 2004; Wine-Lee et al., 2004). To prevent BMP signaling from interfering with ventral neural tube specification, BMP antagonists are expressed in the notochord (Liem et al., 2000; McMahon et al., 1998). Indeed, in mouse mutants lacking the notochord-derived BMP antagonist noggin, floor plate and motor neurons are not specified (McMahon et al., 1998).

Wnt signaling

Wnt signaling is also required for specifying cells in the dorsal neural tube. Two members of Wnt family are specifically expressed in the roof plate, Wnt1 and Wnt3a (Parr et al., 1993). In *Wnt1 Wnt3a* double mutants, the most dorsal progenitors (pdI1 and pdI2) are absent indicating Wnt signaling is needed for dorsal neural tube specification (Muroyama et al., 2002). When over-expressing Wnt signaling mediator, β -catenin, pdI1 cells are expanded. In contrast, pdI1 cells are decreased when β -catenin is down-regulated indicating that Wnt signaling is important for specifying cells in dorsal neural tube, especially the most dorsal region (Zechner et al., 2007).

RA signaling

In contrast with BMP and Wnt signaling, RA is specifically needed for specifying cells in the ventral neural tube. RA is activated by vitamin A, and in vitamin A-deficient chick embryos, p0, p1, p2, and pMN cells are not specified indicating RA is needed for ventral neural tube specification (Diez del Corral et al., 2003). When receptors of RA are blocked, both p0 and p1 cells are not specified indicating more directly that RA signaling

is more important for specifying cells in the most dorsal part of ventral neural tube (Pierani et al., 1999).

Shh signaling

While Shh is clearly required for ventral neural tube specification, its role is increasingly complex. Shh acts as morphogen in a concentration-dependent manner, and specifies five distinct ventral progenitors (p0-p3 and pMN) and the floor plate (Briscoe et al., 2001; Briscoe et al., 1999; Ericson et al., 1997b). In *Shh* null mouse mutants, there are no ventral progenitors indicating that Shh is essential for ventral neural tube specification (Chiang et al., 1996). Shh signaling is mediated by Gli proteins. Full-length Gli proteins can either be processed to become Gli repressor in the absence of Shh, or activated to be Gli activator upon Shh activation (Aza-Blanc et al., 2000; Dai et al., 1999; Litingtung et al., 2002; Ruiz i Altaba, 1998; Sasaki et al., 1997; Wang et al., 2000). Thus Shh morphogen is mediated by the ratio of Gli activator/repressor: higher Shh concentration is mediated by higher ratio of Gli activator/repressor resulting in a more ventral cell fate; more dorsal cell fates are specified resulting from lower ratio of Gli activator/repressor because they are exposed to lower concentration of Shh.

Interactions among different signals in neural tube patterning

These pathways are active at the same time to pattern neural tube and clearly interact with each other. A BMP activity gradient opposing to the Shh activity gradient is mediated by the expression of BMP antagonists in the ventral neural tube (Liem et al., 2000; Liem et al., 1995; McMahon et al., 1998; Patten and Placzek, 2002). Shh activity is repressed in the dorsal neural tube by interacting with BMP and Wnt signaling through Gli repressor: Wnt signaling has been shown to control Gli repressor in the dorsal neural

tube to prevent Shh from specifying dorsal cells (Alvarez-Medina et al., 2008); Gli repressor has been demonstrated that it can physically interact with the effectors of BMP and Wnt signaling, the Smad proteins and β -catenin, respectively (Liu et al., 1998; Ulloa et al., 2007).

In BMP knockout embryos, Wnt1 and Wnt3a expression is reduced suggesting that BMP signaling can work on Wnt in dorsal neural tube patterning (Wine-Lee et al., 2004). Finally, RA signaling can promote p1 cells more efficiently in the presence of Shh (Novitch et al., 2003; Pierani et al., 1999). Taken together, neural tube patterning is not solely dependent on one particular cell signaling.

1.4 Shh signaling and cilia

Series of events occur for neural plate cells from receiving Shh to become specific progenitors. There are two transmembrane proteins that act differently in response to Shh ligand – Patched 1 (Ptch1) and Smoothed (Smo) (Alcedo et al., 1996; Chen and Struhl, 1996; Goodrich et al., 1997; Marigo et al., 1996; Zhang et al., 2001). In the absence of Shh ligand, Ptch1 inhibits Smo resulting in no Shh signaling. In the presence of Shh, Shh relieves Ptch1's repression of Smo resulting in Shh signaling transduction (Denef et al., 2000; Zhu et al., 2003) (Figure 1.3). In vertebrates, Shh signaling is mediated by three transcription factors: Gli1, Gli2, and Gli3 (Hui et al., 1994; Ruiz i Altaba, 1998). Gli1 is not proteolytically processed so always act as activator whereas Gli2 and Gli3 can act as both activator and repressor (Hynes et al., 1997; Lee et al., 1997; Ruiz i Altaba, 1998; Sasaki et al., 1999).

In vertebrates, Shh signaling transduction requires primary cilia. There are two types of cilia: motile cilia and non-motile (primary) cilia. Both cilia are composed by an axeneme containing nine pairs of microtubule doublets, but motile cilia contain additional central microtubule singlets (Figure 1.2). Motile cilia constantly beat in one direction resulting in a movement of a cell or of fluid around cells, such as motile cilia in the respiratory tube that can move mucus (Gudis and Cohen, 2010). The primary cilium exists on almost every vertebrate cell. They can function as mechano-sensory receptors, such as primary cilia on the apical surface of the kidney tubules can monitor the flow of fluid through the tubules (Praetorius and Spring, 2003).

Many components of Shh signaling are localized in primary cilia, and their localization shifts upon Shh stimulation (Corbit et al., 2005; Haycraft et al., 2005; Rohatgi et al., 2007). Ptch1 is localized in the cilium in the absence of Shh, and Smo moves into cilium while Ptch1 moves out in the presence of Shh (Corbit et al., 2005; Rohatgi et al., 2007). Full-length Gli proteins are localized on the tip of cilia, and processed Gli3 repressor is only detected in the nuclei suggesting that Gli proteins leave the cilium to be cleaved and become Gli repressor (Haycraft et al., 2005) (Figure 1.3). Unfortunately, full-length Gli antibody cannot detect activator form of Gli thus it is unclear whether Gli protein is activated in the cilium by immunofluorescence. A negative regulator of Shh signaling, Suppressor of fused (Sufu), enriches on the tip of cilia in the absence of Shh so that full-length Gli proteins cannot be activated (Endoh-Yamagami et al., 2009; Haycraft et al., 2005). Upon Shh stimulation, Sufu-Gli complexes are recruited to cilia and Gli is activated suggesting that Smo can release Gli from the inhibition of Sufu to activate the pathway (Tukachinsky et al., 2010). However, it has

been shown that Sufu can inhibit Shh signaling in the absence of cilia (Chen et al., 2009; Jia et al., 2009). The relationship between Sufu and cilia still remains to be defined, but the main idea is still consistent with the model in which Smo enters the cilium in the presence of Shh, and activates the pathway by inhibiting Sufu thus full-length Gli can be activated (Figure 1.3).

In *Ar113b^{hmn}* mouse embryonic fibroblasts (MEFs), the localization of Gli, Ptch1, and Sufu is not shifted upon Shh stimulation suggesting that Shh signaling components are not regulated properly (Larkins et al., under revision). However, Smo is enriched in cilia even in the absence of Shh, and further enriched upon Shh stimulation in *Ar113b^{hmn}* (Larkins et al., under revision). This is consistent with *Ar113b^{hmn}* neural tube patterning defects that there is a constitutive Shh activation and the activation is Shh-ligand independent (Casparly et al., 2007). The fact that Gli proteins do not move upon Shh stimulation in *Ar113b^{hmn}* argues that the highest Shh activation cannot be achieved, thus there is a constitutive low level of Shh activation results in an expansion of pMN cells in the neural tube.

Since cilia are required for proper Shh signaling transduction in vertebrates and Shh signaling is needed for ventral neural tube specification, it is important to understand how cilia function in the specification of neural progenitors. In cilia-lacking mouse mutants, there is no Shh signaling resulting in the absence of ventral progenitors. Biochemical data show that in the absence of cilia, production of both Gli activator and repressor is absent (Houde et al., 2006; Huangfu et al., 2003; Liu et al., 2005). In contrast, in mouse mutants that generate cilia with buldge structure on the tip, p3 and pMN cells are expanded into dorsal neural tube suggesting that there is an increase of Shh activation

(Cortellino et al., 2009; Qin et al., 2011; Tran et al., 2008). Indeed, the ratio of Gli activator/repressor is increased in mutants with abnormal cilia resulting in higher Shh activation. However, *Arll3b^{hmn}* affects Shh activity and Gli regulation distinctly: genetic and biochemical approaches show that only Gli2 activator is affected, but Gli3 repressor activity and processing are functioned properly in *Arll3b^{hmn}* (Caspary et al., 2007).

It is clear that disrupting Shh activity by either removing Shh or cilia affects ventral neural tube specification indicating Shh is an instructive signal (Briscoe et al., 2000; Briscoe et al., 1999; Chiang et al., 1996; Ericson et al., 1997b). To maintain identities of ventral progenitors over time, continuous Shh signaling is required as ventral progenitors can be specified but then lost when Shh is deleted after initial specification (Dessaud et al., 2010). The continuous requirement of Shh suggests that Shh can be a permissive signal, meaning Shh needs to be present thus can work in concert with other signals to maintain neural tube patterning. This leads us to investigate when Shh is an instructive and a permissive role, and we modulated Shh activity at different time points. We used a conditional *Arll3b* allele to temporally induce a constitutive low level of Shh activation, and we found that an instructive role of Shh is short-lived and Shh becomes a permissive signal right after the initial neural tube specification (chapter 3).

1.5 Oligodendrocyte specification

In mouse, progenitors differentiate as interneurons and MNs from E9.5 to E12.5 in the central nervous system. After E12.5, macroglia including oligodendrocytes and astrocytes are generated. It is becoming clear that precursors of macroglia need to be specified at early development, and the common progenitors of MNs and OLPs – pMN

cells have been studied extensively. The molecular markers for detecting pMN cells are Olig1 and Olig2, the basic helix-loop-helix (bHLH) transcription factors, and they start to express in the pMN cells at E8.5 in mouse (Lu et al., 2002; Zhou and Anderson, 2002). An OLP marker, platelet-derived growth factor receptor α (PDGFR α), starts to co-express with Olig1/Olig2 at E14.5 but the expression of Olig1/2 precedes that of PDGFR α (Zhou et al., 2000). Although molecular markers have been identified to detect OLP specification, the mechanism of how pMN cells can switch from differentiating as MNs to OLPs is still unclear.

In *Olig1* mutants, both MNs and OLPs are specified normally but there is a delay in oligodendrocyte maturation suggesting that Olig1 is necessary for oligodendrocyte differentiation (Lu et al., 2002). *Olig2* mutant embryos lack both MNs and oligodendrocytes indicating that *Olig2* is required for specification of both precursors (Lu et al., 2002). Olig1 and Olig2 have different functions in MN and oligodendrocyte development leading to a model that pMN cells are mixed populations: one population gives rise to MNs while the other one becomes OLPs (Figure 1.4A)

However, this mixed population model has been challenged. Another model proposes that MNs and oligodendrocytes are sequentially generated from the progenitor domain. When a *Cre-loxP* strategy is used to delete Olig1 through expression of a diphtheria-toxin-encoding transgene at E8.5, MNs are absent (Wu et al., 2006). When Olig1 is continuously depleted at E10.5, oligodendrocytes are eliminated. However, Olig2-expressing cells can be detected from E8.5 to E16.5 when Olig1/2-expressing pMN cells should be ablated. Surprisingly, the number of Olig2 cells in these Olig1-depleting mutants is as same as in wild-type at E12.0. TUNEL assay in this study shows

that there is massive cell death between E9.5 and E11.5, so it is unlikely that Olig2 cells at E12.0 are generated prior to E11.5 and maintained until E12.0 (Wu et al., 2006).

Therefore, there might be neuroepithelial stem cells that are Olig negative give rise to Olig positive cells to differentiate as MNs followed by Olig positive cells that become OLPs (Figure 1.4B).

Although the mechanisms of how pMN cells become two distinct cell types remain to be defined, it is known that PDGFR α signaling is required for specification of oligodendrocytes (Klinghoffer et al., 2002). *In vitro*, PDGFR α has been shown to localize to cilia (Schneider et al., 2005). Thus it will be interesting to examine whether disruption of cilia affects PDGFR α signaling in oligodendrocyte specification. *Arl13b^{hmn}* has defective cilia and there are no PDGFR α -expressing OLPs before the embryo die. Therefore, we used a conditional *Arl13b* allele to delete *Arl13b* at E10.5, before pMN cells switch to become OLPs. This will allow us to examine whether the loss of *Arl13b* affect oligodendrocyte specification. We also deleted *Arl13b* specifically in the pMN cells at E8.5, thus we can investigate whether deleting *Arl13b* in oligodendrocyte lineage has any effect on oligodendrocyte development. Surprisingly, in the course of analyzing one of the conditional deletions, we have data that are consistent with the model 2 of NSCs giving rise to pMN cells continuously (chapter 4).

1.6 Signaling in oligodendrocyte development

The complexity of oligodendrocyte development can be simplified into four steps. First, OLPs have to be specified. Second, OLPs undergo extensive proliferation while they migrate to their final location. Third, OLPs differentiate into mature

oligodendrocytes. Finally, oligodendrocytes need to express myelin associate molecules and assemble myelin sheath around the appropriate axons. OLP specification has been introduced in section 1.5, so this section will focus on different signals that are involved in oligodendrocyte proliferation, differentiation, and myelination.

Proliferation of OLPs

OLPs are identified as a bipolar structure, and they undergo massive proliferation while they migrate throughout the CNS. Many growth factors are considered as mitogens for stimulating OLPs to proliferate *in vitro*, but not all of them have been tested *in vivo* (Bogler et al., 1990; McKinnon et al., 1991; McKinnon et al., 1990; Noll and Miller, 1993; Vartanian et al., 1999). Only PDGF has been shown to be essential for OLP proliferation *in vivo* (Calver et al., 1998; Fruttiger et al., 1999). In mice lacking PDGF-A ligands, PDGFR α -expressing OLPs can be specified at the right time and place. However, these normally specified OLPs fail to proliferate in null mice thus the number of oligodendrocytes is greatly reduced at the later stage (Fruttiger et al., 1999). In contrast, the number of OLPs increases dramatically when PDGF-A is over-expressed in the mouse (Calver et al., 1998). After OLPs reach their destinations, proliferation stops and they start to differentiate to multipolar oligodendrocytes.

Differentiation of OLPs

Differentiated oligodendrocytes are characterized by myelin basic protein (MBP), and proteolipid protein (PLP) (Campagnoni, 1988). Shh not only is required for specifying pMN cells that become OLPs, but also involved in oligodendrocyte differentiation. When Gli3 repressor is removed from Shh null embryos, OLP specification can be rescued but oligodendrocytes fail to differentiate suggesting that

intact Shh signaling in differentiation (Tan et al., 2006). Both Notch and BMP signaling have been shown to be important for oligodendrocyte differentiation *in vivo* (Genoud et al., 2002; See et al., 2007). In *Notch1* null mice, OLP specification is normal they precociously differentiate to oligodendrocytes indicating that Notch negatively regulates oligodendrocyte differentiation (Genoud et al., 2002). On the other hand, genetically deleting BMP receptor 1a/b results in a reduction of mature oligodendrocytes (See et al., 2007).

Myelination

Differentiated oligodendrocytes recognize axons of neurons and wrap them with large amounts of specific proteins and lipids to form myelin sheath. Therefore, modulators or effectors in cytoskeleton arrangement are required for formation of oligodendrocyte processes. Wiskott-Aldrich syndrome protein family verprolin homologous (WAVE) proteins mediate rapid rearrangement of actin filaments, and WAVE1 null mice display reduced oligodendrocytes and hypomyelination (Kim et al., 2006; Takenawa and Miki, 2001). The Src-kinase family member Fyn and downstream RhoA GTPase signaling have been shown to regulate outgrowth of oligodendrocytes, and inactivation of RhoA is critical for promoting multi-processed structure of oligodendrocytes (Kippert et al., 2007; Klein et al., 2002; Liang et al., 2004; Osterhout et al., 1999). Signaling from LRR and Ig domain-containing Nogo receptor-interacting protein (LINGO-1) activates RhoA thus inhibits morphological differentiation of oligodendrocytes, and LINGO-1 null mice contain more myelinated axon fibers compared to their wild-type littermates (Lee et al., 2007; Mi et al., 2005).

Once myelin proteins and lipids are transported to the axon-contacting sites, lipid-lipid or lipid-protein interactions are required for creating and maintaining multiple layers of myelin sheets. Thus complexes involved in transporting proteins or lipids play an important role in myelination. Exocyst complexes, including Sec3, Sec5, Sec6, Sec8, Sec10, Sec15, Exo70, and Exo84, are involved in transporting vesicles to the regions of rapid membrane growth (Grindstaff et al., 1998; Hazuka et al., 1999; Hsu et al., 1999; TerBush et al., 1996; Ting et al., 1995). Both Sec6 and Sec8 have been shown to be localized in oligodendrocytes, but only Sec8 is involved in oligodendrocyte differentiation. Over-expression of Sec8 results in an increase of levels of some myelin proteins and a higher membrane complexity, while down-regulation of Sec8 causes shorter processes of oligodendrocytes (Anitei et al., 2006). Interestingly, the major myelin protein MBP is transported as mRNA in granules and then translated to proteins on the myelin membrane indicating that myelination requires a network of RNA, protein, and lipid-transporting machineries (Barbarese et al., 1999).

1.7 Preview

In this dissertation, I will discuss the roles of Arl13b in neural tube development. We generated a conditional *Arl13b* allele, and we deleted Arl13b in specific cell types at specific time points to study the functions of Arl13b in different developmental processes as well as the role of Shh in neural tube patterning. Chapter 3 of this dissertation will discuss when Shh shifts from having an instructive to a permission role in patterning ventral cell fates, and chapter 4 will focus on the role of Arl13b in oligodendrocyte development.

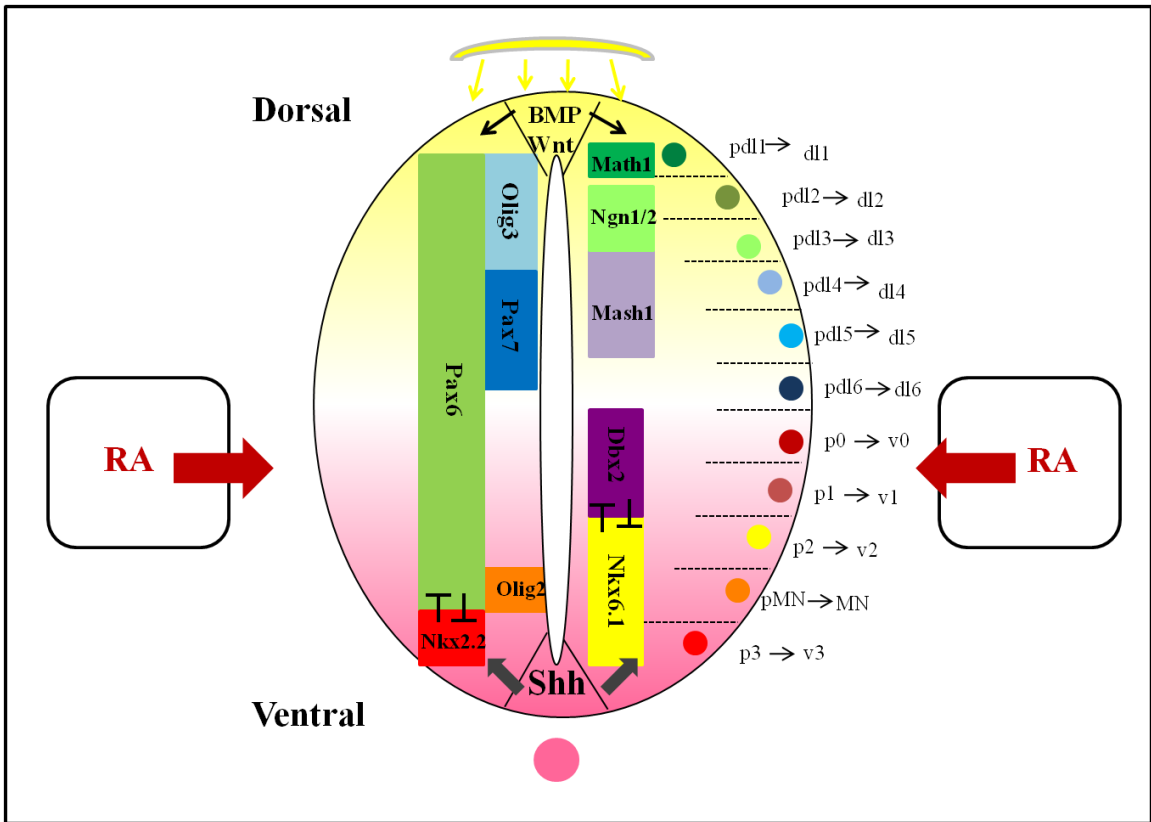


Figure 1.1 Cell signaling and neural tube patterning. Wnt and BMP ligands are secreted from the dorsal ectoderm surface (yellow line on the top), and then the roof plate. Both Wnt and BMP signaling is required for specifying dorsal interneuron progenitors (pdI1 to pdI6). Shh is originally secreted from the notochord (pink dot on the bottom), and is needed for specifying cells in the ventral neural tube to become p0-p3 and pMN cells. RA signaling is from the mesoderm that is adjacent to the neural tube, and is important for p0 and p1 specification. pdI1-pdI6, p0-p3, and pMN cells differentiate to post-mitotic interneurons or motor neurons that are labeled as dI1-dI6, v1-v3, and MN. Math1, Ngn1/2, Mash1, Olig2, Olig3, Pax6, Pax7, Dbx2, Nkx2.2, and Nkx6.1 are transcription factors that are induced by BMP, Wnt, and Shh signaling to define progenitors. Cross repression between Pax6 and Nkx2.2 as well as between Nkx6.1 and Dbx2 can sharpen the boundaries of progenitor domains.

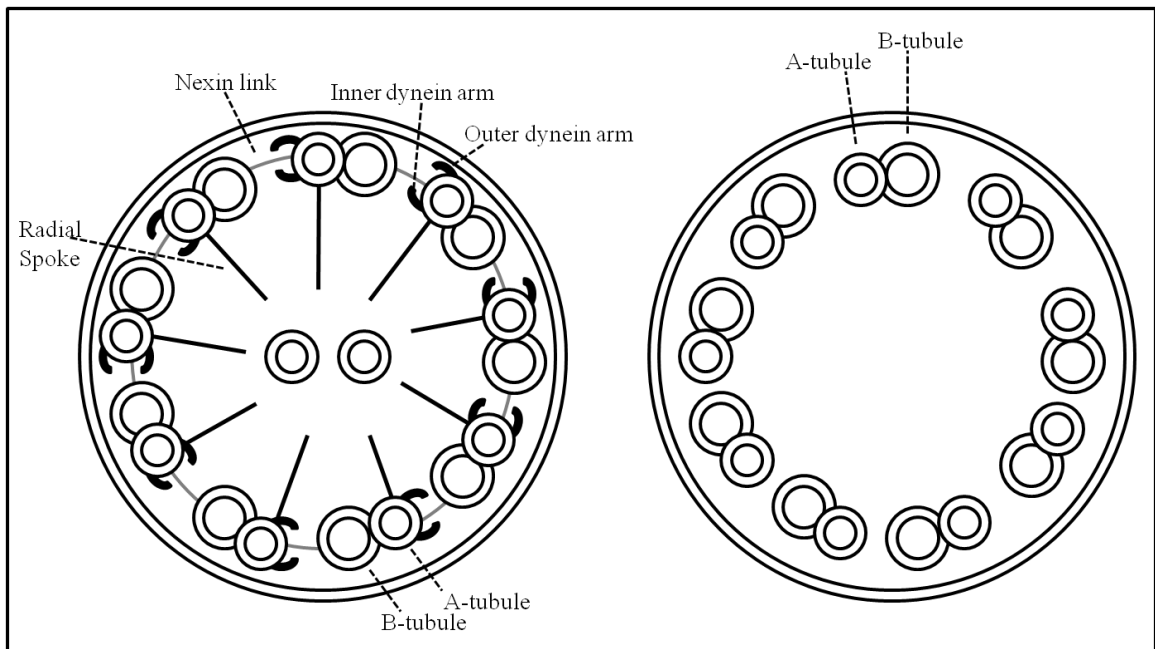


Figure 1.2 Motile and primary cilium. Both motile (left) and primary cilium (right) contain nine doublets of microtubules (A and B-tubule). Motile cilium has a central pair of microtubules, inner and outer dynein arms, radial spoke and nexin link that are not included in primary cilium.

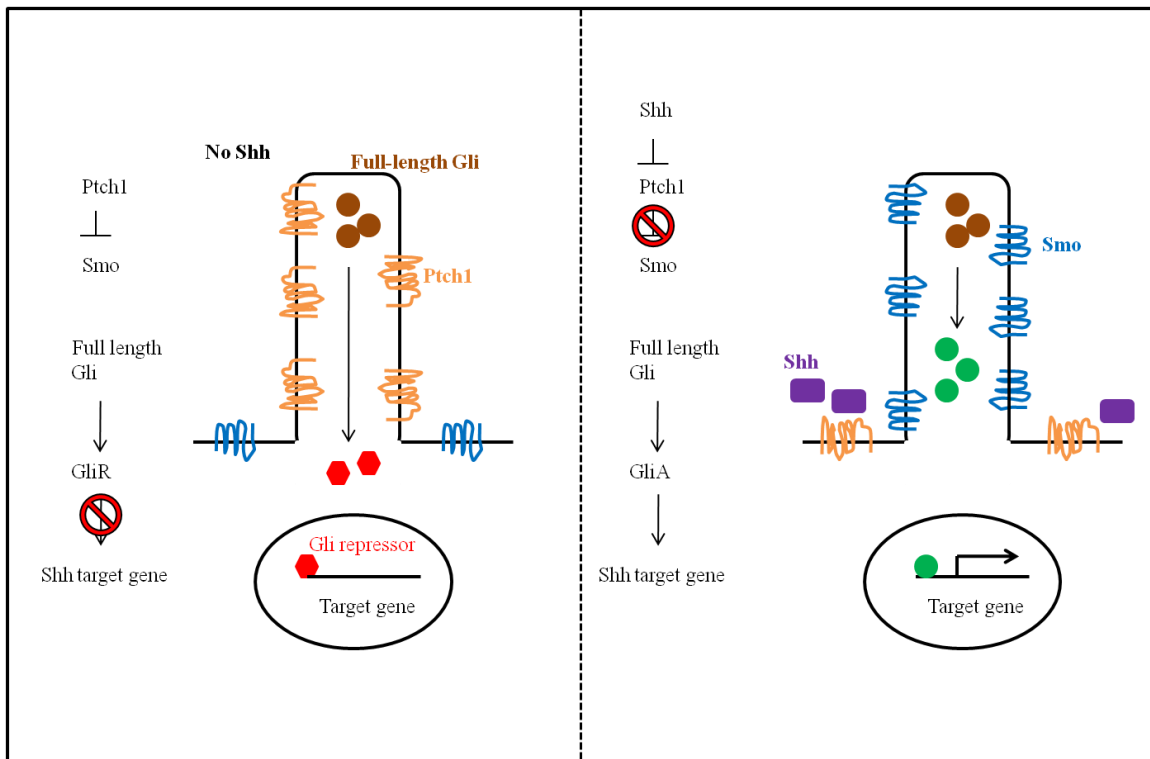


Figure 1.3 Cilia are required for Shh signaling. In the absence of Shh (left), Ptch1 is enriched in the cilium. Full-length Gli is then cleaved to become Gli repressor (GliR) and enters nuclei to inhibit expression of Shh target genes. In the presence of Shh (right), Smo enters cilia to promote full-length Gli proteins to become Gli activator (GliA) resulting in activation of Shh target gene expression.

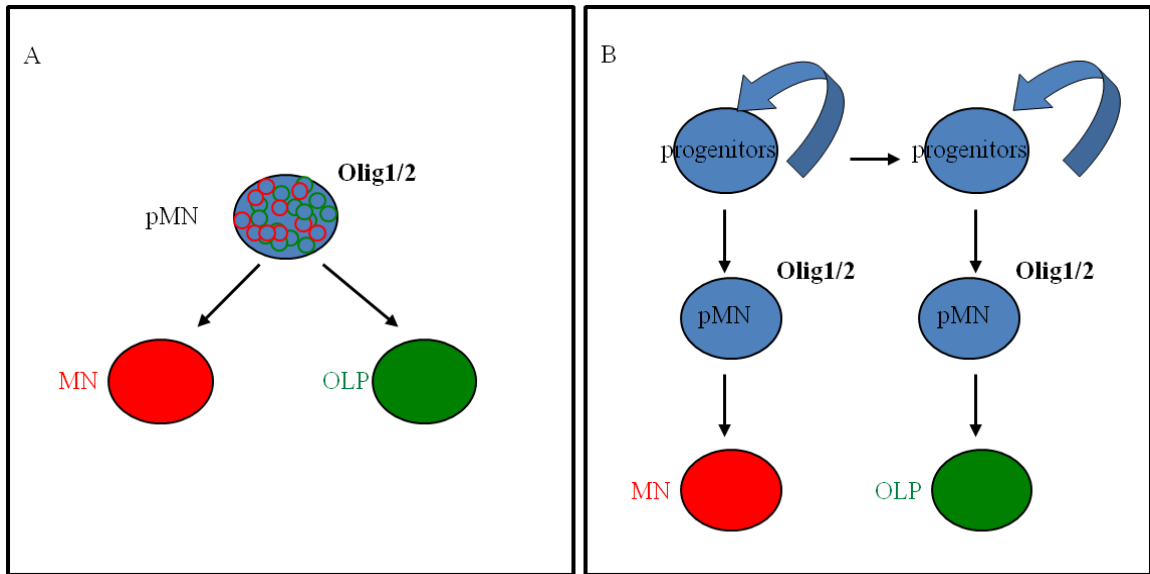


Figure 1.4 Two models of how pMN cells become motor neurons and oligodendrocyte precursors (OLPs). **(A)** There are two populations of pMN cells, and both express Olig1 and Olig2. One population (red) differentiates into motor neurons while the other population (green) becomes OLPs. **(B)** Neuroepithelial stem cells (Olig1/2 negative) give rise to pMN cells (Olig1/2 positive) that differentiate to motor neurons, and subsequently give rise to pMN cells that become OLPs.

CHAPTER 2
MATERIALS AND METHODS

2.1 Generation of a conditional *Arll3b* allele

In order to generate the targeting construct that flanked exon 2 of *Arll3b* with loxP sites, three fragments of *Arll3b* containing exon 2 and 3 were amplified from the bMQ55p06 (the Wellcome Trust Sanger Institute). Fragment 1 contained partial intron 1 that was amplified by using forward primer: 3' – cctcaagccgtgagctatg and reverse primer 3' – cagtgttctcaaccgtcct. Forward primer of fragment 1 was 4124 bp upstream of first base pair of exon2, and reverse primer of fragment 1 was 106 bp upstream of first base pair of exon2 (plasmid #47). Fragment 2 was amplified with: 3' – ggacgggtgagaaccactgt and 3' – aagccagcttgggttattt. Forward primer of fragment 2 was 123 bp upstream of first base pair of exon2, and reverse primer of fragment 2 was 404 bp downstream of first base pair of exon2 (plasmid #46). Fragment 3 was amplified by 3' – ttgatcagcaggagacagga and 3' – tcaacaaaggtccccttca. Forward primer of fragment 3 was 365 bp downstream of first base pair of exon2, and reverse primer of fragment 3 was 4835 bp downstream of first base pair of exon2 (plasmid #48).

The three fragments were cloned into pFlexible and then cloned into pFlexible, and the whole sequences of which are available on the website of the Wellcome Trust Sanger Institute or <https://www.sanger.ac.uk/Teams/Team82/docs/pFlexible.pdf>. Fragment 1 was digested with PmeI and AscI, fragment 2 was digested with PacI, and fragment 3 was cut with Sbf1 (Figure 2.1). Restriction digests confirmed all fragments were in the correct orientation. As a result, exon 2 of *Arll3b* was flanked with LoxP sites. This construct was then linearized with NotI, and the Emory Transgenic Mouse & Gene Targeting Core facility electroporated the construct into ES cells and selected ES cell clones with puromycin. 288 ES cell clones were screened and 18 clones were identified

by Southern blotting that had undergone homologous recombination. DNA was extracted from tails, and genomic DNA was digested with BamHI and BglII enzymes for Southern blotting. 5' external probe was generated from bMQ55p06 by using forward primer 3'-ctctccacctgaccatctc, and reverse primer 3'-gatgcctcttctggtgtgt. Forward primer of 5' external probe was 6195 bp upstream of first base pair of exon2, and reverse primer was 4998 bp upstream of first base pair of exon2. A 1197-bp fragment of 5' external probe was then cloned into pCRII, thus 5' external probe was able to be obtained by digesting plasmid #54 with EcoRI. 3' external probe was generated from bMQ55p06 by using forward primer 3'-aaggggaccttgggaacc and reverse primer 3'-ggcggtgacactgtaagaca. Forward primer of 3' external probe was 4818 bp downstream of first pair of exon2, and reverse primer of 3' external probe was 5822 bp downstream of first pair of exon2. A 1004-bp fragment of 3' external probe was cloned into pCRII, and 3' external probe could be generated by digesting plasmid #52 with EcoRI. The sizes of wild-type and targeted *Ar13b* alleles were 13.5 kb and 8.6 kb by using 5' external probe, respectively. The sizes of wild-type and targeted *Ar13b* allele were 13.5 kb and 7.5 kb by using 3' external probe, respectively (Figure 2.2).

Two clones were selected and injected into blastocysts to obtain chimera mice. Chimera males were set up with C57BL/6J females to obtain pups with germline transmission of the targeted allele. The puromycin cassette was removed by breeding with Flp mice (Rodriguez et al., 2000), and *Ar13b^{flxed}* allele was detected by Southern blotting with 5' internal probe. 5' internal probe was obtained from plasmid #47 (5' arm in TOPO), and a 607-bp band was purified by Gel Extraction Kit (Qiagen 28706) after

digesting with HindIII. The sizes of wild-type and *Arl13b*^{floxed} allele were 9.1 kb and 3.9 kb by using 5' internal probe after digesting with PstI, respectively (Figure 2.3).

Ear pieces were digested in Direct lysis buffer (Viagen 102-T) containing 4 mg/ml proteinase K at 55°C overnight, and proteinase was inactivated at 85°C for 45 minutes. *Arl13b*^{floxed} allele could be amplified by using Polymerase chain reaction (PCR) program – conditional arl13b: 94°C for 20sec, 65°C for 30sec, 72°C for 3min, repeated thirty-five times. AmpliTaq Gold (Applied Biosystems N808-0249) was required for genotyping *Arl13b*^{floxed} allele.

Cond Forwar primer: AGG ACG GTT GAG AAC CAC TG

Cond Reverse primer: AAG GCC AGC TTG GGT TAT TT

PCR products by using Cond primers were 526 bp, 679 bp, and 109 bp for the wild-type, *Arl13b*^{floxed}, and deleted allele, respectively (Figure 2.4).

2.2 Genotyping for mouse strains

Mouse strains used were: *CAGG-CreER*TM (JAX 004682), *EIIa-Cre* (JAX 003724), *Ptch1-lacZ* (D allele, from M.P. Scott), *Brn4-Cre* (Tg(Pou3f4)32Cren, from B. Crenshaw), *R26R* (Gt(ROSA)26Sor^{tm1Sho}; JAX 003504), Flp (JAX003800), and *Olig1-Cre* (*Olig1*^{tm1(cre)Rth}, from D. Rowitch). DNA was obtained from ear pieces that were digested in Direct lysis buffer (Viagen 102-T) containing 4 mg/ml proteinase K at 55°C overnight, and proteinase was inactivated at 85°C for 45 minutes. DNA was then diluted 1:10 in water, and PCR was performed for genotyping using primers (5' to 3') and conditions that were described below:

Cre PCR program for *EIIa-Cre*, *Brn4-Cre*, *Olig1-Cre*, and *CAGG-CreERTM* lines:

94°C for 2min; (94°C for 30sec, 60°C for 1min, 72°C for 1min) x 35; 72°C for 7min.

oIMR1084: GCGGTCTGGCAGTAAAACTATC

oIMR1085: GTGAAACAGCATTGCTGTCACCTT

oIMR7338: CTAGGCCACAGAATTGAAAGATCT

oIMR7339: GTAGGTGGAAATTCTAGCATCATCC

oIMR1084 and 1085 were used for amplifying Cre transgene. oIMR7338 and 7339 were used for amplifying a housekeeping gene as a control.

Amptaq PCR program for *Ptch1-lacZ* and *R26R* mouse lines: 94°C for 12min; (94°C for 20sec, 55°C for 30sec, 72°C for 45sec) x 55; 72°C for 7min.

LacZ2F: TGCCACTCGCTTTAATGATG

LacZ2R: CAGCAGCAGACCATTTTCAA

WT3: CTGCGGCAAGTTTTGGTTG

WT4: AGGGCTTCTCGTTGGCTACAAG

LacZ2F and LacZ2R were used for amplifying a LacZ transgene, and WT3/4 were amplifying a housekeep gene as a control.

Eppitaq PCR program for *Arl13b^{hmn}* allele: 94°C for 2min; (94°C for 20sec, 55°C for 30sec, 72°C for 30sec) x 55; 72°C for 7min.

Hnn147 Forward: AATGCCTCAAGTGCCTCTTT

Hnn147 Reverse: GGGACTCATCTTTGGGAACA

Hnn174 Forward: TGTGGGTGGCATATGTAGGA

Hnn174 Reverse: GCTAGCTATTTTCTGTTGCTGGA

Flp PCR program for flp mouse line: 94°C for 12min; (94°C for 30sec; 58°C for 1min; 72°C for 1min) x 55; 72°C for 7min.

oIMR0042: CTAGGCCACAGAATTGAAAGATCT

oIMR0043: GTAGGTGGAAATTCTAGCATCATCC

oIMR1348: CACTGATATTGTAAGTAGTTTGC

oIMR1349: CTAGTGCGAAGTAGTGATCAGG

oIMR0042 and 0043 amplify a 324 bp DNA fragment from the wild-type allele.

oIMR1348 and 1349 amplify a 725 bp fragment from the Flp transgene.

All genotyping was performed with Choice Taq (Denville Scientific Inc.), except AmpliTaq Gold was used in Amptaq program.

2.3 Preparation of genomic DNA from mouse tails

0.5 cm of tail was cut and 500 µl of SNET solution containing 1 mg/ml of proteinase K (dissolved in 0.01M Tris (pH7.5), 0.01mM CaCl₂, and 50% glycerol) was added. SNET solution contained 20mM Tris (pH 8.0), 5mM EDTA (pH8.0), 400mM NaCl, 1% (w/v) SDS, and was sterilized by filtering through a 0.45 µm nitrocellulose filter. Tail pieces in SNET solution was then incubated overnight at 55°C in a horizontal position on a rocking platform or with agitation in a shaking incubator. 500 µl of phenol:chloroform:isoamyl alcohol (Sigma P3803) was added, the tube was sealed, and incubated on a rocking platform for 30 minutes at room temperature (RT). The organic and aqueous phases was separated by centrifuging at the maximum speed (Eppendorf Centrifuge 5415 R) for 5 minutes at RT, and the upper aqueous phase was transferred to a

fresh microfuge tube (~350 μ l). An equal volume of chloroform was added, the contents of the tube was mixed by inversion several times, and centrifuge at the maximum speed for 5 minutes at RT. The upper aqueous phase was transferred to a fresh microfuge tube (~250 μ l). DNA was precipitated by adding 0.1 volume of 3M NaOAc (pH 5.2) and 2 volumes of cold 100% ethanol (keep at -20°C). The tube was inverted several times, and incubated at 4°C for at least 30 minutes. The precipitated DNA was collected by centrifuging at the maximum speed for 15 minutes at 4°C, and ethanol was carefully removed. The pellet of DNA was washed with 1 ml of 70% ethanol, and then centrifuged at the maximum speed for 5 minutes. Ethanol was removed, and the pellets were dried at RT for 5 minutes. 50~100 μ l of TE buffer containing 10mM Tris (pH7.5) and 10mM EDTA (pH8.0) was added to each pellet, and incubated on a 55° heat plate with the lid open for 5 minutes. The pellets were resuspended by gently pipetting up and down, and stored at 4°C.

2.4 Southern Blotting

Genomic DNA was extracted from tails, and 15 μ g of DNA was digested with the appropriate enzyme in a 30 μ l reaction at 37°C overnight. Digested genomic DNA was loaded on a 1% agarose gel in 1x TAE buffer, and run overnight at 40 volts. The next day, the gel was stained with ethidium bromide for 20 minutes and then a picture was taken with a ruler. Proper digestion was detected by a smear of DNA representing all size fragments. The gel was washed in 500 ml of 0.25 HCL for 15 minutes, and then washed in 500 ml of 0.5N NaOH/1M NaCl for 15 minutes. The gel was then neutralized by

washing three times in 0.5M Tris (pH 8.0) with 3M NaCl for 30 minutes each. DNA was transferred to a nitrocellulose membrane in 20X SSC (3M NaCl/0.3M sodium citrate) overnight at RT. The membrane was cross linked by UV light, and pre-hybridized in 10-15 ml of hyb buffer (GE healthcare, NIF939) at 65°C for 1 hour. A probe was radioactivity-labeled by using the Rediprime II kit (GE healthcare, RPN1636), and once the labeled probe was spun down, 100 µl of H₂O, 500 µl of salmon sperm, and 25 µl of COT DNA was added. The probe was boiled for 10 minutes, and added to the bottle containing the membrane and hybridized at 65°C overnight. The membrane was washed in 0.1xSSC/0.1% SDS twice at RT and subsequently twice at 65°C for 15 minutes per wash. The membrane was placed on film (Kodak BioMax MsFilm 8294985) at -80°C overnight and then developed on the Konica MinoLTA developer (SRX-101A).

2.5 Immunofluorescence

Embryos were dissected in phosphate buffer saline (PBS) with 0.4% bovine serum albumin (BSA), and fixed in 4% paraformaldehyde (PFA) at 4°C for 1 hour. The fix was removed by washing in PBS at 4°C for 2 hours before being placed in 30% sucrose at 4°C overnight. Embryos were washed in OCT at least twice prior to being embedded in OCT. Frozen embryos were sectioned at 10-µm thickness. Slides were washed in antibody solution (10% heat-inactivated goat serum and 0.1% Triton X-100 in PBS) at RT for 10 minutes, and incubated with primary antibodies at 4°C overnight. After washing several times in antibody solution at RT, slides were incubated with secondary antibodies for 1 hour at RT in dark. Slides were washed, and mounted with

prolong antifade mounting solution. Primary antibodies used were rabbit anti-Arl13b (serum 503, 1:1500), mouse anti-Cre (Sigma C7988, 1:500), rabbit anti-Olig2 (Millipore AB9610, 1:300), PDGFR α (GeneTex 558774, 1:100), and rabbit anti-Smoothed (Dr. Kathryn Anderson, 1:500). Mouse anti-FoxA2, HB9, Nkx2.2, Nkx6.1, Pax6, and Shh primary antibodies were obtained from Developmental Studies Hybridoma Bank, and the 1:10 dilution was used. Secondary antibodies were obtained from Invitrogen for AlexFlour series of anti-rabbit (A11034 for 488nm; A11011 for 568 nm), anti-mouse (A11029 for 488nm; A11031 for 568 nm), and anti-rat (A21471 for 594 nm). The dilution for secondary antibodies was 1:200. For staining mouse embryonic fibroblasts, cells were washed with PBS and fixed in 4% PFA for 10 minutes and then stained as described for embryonic frozen sections.

For whole mount staining, E8.5 embryos were fixed in 2% PFA for 20 minutes at RT and washed with PBS for 10 minutes. Embryos were then permeabilized in PBS with 0.1% Triton X-100 and 100mM glycine for 10 minutes, and washed in PBS for 10 minutes. After blocking in blocking buffer (10% calf serum, 0.1% BSA, and 1.5% heat-inactivated sheep serum (HISS) in TBST containing 20mM Tris, 150mM NaCl, 0.05% Tween-20) at RT for 3 hours, embryos were incubated with primary antibody in TBST with 0.1% BSA and 1.5% HISS at 4°C overnight. The next day, embryos were washed in TBST and then incubated with secondary antibody in TBST at RT for 3 hours in dark. Embryos were washed in TBST several times and taken pictures by Leica MZFLIII stereomicroscope.

2.6 Western Blotting

E12.5 embryos were dissected in PBS, and weighed to determine the amount of lysis buffer (250mM sucrose, 20mM pH7.9 Tris, 0.45M NaCl, 2mM MgCl₂, 2mM CaCl₂, 1% Sodium cholate, and protease inhibitor) that needed to be added. 1.5ml of lysis buffer was added to 1g of embryo weight, and tissue was homogenized by using a pestle on ice. Homogenized tissue was incubated on ice for 20 minutes, and protein was obtained by centrifuge at 58000 rpm for 1 hour at 4°C. The supernatant was transferred to a new tube, and protein concentration was determined by Bradford assay. 50 µg of protein was loaded to a 10% SDS-PAGE gel, and the proteins were separated at 200 volts for 40 minutes. After transferring proteins to a nitrocellulose membrane at 100mA at 4°C overnight, the membrane was blocked in 5% milk in TBST (0.1% Tween-20 in 1X TBS) for 1 hour. Affinity purified Arl13b antibody (1:1000) was incubated with the membrane at RT for 1 hour, and the membrane was washed with TBST for 5 minutes three times. Anti-rabbit HRP (1:5000, GE healthcare NA934) was incubated with the membrane for 1 hour, and proteins were visualized by ECL method (GE Healthcare, RPN2432). Actin antibody (1:5000, Sigma A5060) was used for a loading control.

2.7 RNA *in situ* hybridization

E12.5 embryos were dissected in PBS with 0.4% BSA, and the head was removed and the body was cut into halves for whole mount RNA *in situ* hybridization. Embryos were fixed in 4% PFA overnight at 4°C, and dehydrated through 25, 50, 75, and 100% Methanol in PBS. When embryos were ready for *in situ* hybridization, they were rehydrated through 75, 50, and 25% Methanol. Embryos were washed in PBSw (0.1% Tween-20 in 1x PBS) for three times, and 5 minutes each time. Embryos were incubated

in 10 µg/ml proteinase K in PBSw for 15 minutes, and washed twice in 2mg/ml glycine in PBSw. After rinsing in PBSw twice for 5 minutes, embryos were fixed in 4%PFA containing 0.2% glutaraldehyde for 15 minutes and then washed in PBSw three times. Embryos were washed in 1:1 ratio of hyb buffer (see below) and PBSw for 5 minutes, in hyb buffer for 5 minutes at RT, and in hyb buffer at 65° for 2 hours. Before hybridizing with a probe, 200ng of *Ptch1* probe was added into 100µl of hyb buffer and then heated at 95°C for 5 minutes. Heated probe was added to 900µl hyb buffer and embryos, and incubated at 70°C overnight.

The next day, embryos were washed in 800µl hyb buffer for 5 minutes at 70°C and then 400µl of 2xSSC pH4.5 was added to the embryos for three times. Embryos were washed in 2xSSC pH7.0 with 0.1% CHAPS twice at 70°C, 30 minutes for each time. After rinsing with MAB (50ml of 1M maleic acid, 15ml of 4M NaCl, 400mk H₂O, and bring pH to 7.5) at RT for 10 minutes twice, embryos were washed in MAB buffer at 70°C for 30 minutes twice. Embryos were washed in PBS at RT for 10 minutes twice, and then in PBSw for 5 minutes. After incubating in 1ml blocking solution (1% boehringer blocking reagent and 10% goat serum in PBSw) for 2 hours at 4°C, embryos were incubated in 1.5 ml of blocking buffer with 0.1µl/ml of anti-DIG antibody (AP) at 4°C overnight.

The last day, embryos were rinsed in PBSw+0.1%BSA for 45 minutes five times. After washing in PBSw for 30 minutes twice, embryos were washed in AP1 buffer (2ml of 1M Tris pH9.5, 0.5ml of 4M NaCl, 1ml of 1M MgCl₂, and 6.5ml of H₂O) for 10

minutes twice. Embryos were then incubated in 1ml BM purple in the dark until signal was developed.

Hybridization buffer (hyb buffer) was prepared by mixing 0.5g Boehringer Block, 25ml formamide, 12.5ml of 20x SSC pH 7.0 (175.3g NaCl and 88g Sodium citrate into 1L H₂O), 500µl of 0.5M EDTA pH8.0, 10ml of 5mg/ml torula RNA, 100µl of 50mg/ml Hepairn, 500µl of 10% CHAPS, and 50µl Tween20.

The plasmid (#61) of *Ptch1* probe was obtained from Matthew P. Scott's lab (Goodrich et al., 1996). *Ptch1* plasmid was linearized at 37°C for 2 hours, and the reaction contained 8.3 µl of plasmid#61, 2µl of NEB buffer2, 1µl of BamHI, and 8.7 µl of sterile water. 2 µl of 3M NaOAc and 40 µl of 100% EtOH was added to the linearized DNA, and the tube was incubated at RT for 10 minutes. Then DNA was spun down for 3 minutes at the full speed, and 1 ml of 70% EtOH was added. After centrifuging for 3 minutes, supernatant was removed and the pellet was air dried for few minutes. 5 µl of sterile water was added to resuspend the DNA. The *Ptch1* probe was labeled at 37°C for 2 hours with 1 µl of T3 polymerase in 1 µl of 10x transcription buffer, 10X of DIG labeling mix, 100mM DTT, and RNase OUT. After 2 hours, 50 µl of 0.2M NaOAc was added immediately. 15 µl of 4M LiCl and 300 µl of cold 100% EtOH were added to the probe, and the probe was incubated at 4°C for at least 30 minutes. Then the RNA probe was spun down at 4°C for 15 minutes, and 1 ml of cold 70% EtOH was added. After spinning down for 2 minutes, supernatant was removed and the pellet was air dried for few minutes. Then the pellet was resuspended in 75 µl of hyb buffer, and stored at -80°C.

2.8 X-gal staining

Embryos were fixed in fixative solution containing 0.1M sodium phosphate buffer, 0.2% glutaraldehyde, 5mM EGTA, 2mM MgCl₂ at RT for 15 minutes. Fixed embryos were rinsed three times in detergent rinse containing 0.1M sodium phosphate buffer, 2mM MgCl₂, 0.01% sodium deoxycholate, and 0.02% NP-40 at RT. X-gal was added in detergent rinse with 1M Tris (pH 7.5), 5mM potassium ferricyanide, 5mM potassium ferrocyanide, and final concentration of X-gal was 1 mg/ml. Embryos were incubated at RT in dark until blue color was visualized.

2.9 Tamoxifen injection

Tamoxifen (Sigma T5648) was dissolved in 100% ethanol to a final concentration of 10 mg/ml. When injecting mice at E6.5, E7.5, or E7.75, 0.1 mg tamoxifen per 1 g body weight was dissolved in 300 µl of corn oil (Sigma C8267) by using a vacuum centrifuge at medium speed for 20 min. When injecting mice at E8.5, 0.15 mg of tamoxifen was used per 1g body weight. Pregnant females were injected intraperitoneal once a day with 25G needle (blue).

2.10 Quantitative analysis

Cells in the neural tube were stained with Olig2 and HB9 according to the protocol in 2.5. When slides were incubated with secondary antibodies, a nuclear marker (Hoechst, 1:3000) was also added thus the neural tube was triple stained at RT for 1 hour. Olig2 cells, HB9 cells, and nuclei were visualized by Leica DM6000 B upright fluorescence microscope. Pictures were taken at 40x objective with three different

channels. Cells were counted by Image J (NIH), and three color channels were separated so Olig2, HB9, or Hoechst-staining cells could be counted in its own channel. RGB color was converted to grayscale by clicking conservations to scale when converting under options of Edit, and then by clicking Image -> Type -> 16 bit. Cells were highlighted by using Threshold under Adjust of Image, and some big areas could be separated by clicking Watershed under Binary of Process. Total cells were counted by Analyze Particles under Analyze, and size range was from 100 to infinity. Three different sections were counted for one embryo. Olig2 and HB9 positive cells were normalized to the total number of cells in the neural tube. Five embryos were counted for each genotype, and averages with standard deviations were calculated. The averages of normalized Olig2 or HB9 cells in mutant embryos were compared to the averages of which in wild-type or *Ar113b^{floxed/+}*. After calculating with student's t test, there was a significant difference when $p < 0.005$. Acetylated α -tubulin or Arl13b-staining cilia in mouse embryonic fibroblasts were also counted by Point selections of Image J, and shift was pressed while clicking individual cilium so final number could be obtained.

2.11 Generation of mouse embryonic fibroblasts (MEFs)

Before dissection, 6 ml of 0.1% gelatin was added to a 10-cm tissue culture plate and incubated at 37°C incubator for at least 1 hour. E12.5 embryos were dissected in PBS with 4% BSA, and heads and organs were removed. Single embryo was transferred to PBS and sucked into a 1ml syringe, and excess PBS was removed. A 18G needle (pink) was assembled to a syringe, and an embryo was re-suspended up-and down in 1 ml of MEF medium {DMEM (high glucose), 10% of FBS, and penicillin/ Streptomycin} for 5-

10 times until there was no big mass of pieces. The embryo cell suspension was transferred to a gelatinized 10-cm plate containing 10 ml of MEF medium, and incubated at 37°C overnight. Fresh medium was changed the next day, and then one plate of cells was trypsinized and plated to five 10-cm plates after cells were confluent.

2.12 Arl13b deletion in MEFs

MEFs were obtained from *Arl13b*^{floxed/+} and *Arl13b*^{hnn/floxed}; *CAG-Cre/+* embryos, and plated on a 6-well plate containing coverslips that were coated with 0.1% gelatin in a density of 800,000 cell/well in MEF medium. The next day, MEF medium was replaced by DMEM/high glucose medium without serum for 24 hours. Tamoxifen (2 μM as final concentration, Sigma H7904) was added in DMEM/high glucose with or without serum for 24 and 48 hours, and coverslips were collected for immunofluorescence.

Acknowledgement

I am thankful for Michael J. Hillman for generating a conditional *Arl13b* allele construct.

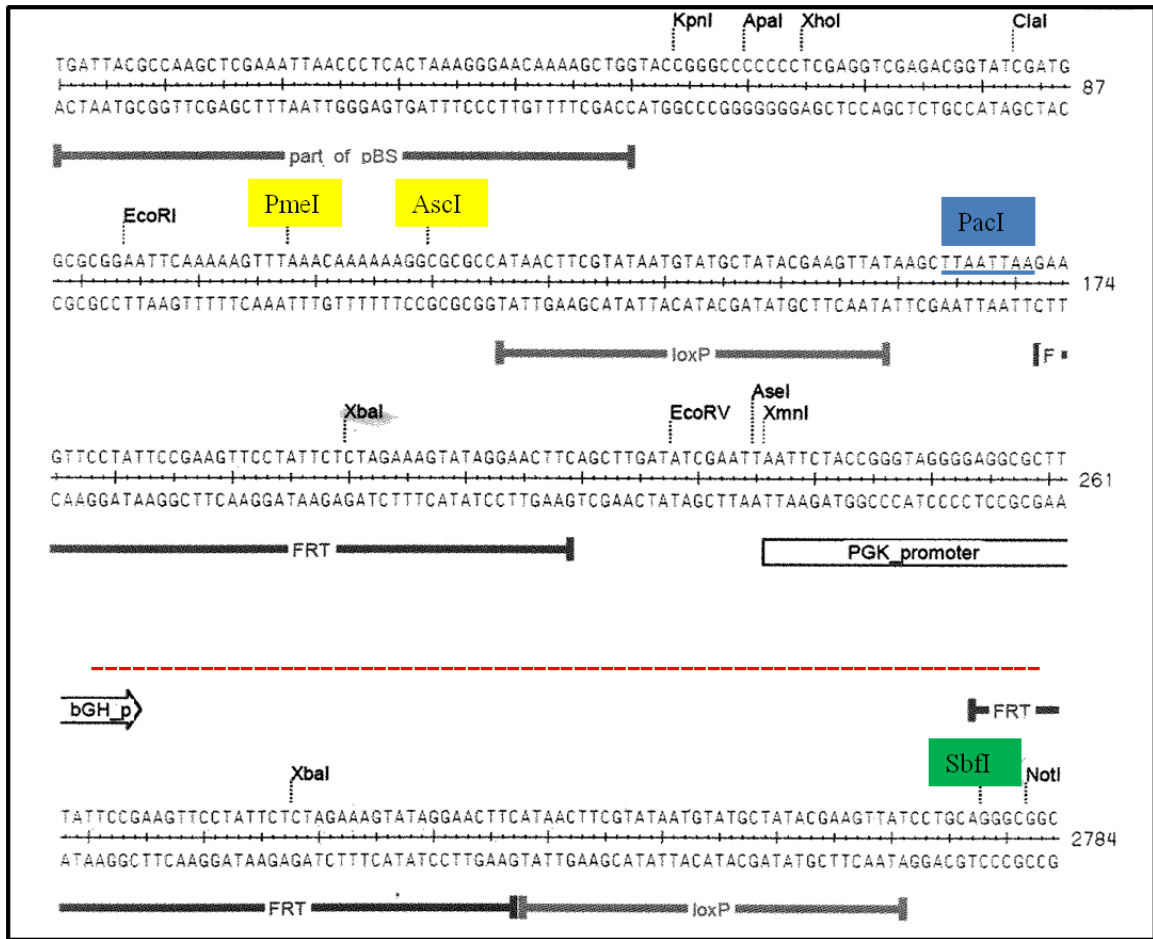


Figure 2.1 Cloning sites of 5' arm, exon 2 of *Arl13b*, and 3' arm on pFlexible. Fragment 1 containing 5' arm of the conditional *Arl13b* allele is inserted between PmeI and AscI (yellow). Fragment 2 contains exon 2 of *Arl13b* and is inserted into PacI locus on pFlexible. Fragment 3 containing 3' arm of the conditional *Arl13b* allele is inserted at SbfI locus on pFlexible.

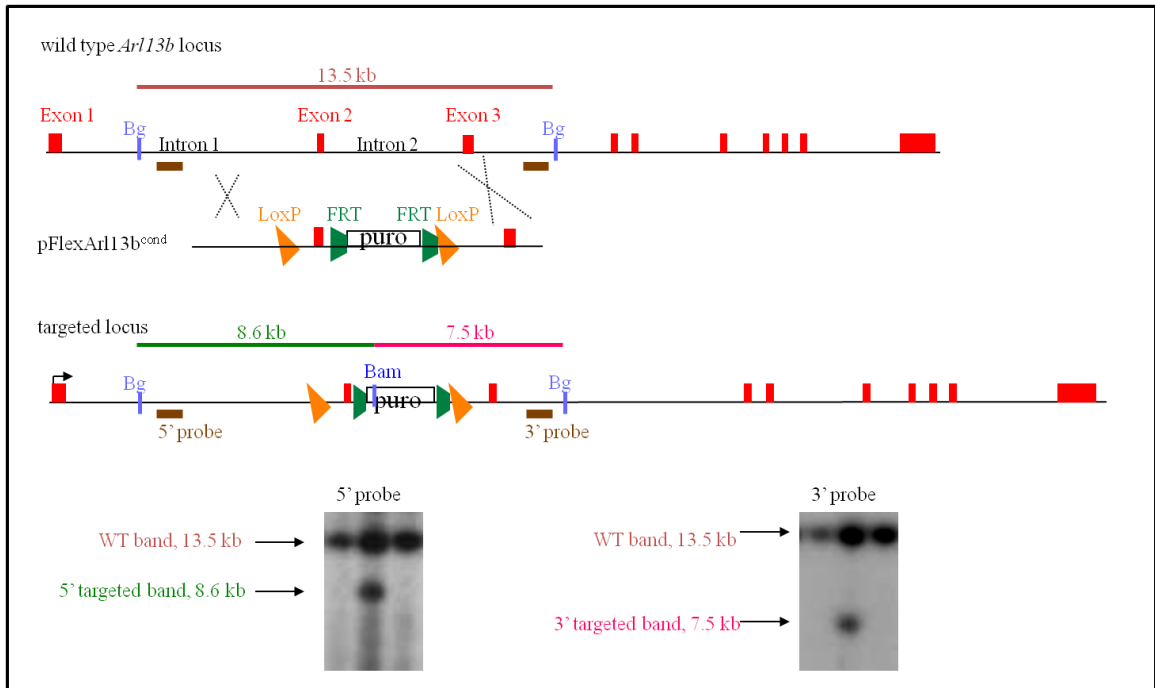


Figure 2.1 The construct of a conditional *Arl13b* allele. Above is a schematic figure showing that a conditional *Arl13b* allele construct is inserted into the endogenous *Arl13b* locus by homologous recombination. The construct creates a BamHI-cutting site to generate two unique fragments when digesting with BglII, and wild-type and targeted alleles can be detected by Southern blotting.

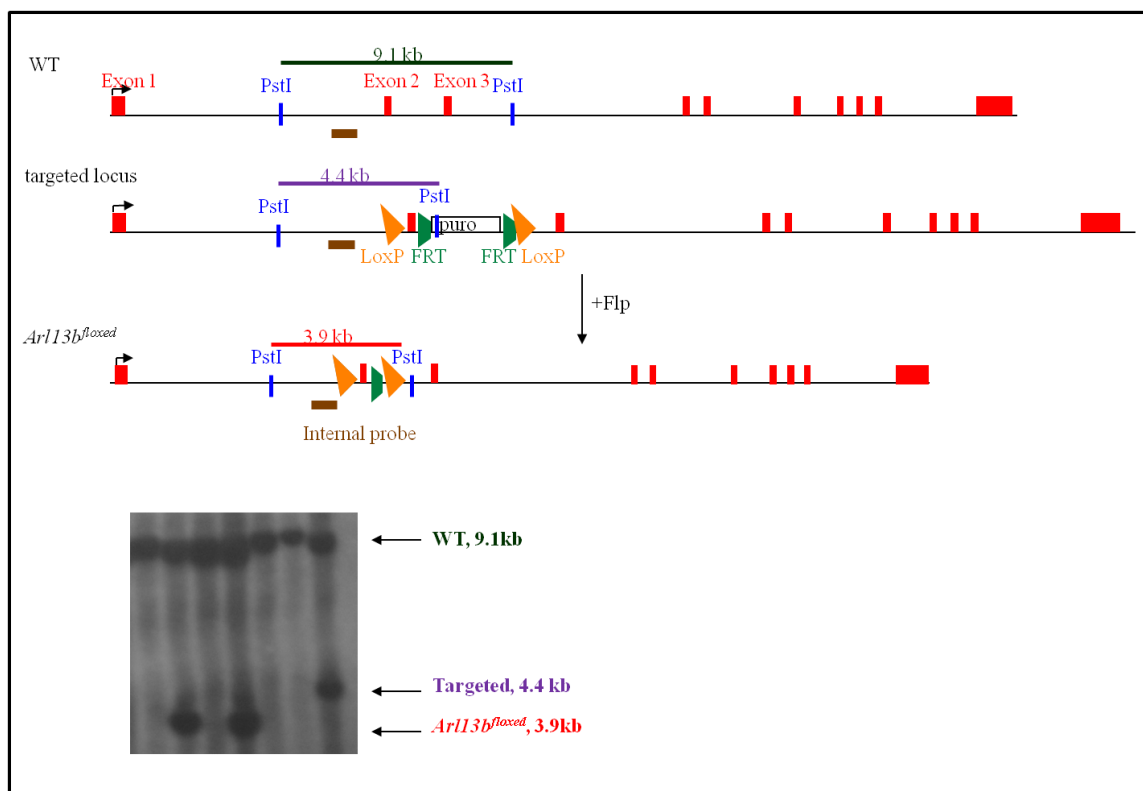


Figure 2.3 The generation of a *Arl13b*^{floxed} allele. Above is a schematic figure showing the differences between wild-type, targeted allele with a puromycin cassette, and targeted allele without a puromycin cassette after crossing with *Flp* mice. Flp recombinase recognizes FRT sequences, and removes the area between two FRT sites. Genomic DNA is digested with PstI, and an internal probe is used to distinguish different alleles.

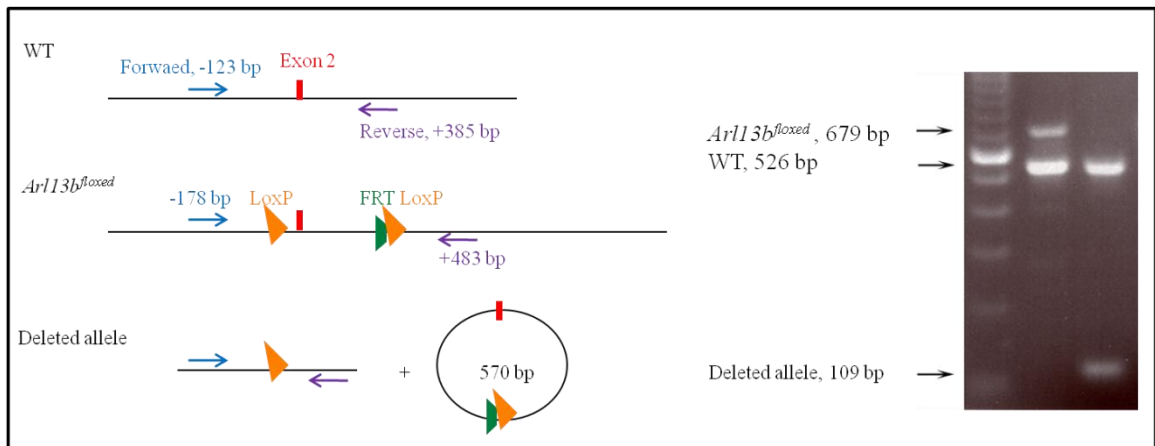


Figure 2.4 Exon two of *Arl13b* can be deleted upon *Cre* recombination. A schematic figure (left) shows the relative locations of primers for detecting wild-type, *Arl13b^{floxed}*, and a deleted allele. *Cre* recombinase recognizes LoxP sequences, thus exon 2 of *Arl13b* can be removed by crossing to *Cre* lines. A picture (right) shows PCR result by using primers to detect different alleles.

CHAPTER 3

SHH ACTS FIRST AS AN INSTRUCTIVE MORPHOGEN AND THEN AS A
PERMISSIVE SIGNAL IN MAMMALIAN NEURAL TUBE PATTERNING

3.1 Summary

Cilia are necessary for Sonic hedgehog (Shh) signaling, which is required to pattern the neural tube (Chiang et al., 1996; Huangfu et al., 2003). The five ventral neural cell fates are defined by a specific cohort of transcription factors that are induced by distinct thresholds of Shh activity (Briscoe et al., 2000; Briscoe et al., 1999; Ericson et al., 1997a; Ericson et al., 1997b). Despite this understanding, the role of Shh as an instructive morphogen has become increasingly complex as models integrate concentration and time (Dessaud et al., 2007; Ribes et al., 2010). Recent work in mouse showed that if Shh expression is extinguished just after the ventral cell fates are specified, those cell fates are lost, demonstrating that Shh signaling must be maintained once neural fates are specified (Dessaud et al., 2010). To determine if normal neural patterning occurs when the Shh activity gradient is not maintained, we temporally induced low level constitutive Shh activity by deleting the cilia protein *Arl13b* in mouse embryos. We defined a critical period prior to E10.5 when changes in Shh activity cause cells to change their fate in the caudal neural tube. However, when we induced constitutive, low level Shh activity after that critical period, improperly patterned cells converted to the wild-type pattern, indicating ungraded Shh activity during this time permits the rescue of cell fates. Our studies show that Shh has two different types of activity during neural patterning. Shh first acts an initial instructive role when the activity level determines final cell fates. Subsequently, Shh activity needs to be present for differentiation to proceed but cells are already committed. Interestingly, we always observe normal patterning in the rostral neural tube regardless of the timing of *Arl13b* deletion suggesting that Shh acts mainly as

a permissive signal rostrally. These data argue that Shh plays a short-lived morphogen role and a long-term, essential permissive function in neurogenesis.

3.2 Introduction

Cells in the ventral neural tube interpret Shh signaling levels over time to specify five different ventral cell fates (Briscoe et al., 2000; Briscoe et al., 1999; Ericson et al., 1997a; Ericson et al., 1997b). Since the discovery that Shh signaling is required for spinal cord cell fates, the mechanism through which the morphogen gradient functions has emerged as increasingly complex (Chiang et al., 1996). The first model suggested that Shh acts as a simple diffusible morphogen, where its activity was a simple function of its concentration, which was determined by the distance of a cell from the morphogen source (Briscoe et al., 2000; Briscoe et al., 1999; Ericson et al., 1997a; Ericson et al., 1997b). However, this model did not account for how a stable pattern could be specified while the tissue being patterned was growing simultaneously. Recent data have shown that the duration and level of Shh signaling are integrated to determine cell fate (Dessaud et al., 2010; Dessaud et al., 2007; Ribes et al., 2010). In this temporal adaptation model, cells become progressively less sensitive to Shh ligand as it induces expression of the negative regulator of the pathway, Patched1 (Ptch1) (Chen and Struhl, 1996; Goodrich et al., 1997; Jeong and McMahon, 2005; Marigo and Tabin, 1996). This negative feedback loop demands that cells be stimulated with higher concentrations of Shh over a longer period of time to achieve the highest Shh response. This implies that Shh signaling must be continuous and, indeed, recent work showed that ventral neural cell fates are lost if Shh

signaling is not maintained (Dessaud et al., 2010). However, it is unclear whether proper neural cell fates continuously require graded Shh activity.

Vertebrate Hedgehog signaling requires the primary cilium, and components of the pathway are localized to cilia (Corbit et al., 2005; Haycraft et al., 2005; Huangfu et al., 2003; Rohatgi et al., 2007). Ptch1 is a Shh receptor and is localized to the cilium in the absence of Shh, while Smoothed (Smo) enters the cilium upon Shh stimulation (Corbit et al., 2005; Marigo and Tabin, 1996; Rohatgi et al., 2007). Gli proteins mediate the transcriptional response to Hh signaling and are processed to either activator (GliA) or repressor (GliR) forms (Aza-Blanc et al., 2000; Ruiz i Altaba, 1998). Normally, the relative localization of Ptch1 and Smo shifts upon Shh stimulation, permitting Gli proteins to be enriched in cilia (Chen et al., 2009; Haycraft et al., 2005; Rohatgi et al., 2007; Tukachinsky et al., 2010).

Mouse mutants that lack specific intraflagellar transport (IFT) proteins do not have cilia, which results in an absence of GliR and GliA function and a lack of ventral neural cell fates (Houde et al., 2006; Huangfu et al., 2003; Liu et al., 2005; May et al., 2005; Tran et al., 2008). In contrast, we have found that in mouse mutants lacking the ciliary protein Arl13b (called *Arl13b^{hennin(hmm)}*), there is a constitutive low level of Shh activation that corresponds to the specification of progenitors of motor neurons (pMN) through most of the neural tube (Casparly et al., 2007). *Arl13b^{hmm}* mutants possess abnormal cilia that allow a constitutive low level of Shh activity in the spinal cord through changes in GliA, but not GliR activity. Components of Shh signaling are not regulated properly in the absence of Arl13b: Ptch1 and Smo localize to cilia regardless of Shh stimulation, and there is no Gli enrichment in cilia upon Shh stimulation (Larkins et

al., under revision). This is consistent with the constitutive activation of Shh signaling in the *Arl13b^{hmn}* mutant neural tube being ligand-independent (Casparly et al., 2007).

Here, we use a targeted conditional null allele of *Arl13b* to temporally control Shh signaling activity in the mouse neural tube. Our analysis of the resulting phenotypes supplies *in vivo* evidence that cells in the mouse neural tube are only sensitive to the level of Shh activity prior to E10.5 in caudal neural tube. In contrast to complete ablation of Shh signaling after the establishment of morphogen gradient, when ventral cell fates are initially specified and then lost (Dessaud et al., 2010), we show that mis-patterned cells experiencing constitutive low levels of Shh signaling are able to correct their fates if they are initially exposed to a normal Shh gradient. As this phenotype contrasts with the *Arl13b^{hmn}* germline null phenotype, our data define the timeframe during which Shh acts as an instructive morphogen and reveal the timeframe of its subsequent permissive signaling role.

3.3 Results

Neural progenitors are sensitive to changes in Shh activity at E9.5, but not at E10.5

To temporally alter Shh activity in the neural tube during development, we generated a conditional null *Arl13b* allele (Figure 3.1A; construct was generated by Michael J. Hillman). By combining a ubiquitous, tamoxifen-inducible *Cre* line, *CAGG-CreERTM*, with the *Arl13b^{floxed}* allele and injecting the pregnant dams with tamoxifen, we controlled the timing of *Arl13b* deletion (Hayashi and McMahon, 2002) (Figure 3.1I and J; 3.3A). Via immunofluorescence, we saw a reduction of Arl13b starting 24 hours (h) post-injection and a complete loss of Arl13b expression at 42 h post-injection (Figure

3.2). Indeed, when we induced deletion in the germline by *EIIa-Cre*, the conditional allele recapitulated the *Arl13b^{hmn}* phenotype indicating the same constitutive low level Shh activity as in *Arl13b^{hmn}* (Figure 3.1C-F).

To investigate when cells are sensitive to changes in Shh activity, we first analyzed the consequences of removing *Arl13b* as neural patterning is established, around E9.5. By injecting tamoxifen at E7.75, we obtained full deletion of *Arl13b* by E9.5, and refer to embryos with this time of deletion as *Arl13b^{ΔE9.5}* (Figure 3.3A ii and H). In the caudal neural tube at E9.5, we found an equivalent expansion of *Olig2* cells in the *Arl13b^{ΔE9.5}* neural tube as in *Arl13b^{hmn}* embryos (Figure 3.3E and I). We also saw that, compared to control *Arl13b^{flxed/+}* embryos, the progenitor marker *Nkx6.1* was expanded dorsally in the *Arl13b^{ΔE9.5}* neural tube, albeit not as far dorsally as in *Arl13b^{hmn}* embryos (Figure 3.8A'', D'', and J'').

Next, to examine whether cells are sensitive to changes in Shh activity at E10.5, we examined *Arl13b^{ΔE10.5}* embryos, whose mothers were injected with tamoxifen at E8.5 (Figure 3.3A iii, J, and L). We found *Olig2* expression was normal at E10.5, indicating that cells were no longer sensitive to changes in Shh activity and arguing the the cells are committed at E10.5 (Figure 3.3K and M). Thus cells in the mouse neural tube are sensitive to changes in Shh activity levels for a developmental window after E8.5 and prior to E10.5, implying that Shh is not a potent instructive signal *in vivo* after E10.5.

***In vivo* modulation of Shh activity level and regulation of Smo localization**

To confirm that temporal loss of *Arl13b* affected Shh signaling in the same mechanistic manner as constitutive loss of *Arl13b*, we turned to *Arl13b* deletion in cell

culture with *Arl13b*^{floxed/+} and *Arl13b*^{hmn/floxed; CAGG-Cre/+} (*Arl13b*^{ΔCAGG-Cre}) mouse embryonic fibroblasts (MEFs). We cultured the MEFs under two conditions: in serum-free media for 24 h (to induce cilia formation) followed by tamoxifen treatment to delete *Arl13b*, or in serum-containing media with tamoxifen, which permits the cells to proliferate as they would *in vivo*. Consistent with what we had seen *in vivo*, we saw a slight decrease of Arl13b 24 h after tamoxifen addition and an absence of Arl13b between 36 and 42 h after tamoxifen treatment (Figure 3.4A-F, I, J-O, and R). These data establish that Arl13b protein was abolished 42 h after tamoxifen injection and implied that Arl13b-dependent phenotypes could be analyzed *in vivo* two days post-injection (Figure 3.4G, H, P, and Q).

The germline deletion of the conditional allele recapitulated the *Arl13b*^{hmn} neural patterning phenotype, arguing that the *Arl13b* conditional deletion globally affected Shh activity as expected (Figure 3.1C-F). At the cellular level, this is due to a lack of regulation of key components of the pathway; Smo requires Shh stimulation to localize to cilia in wild-type MEFs, but was found in the cilia of *Arl13b*^{hmn} MEFs regardless of Shh stimulation (Larkins et al., under revision). Therefore, we tested whether the conditional deletion of Arl13b affected ciliary Smo localization like the null allele. We examined Smo localization in *Arl13b*^{floxed/+} and *Arl13b*^{ΔCAGG-Cre} MEFs at 36 h post-tamoxifen treatment, as well as at 48 h, when we detected no Arl13b. As expected, we found that when Arl13b protein was present in *Arl13b*^{floxed/+} or in *Arl13b*^{ΔCAGG-Cre} MEFs at 36 h, Smo localized to cilia only upon Shh stimulation (Figure 3.5A-H). By 48 h in *Arl13b*^{floxed/+}, we no longer found Smo in cilia, consistent with the observation that continued Shh response requires continuous stimulation (Figure 3.5J, K, N, O, and R;

(Dessaud et al., 2007)). In contrast, Smo localized to cilia in *Arl13b*^{ΔCAGG-Cre} at 48 h with or without Shh stimulation (Figure 3.5L, M, P, Q, and R). This indicates that temporal deletion of *Arl13b* results in the same kinetics of loss of Smo regulation found in *Arl13b*^{hmn} MEFs (Larkins et al., under revision). Thus the temporal deletion of *Arl13b* with *CAGG-CreER*TM *in vivo* results in constitutive low level of Shh activity.

Rescue of neural tube patterning over time in *Arl13b*^{ΔE9.5} embryos demonstrates active role for low level Shh activity

The loss of cell fates over time in the *Shh* conditional mice indicated that Shh expression must be maintained for patterning to persist (Dessaud et al., 2010). To test the consequence of altering Shh activity via loss of *Arl13b* on ventral cell fates over time, we examined the *Arl13b*^{ΔE9.5} embryos at several time points. Differentiated motor neurons are normally restricted to the ventrolateral neural tube, but are expanded in *Arl13b*^{hmn} null embryos from E10.5 through E12.5 (Figure 3.6A, B, I, and J). In E10.5 *Arl13b*^{ΔE9.5} embryos, we detected an expansion of Olig2 and HB9 cells identical to the E10.5 *Arl13b*^{hmn} null phenotype (Figure 3.6B and D). However, by E12.5 we found the same number of Olig2- and HB9-positive cells in *Arl13b*^{ΔE9.5} embryos as in control embryos (Figure 3.6 Q). Furthermore, their expression domain resembled the wild-type pattern, not the *Arl13b*^{hmn} null embryo pattern (Figure 3.6I and L). This recovery of patterning from E10.5 to E12.5 was surprising, since graded Shh does not direct different ventral neural cell fates after E10.5. Thus not only must Shh signaling be maintained for normal neural cell fates to be specified but the maintenance of Shh signaling permits abnormally specified cells to be rescued to a wild type fate over time.

The recovery of patterning was unexpected so we investigated two potential limitations stemming from our inducing deletion of *Arl13b*. A trivial explanation for the rescue of patterning we see is that *Cre*-induced deletion may not be complete. In such a scenario, wild-type cells might out-compete mutant cells over time. We ruled out this possibility by examining *Arl13b* expression via immunofluorescence (Figure 3.7E and F) and Western blotting (Figure 3.7G), as well as by confirming *Arl13b* deletion via PCR of the deleted *Arl13b^{floxed}* allele (Figure 3.7H). In all cases, we could detect no protein or unrecombined DNA allele, indicating that the deletion was ubiquitous and no wild-type cells remained.

The second potential limitation that could underlie the recovery of patterning was that, in contrast to *Arl13b^{hmn}* embryos that never expressed *Shh* in the floor plate, *Shh* was expressed in the floor plate in *Arl13b^{ΔE9.5}* embryos at E9.5, E10.5, and E12.5 (Figure 3.3E' and I'; 3.6F, H, N, and P). We thought it extremely unlikely that the *Shh* expression in the floor plate could drive the recovery since the *Arl13b^{ΔE10.5}* embryos showed ventral neural cells are insensitive to shifts in *Shh* activity after E10.5. Furthermore, *Shh* *Arl13b^{hmn}* double mutant analysis has shown that the absence of *Arl13b* results in ligand-independent constitutive *Shh* activity (Casparly et al., 2007). However, we reasoned that we could eliminate this possibility if we observed the same recovery of patterning when *Shh* expression in the floor plate was extinguished. To test this directly, we deleted *Arl13b* by injecting tamoxifen at E7.5, six hours before the injection that generated the *Arl13b^{ΔE9.5}* embryos, and called these embryos *Arl13b^{ΔE9.25}* (Figure 3.3A i). *Shh* was absent in the floor plate in the *Arl13b^{ΔE9.25}* embryos at E9.5, as in *Arl13b^{hmn}* embryos (Figure 3.3E' and G'). We did find an expansion of the *Olig2*-positive domain at E9.5

and E10.5 in the *Arl13b*^{ΔE9.25} embryos (Figure 3.3G; 3.6C); however, by E12.5, Olig2 was restricted to its normal wild-type domain (Figure 3.6K). The equivalent recovery of patterning by E12.5 in *Arl13b*^{ΔE9.25} as in *Arl13b*^{ΔE9.5} embryos indicates that Shh expression in the floor plate of *Arl13b*^{ΔE9.5} embryos cannot explain the recovery.

Rescue of neural patterning over time is not due to reactivation of Shh gradient

The question then became whether Shh activity gradient was re-established at E12.5 resulting in recovery of patterning in *Arl13b*^{ΔE9.25} and *Arl13b*^{ΔE9.5}. While it is well known that Shh activity initiates in a steep gradient at E8.5 and is maintained at E9.5 and E10.5, its subsequent status is unclear (Goodrich et al., 1996). We examined the gradient at E12.5 using the *Ptch1-lacZ* allele and *Ptch1* in situ hybridization and found Shh activity through most of the ventricular zone. This pattern did not correlate with the distinct cell fates of the E12.5 ventral neural tube (Figure 3.7A and C). In fact, cells at intermediate levels of the neural tube had higher *Ptch1* expression than those in the ventral midline, despite the midline being the source of ligand. The observation that cell fates do not reflect the level of Shh activity at E12.5 is consistent with our genetic analysis, arguing that alterations in Shh activity do not change ventral cell fates after E10.5 (*Arl13b*^{ΔE10.5} embryos).

We also examined *Ptch1* expression in *Arl13b*^{ΔE9.5} embryos, to determine whether the Shh activity gradient was abnormally maintained in the conditional mutant. However, we saw no difference from wild-type, indicating that novel alterations in the gradient could not account for the recovery of patterning (Figure 3.7B and D). Curiously, *Ptch1* expression was absent across the ventral midline, despite the expression of Shh in the

floor plate in both wild-type and *Arl13b*^{AE9.5} embryos. The absence of a Shh activity gradient at E12.5 is consistent with our functional data that graded activity need not be maintained for proper spinal cord cell specification.

Recovery of patterning is complete indicating a permissive role of Shh

To determine the extent of recovery of patterning in *Arl13b*^{AE9.25} and *Arl13b*^{AE9.5} embryos, we examined other markers affected in the *Arl13b*^{hmn} null neural tube. Normally at E12.5, Nkx6.1 marks all ventral progenitors, within which the subdomains are demarcated by FoxA2 in the floor plate, Nkx2.2 in the p3 cells, and Olig2 in the pMN cells (Figure 3.8C, C', and C''). In *Arl13b*^{hmn} embryos, we rarely saw FoxA2-expressing cells; Nkx2.2-expressing cells were specified across the ventral midline, intermingled with Olig2 cells; and Nkx6.1 cells were expanded into dorsal neural tube (Figure 3.8F, F', and F''). When we examined these markers in E12.5 *Arl13b*^{AE9.25} and *Arl13b*^{AE9.5} embryos, we found they were similar to control embryos, providing evidence that the pattern was rescued (Figure 3.8I, I', I'', L, L', and L''). Nkx6.1 was specified normally in the ventricular zone in E12.5 *Arl13b*^{AE9.25} and *Arl13b*^{AE9.5}, although its expression pattern was different in the motor neuron domain (Figure 3.8I'' and L''). At E9.5, FoxA2 was present in both *Arl13b*^{AE9.25} and *Arl13b*^{AE9.5} caudal neural tubes, consistent with the initial Shh activity establishing FoxA2 expression (Figure 3.8G and J); however, by E10.5, there were FoxA2-positive cells in more dorsal positions than normal, possibly reflecting the change in Shh activity due to the loss of *Arl13b* (Figure 3.8H and K). Nkx2.2 expression shifted over time in both the *Arl13b*^{AE9.25} and *Arl13b*^{AE9.5} caudal neural tube, but Nkx6.1 was expanded at both E9.5 and E10.5 (Figure 3.8G', G'', H', H'', J', J'', K', and K'').

Therefore, the global neural tube pattern resembled that of wild-type embryos indicating that improperly patterned cells along the dorsal ventral axis were rescued and that Shh plays an active permissive role through most of the neural tube.

Shh activity is altered in rostral and caudal *Arl13b*^{hmn} neural tube.

Mouse mutants with defects in cilia proteins often display distinct phenotypes along the rostral-caudal axis so we examined the patterning phenotype in the rostral neural tube of *Arl13b*^{hmn} mutants (Cortellino et al., 2009; Eggenschwiler et al., 2006; Huangfu and Anderson, 2005; Qin et al., 2011; Tran et al., 2008). We found a modest, statistically significant expansion of Olig2-positive pMN cells compared to the caudal neural tube but no change in the differentiated HB9-positive motor neurons in the rostral neural tube although the expansion was not as significant as in the caudal neural tube (Figure 3.9A-D, and I). Normally, there is a steep gradient of Shh activity extending dorsally from the ventral midline that we can visualize with the *Ptch1-lacZ* reporter line (Figure 3.9E and G). The Shh activity gradient in the *Arl13b*^{hmn} rostral neural tube extended further dorsally than in wild-type, albeit not as far dorsally as in the caudal neural tube (Figure 3.9 F and H). Thus deletion of *Arl13b* alters Shh activity along the rostral-caudal axis of the *Arl13b*^{hmn} neural tube. Given that the rostral neural tube is temporally advanced compared with the caudal neural tube and that the duration of Shh signaling is known to be important for determining cell fates, the rostral *Arl13b*^{hmn} phenotype raised questions about the temporal requirement for graded Shh activity.

Rostral neural tube does not require graded Shh activity for its patterning

We examined the rostral neural tube of *Arl13b*^{ΔE9.25}, *Arl13b*^{ΔE9.5}, and *Arl13b*^{ΔE10.5} embryos to determine whether cells in the rostral neural tube are sensitive to shifts in Shh activity, or whether they require maintenance of a graded Shh response for their normal specification and differentiation. We observed normal patterning in all three inducible deletions at all time points (Figure 3.10). We have shown that there is a specific time window when cells are sensitive to changes in Shh activity in the caudal neural tube, it is possible that cells are no longer sensitive to shifts of Shh activity level in the rostral neural tube by the time we examined the patterning. This result also suggests that Shh is mainly a permissive signal rostrally, a normal neural pattern can be achieved in the presence of ungraded Shh activity.

3.4 Discussion

Cells in the caudal neural tube are sensitive to shifts in Shh activity level for a discrete time window

Our genetic studies dissect the temporal requirement for graded Shh activity in neural tube patterning and suggest a plausible mechanism behind the robustness of maintaining neural tube patterning, as they argue that Shh shifts from an instructive morphogen to a permissive signal around E9.25 in the mouse. This shift corresponds to the time during which naïve cells in the neuroepithelium are specified and points to these cells being committed at E10.5. Furthermore, we found the gradient of Shh activity normally dissipates over time, indicating that cell fates in E12.5 wild-type embryos do not correlate with the Shh activity gradient as they do at E9.5.

Our comparison of the germline null *Arl13b*^{hmn} embryos to the *Arl13b*^{AE9.25} and *Arl13b*^{AE9.5} embryos underscores the critical role of the initial Shh activity gradient in the mammalian neural tube (Figure 3.11). At E12.5, abnormal patterning persists in *Arl13b*^{hmn} mutants, while patterning recovers to wild-type in *Arl13b*^{AE9.25} and *Arl13b*^{AE9.5} embryos, suggesting that the initial establishment of the Shh activity gradient in *Arl13b*^{AE9.25} and *Arl13b*^{AE9.5} embryos provides the instructive signals that guide each cell's ultimate fate (Figure 3.11). This is in keeping with the prevailing view of Shh as an instructive morphogen.

The permissive role of Shh signaling in patterning

Earlier evidence has hinted at a permissive role for Shh signaling *in vivo*. For instance, when mutations that abolish Shh signaling are combined with mutations in genes that normally repress the pathway, some ventral cell fates are rescued (Eggenchwiler et al., 2001; Litingtung and Chiang, 2000; Persson et al., 2002; Wijgerde et al., 2002); however, the patterning that is seen in *Shh Gli3*, *Smo Gli3*, or *Shh Rab23* double mutants is not the same as wild-type indicating that derepressing the pathway alone is not sufficient to specify the diversity of cell fates in the neural tube.

The shift of Shh activity from an instructive to a permissive role raises several important questions. First, how does a cell that is inappropriately specified at E10.5 “remember” the instructive signal it received prior to *Arl13b* deletion? Second, does the permissive role Shh activity plays demand the regulation of GliR, the presence of GliA, or a combination of the two? Finally, and most fundamentally, what are the other pathways that require Shh signaling to pattern the neural tube?

The recovery of patterning we see in the embryos is complete; the cells outside the normal pMN domain that express Olig2 at E9.5 switch to expressing the markers of the adjacent dorsal and ventral domains. Since *Arl13b* is deleted in all cells, properly patterned cells are not arising from proliferating wild-type cells; however, since no recovery takes place in *Arl13b^{hmn}* mutants, the cells that are mis-patterned at E9.5 in *Arl13b^{AE9.25}* and *Arl13b^{AE9.5}* embryos clearly experienced the initial Shh activity gradient. This interpretation suggests that the few stray Olig2+ cells that are evident in the neural tubes of E12.5 *Arl13b^{AE9.25}* but not E12.5 *Arl13b^{AE9.5}* mutants likely represent cells that deleted *Arl13b* prior to responding to the Shh morphogen (Figure 3.6K and L). Shh signaling activates a distinct transcriptional repertoire of transcription factors in the five ventral cell types, and a gene regulatory network among these genes helps to establish and maintain the tight regulation of the domains (Briscoe et al., 1999; Ericson et al., 1997b; Novitch et al., 2001; Sander et al., 2000; Vallstedt et al., 2001). The documented collaboration among transcription factors and external signals in the dorsal spinal cord to recruit epigenetic marks could be responsible for the cellular memory we observe (Lee et al., 2009).

The dorsal and ventral expansion of Olig2-positive cells in *Arl13b^{AE9.25}* and *Arl13b^{AE9.5}* mutants but not in *Arl13b^{AE10.5}* mutants argues that neural progenitors are transiently competent to respond to both increases (dorsal expansion) and decreases (ventral expansion) in the ratio of Gli activator to repressor. While the cells are subsequently insensitive to shifts in the level of Shh activity, our data show that they remain specified when Shh signaling continues. The relative roles of Gli activator and repressor when Shh signaling switches to become a permissive signal remain to be

clarified. Since the absence of *Arl13b* permits normal Gli3 repressor function and constitutive low-level Gli2 activator (Casparly et al., 2007), it is possible that the permissive role of Shh signaling in the ventral neural tube is mediated either by the absence of repressor or by the presence of activator, or by a combination of the two.

The loss of neural cell fates in the *Shh* conditional mice could be explained simply by the accumulation of Gli repressor in the absence of ligand (Dessaud et al., 2010). In mouse mutants lacking proteins of the anterograde IFT machinery, full-length Gli proteins are not processed to the repressor form or modified to be bone fide activators, resulting in an absence of ventral cell fates (Houde et al., 2006; Huangfu and Anderson, 2005; Huangfu et al., 2003; Liu et al., 2005; Tran et al., 2008). In contrast, *Gli2 Gli3* double mutants lack all Gli protein and ventral-most fates but specify motor neurons (Bai et al., 2004; Lei et al., 2004; Motoyama et al., 2003). Although genetic analysis in the IFT mutants demonstrated an absence of Gli activator or repressor function, the discrepancy in phenotype when compared with the mutants that actually lack all Gli production indicates a functional distinction. The *Gli2 Gli3* double mutant phenotype indicates that cell fates like motor neurons can develop in the absence of Gli activator, at least when Gli repressor is absent (Bai et al., 2004; Lei et al., 2004; Motoyama et al., 2003). This suggests that although Gli activator is present in the absence of *Arl13b*, it may be the proper regulation of GliR that is responsible for the recovery of patterning we see in the *Arl13b*^{AE9.25} and *Arl13b*^{AE9.5} embryos.

Most of the pathways known to play patterning roles in the neural tube, including bone morphogenetic protein (BMP), Wingless (Wnt), and retinoic acid, interact with Shh signaling (Nishi et al., 2009). Retinoic acid signaling from the paraxial mesoderm works

with Shh signaling to specify ventral progenitors (Novitch et al., 2003; Pierani et al., 1999; Wichterle et al., 2002). A BMP activity gradient reciprocal to the Shh activity gradient is mediated by the expression of BMP antagonists in the ventral neural tube (Liem et al., 2000; McMahon et al., 1998; Patten and Placzek, 2002). In fact, BMPs could be providing the instructive cues as in chick, where graded BMP signaling is capable of eliciting all ventral cell fates in the presence of Shh signaling (Mizutani et al., 2006). BMPs and Wnts are expressed at the dorsal midline of the neural tube and are needed for specifying dorsal progenitors (Chesnutt et al., 2004; Lee et al., 2000; Lee et al., 1998; Liem et al., 1997; Liem et al., 1995; Muroyama et al., 2002; Parr et al., 1993; Timmer et al., 2002; Wine-Lee et al., 2004; Zechner et al., 2007). Shh signaling interacts with both the Wnt and BMP pathways; Wnts directly regulate GliR, and Gli3 activity can regulate canonical Wnt signaling (Alvarez-Medina et al., 2008; Ulloa et al., 2007; Yu et al., 2008). Furthermore, Wnt signaling regulates ventral neural fates through Gli3 in a time-dependent manner (Yu et al., 2008). Effectors of both BMP and Wnt signaling interact with Gli3 repressor (Liu et al., 1998; Meyer and Roelink, 2003; Ulloa et al., 2007). The observation that Gli3 repressor expression is normal in the absence of Arl13b suggests that Gli3 repressor could interact normally with these pathways, making them reasonable candidates to explain the recovery of patterning we observe.

Our findings clarify the role of Shh signaling in neural patterning during development (Figure 3.12). Our understanding of Shh as a morphogen has evolved from a linear concentration-dependent model to a temporal adaptation model. Our data uncover a novel mechanism of adaptation over time and show that Shh shifts from an instructive

to a permissive signal, revealing a fundamental second mechanism through which Shh signaling functions to properly specify cell fates in the mammalian spinal cord.

This chapter has been submitted to PLoS Biology by Chen-Ying Su, Michael J. Hillman, and Tamara Caspary.

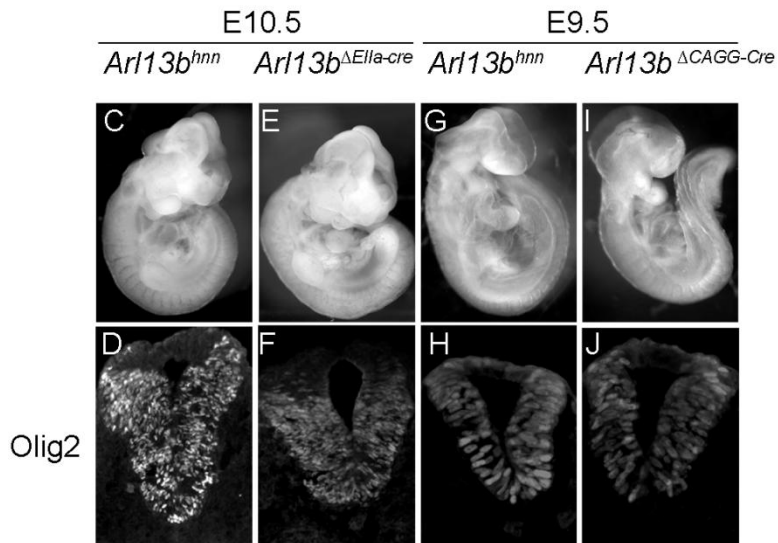
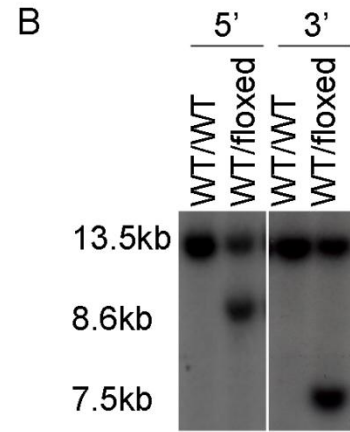
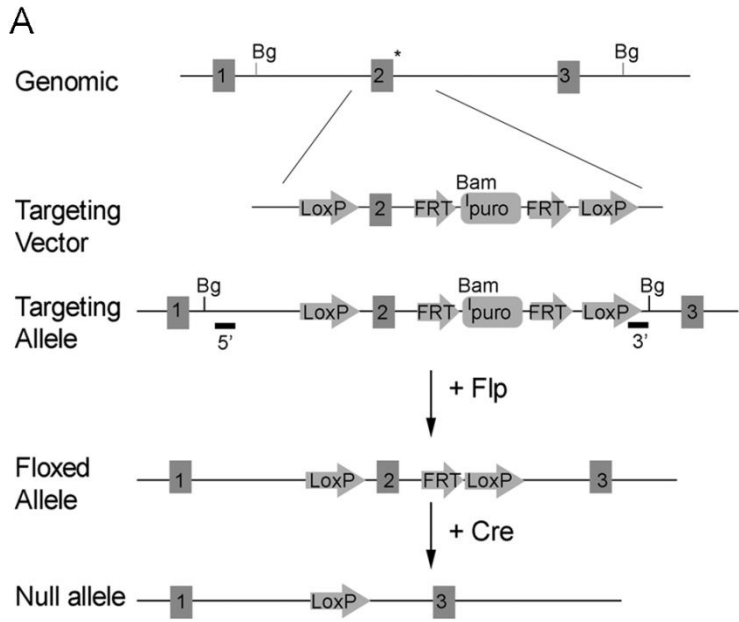


Figure 3.1 The generation of a conditional *Arl13b* allele. **(A)** Schematic figure shows that exon 2 of the wild-type *Arl13b* locus is flanked by LoxP sites with a puromycin-resistant cassette. The mutation (*) disrupts the splice site of exon 2 of *Arl13b* in *Arl13b^{hmn}*. A puromycin-resistant cassette is removed by *Flp* recombinase, and exon 2 can be deleted upon *Cre* recombination. Genomic DNA is digested with BglIII (Bg) and BamHI (Bam) and probed with two unique external probes (black bars) to confirm homologous targeting. **(B)** The targeted locus creates a BamHI site that reduces a 13.5-kb BglIII fragment into one 8.6-kb and one 7.5-kb fragment that can be detected by unique 5' and 3' external probes, respectively. **(C - F)** When *Arl13b* is deleted by a germline-expressed *Ella-Cre*, E10.5 *Arl13b^{ΔElla-Cre/hmn}* embryo shows exencephaly (E) and an expansion of Olig2 cells (F) that are identical to *Arl13b^{hmn}* (C and D). **(G - J)** When a high dose of tamoxifen is injected at E6.5, *Arl13b^{ΔCAGG-Cre}* can recapitulate the null phenotype by embryo morphology (G and I) and the expansion of Olig2 cells (H and J) at E9.5.

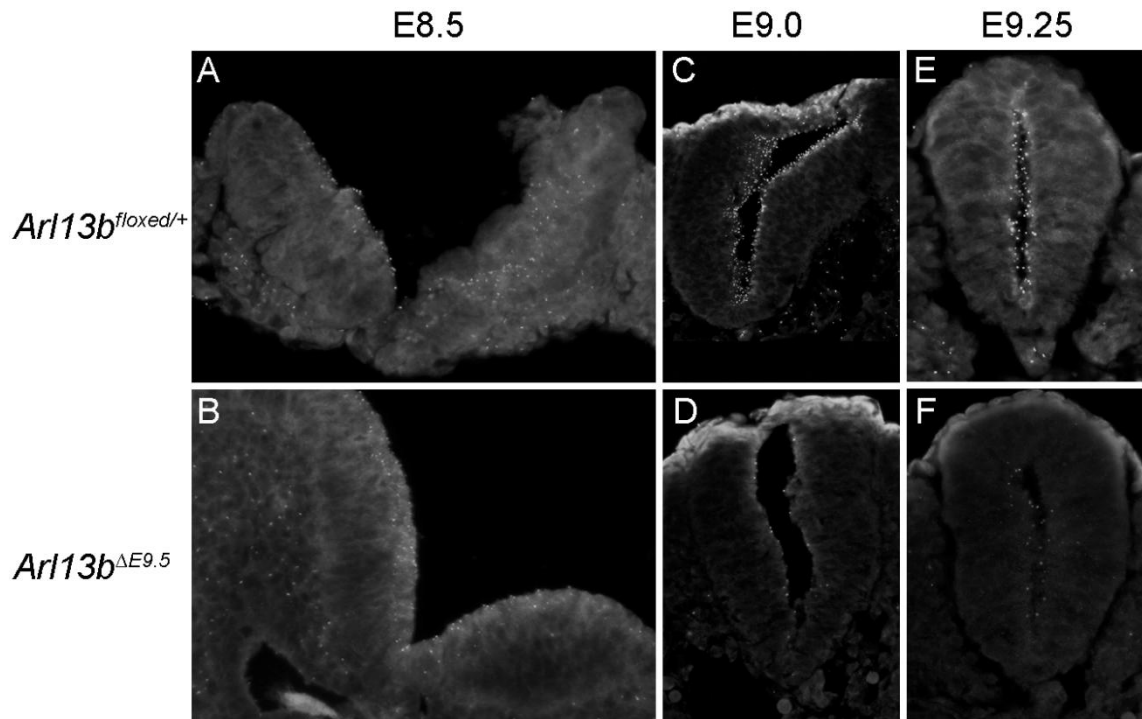
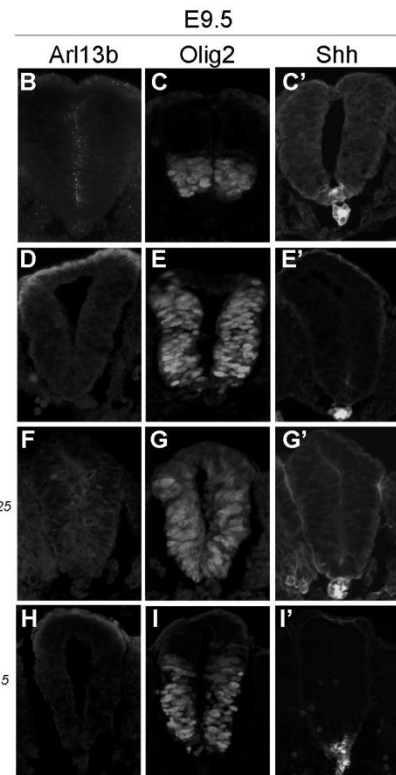
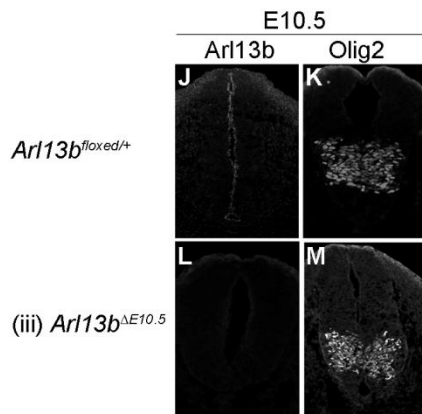
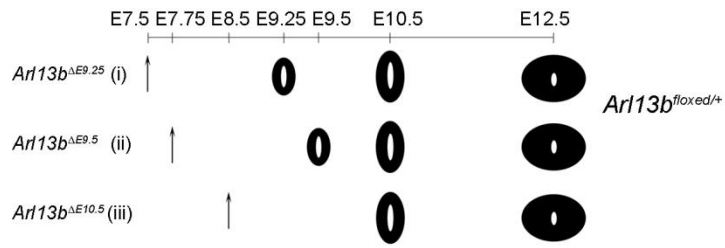


Figure 3.2 The rate of Arl13b protein turnover *in vivo*. **(A-B)** Arl13b can be detected in all the cilia at E8.5 in *Arl13b^{floxed/+}* (A) while some cells do not have Arl13b in *Arl13b^{ΔE9.5}* (B). **(C-F)** The expression of Arl13b can be observed along the ventricular zone in *Arl13b^{floxed/+}* at E9.0 (C) and E9.25 (E). However, there is a dramatic decrease of Arl13b expression in *Arl13b^{ΔE9.5}* at both stages (D-F).

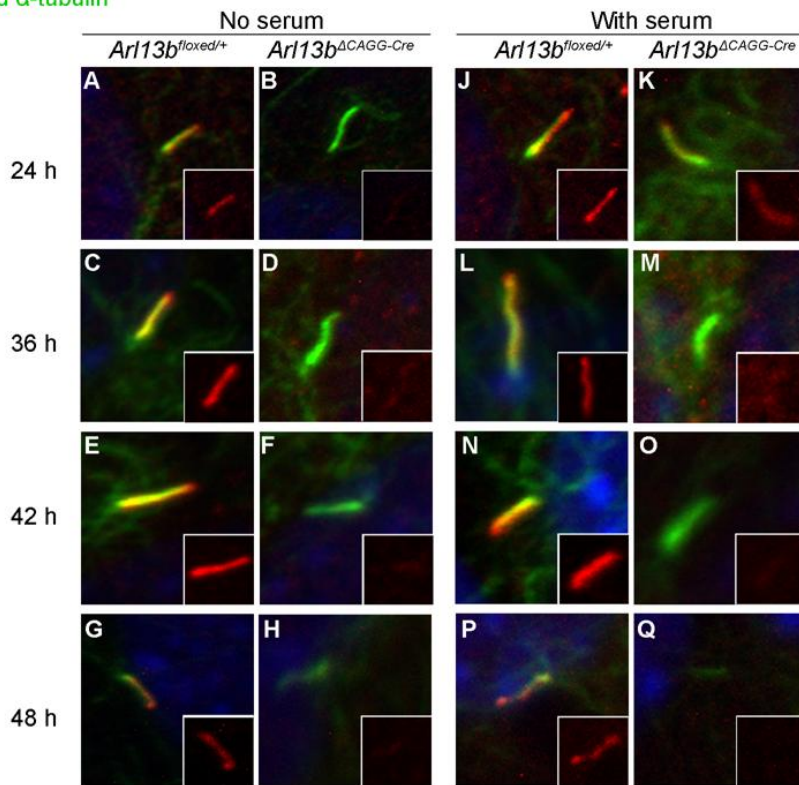
A Injection schematic diagram



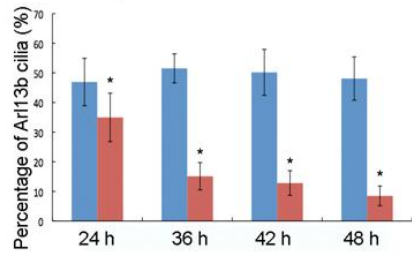
Su Figure 1

Figure 3.3 Temporal deletion of *Arl13b* results in different neural tube patterning. **(A)** Experimental design of tamoxifen injection for deleting *Arl13b*. (i-iii). A high dose (solid arrow) of tamoxifen is injected at E7.5 (i), E7.75 (ii), or E8.5 (iii), and embryos are collected at E9.5, E10.5, or E12.5 to examine neural tube patterning. Black neural tube represents ubiquitous *Arl13b* deletion based on immunofluorescence with Arl13b antibody. **(B, D, F, and H)** Arl13b expression can be observed in the ventricular zone of E9.5 *Arl13b^{flxed/+}* caudal neural tube (D), but not in E9.5 *Arl13b^{hmn}* (D), *Arl13b^{ΔE9.25}* (F), or *Arl13b^{ΔE9.5}* (H). **(C, E, G, and I)** Olig2 cells are specified in a restricted domain in E9.5 *Arl13b^{flxed/+}* (C), but are expanded in *Arl13b^{hmn}* (E), *Arl13b^{ΔE9.25}* (G) and *Arl13b^{ΔE9.5}* (I) caudal neural tube. **(C', E', G', and I')** Shh is expressed in the notochord and floor plate in both E9.5 *Arl13b^{flxed/+}* and *Arl13b^{ΔE9.5}* (C' and I'). Shh is only observed in the notochord in *Arl13b^{hmn}* and *Arl13b^{ΔE9.25}* (E' and G'). **(J and L)** Arl13b is expressed in the ventricular zone of E10.5 *Arl13b^{flxed/+}* caudal neural tube (J), but is absent in *Arl13b^{ΔE10.5}* (L). **(K and M)** Olig2 cells are specified in their restricted domain in both *Arl13b^{flxed/+}* (K) and *Arl13b^{ΔE10.5}* (M).

Acetylated α -tubulin
Arl13b



I Arl13b expression in serum-free condition



R Arl13b expression in serum-containing condition

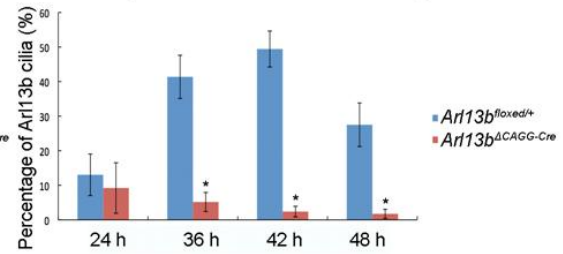
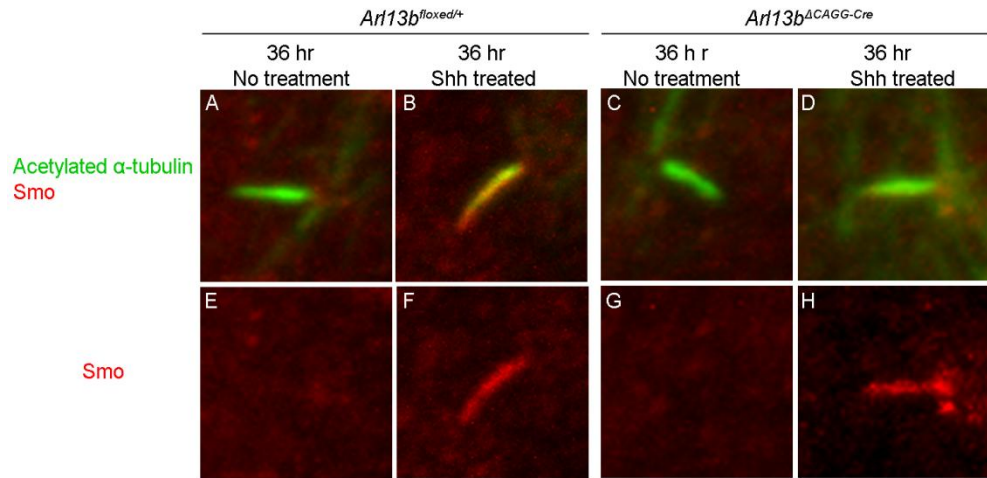
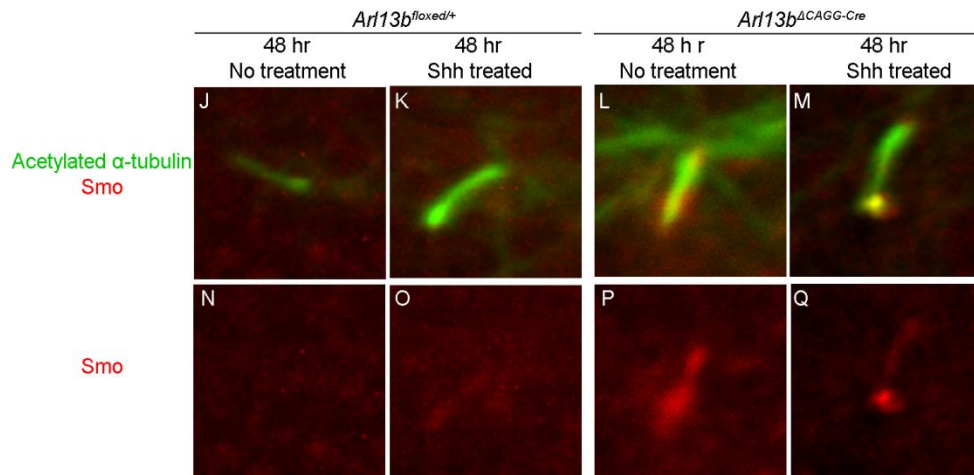
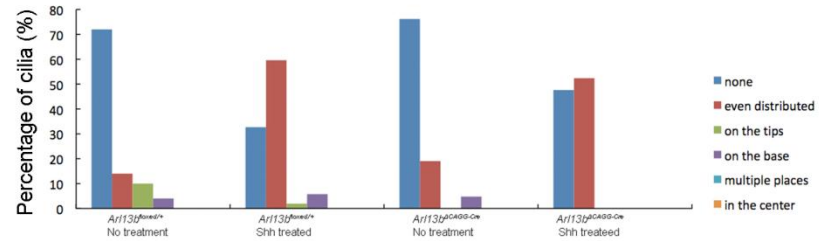


Figure 3.4 The kinetics of Arl13b protein deletion in conditional Arl13b knockout MEFs is similar to *in vivo*. **(A-I)** Arl13b (red) is localized in the cilium, stained by acetylated α -tubulin (green), in control MEFs under serum-free condition (A, C, E, and G). Arl13b expression in *Arl13b*^{ΔCAGG-Cre} MEFs is hardly detected after tamoxifen treatment for 24 (B), 36 (D), 42 (F), and 48 (H) hours in serum-lacking condition. The small insets show Arl13b staining alone. Quantification of Arl13b-expressing cells in *Arl13b*^{flxed/+} (blue) and *Arl13b*^{ΔCAGG-Cre} (purple) shows in I. **(J-R)** Arl13b (red) is co-localized with acetylated α -tubulin (green) in control MEFs under serum-containing condition (J, L, N, and P). The decrease of Arl13b expression is more dramatically in *Arl13b*^{ΔCAGG-Cre} MEFs that are cultured in serum-containing media for 24-48 hours after adding tamoxifen (K, M, O, and Q). R shows quantitative result of Arl13b expression in control (blue) and *Arl13b*^{ΔCAGG-Cre} (purple) MEFs.



I Smo localization in cilia



R Smo localization in cilia

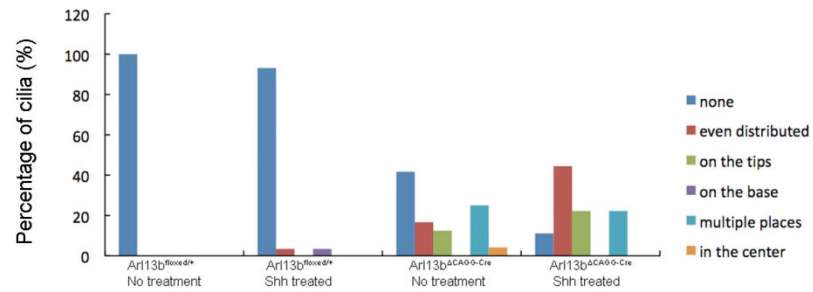
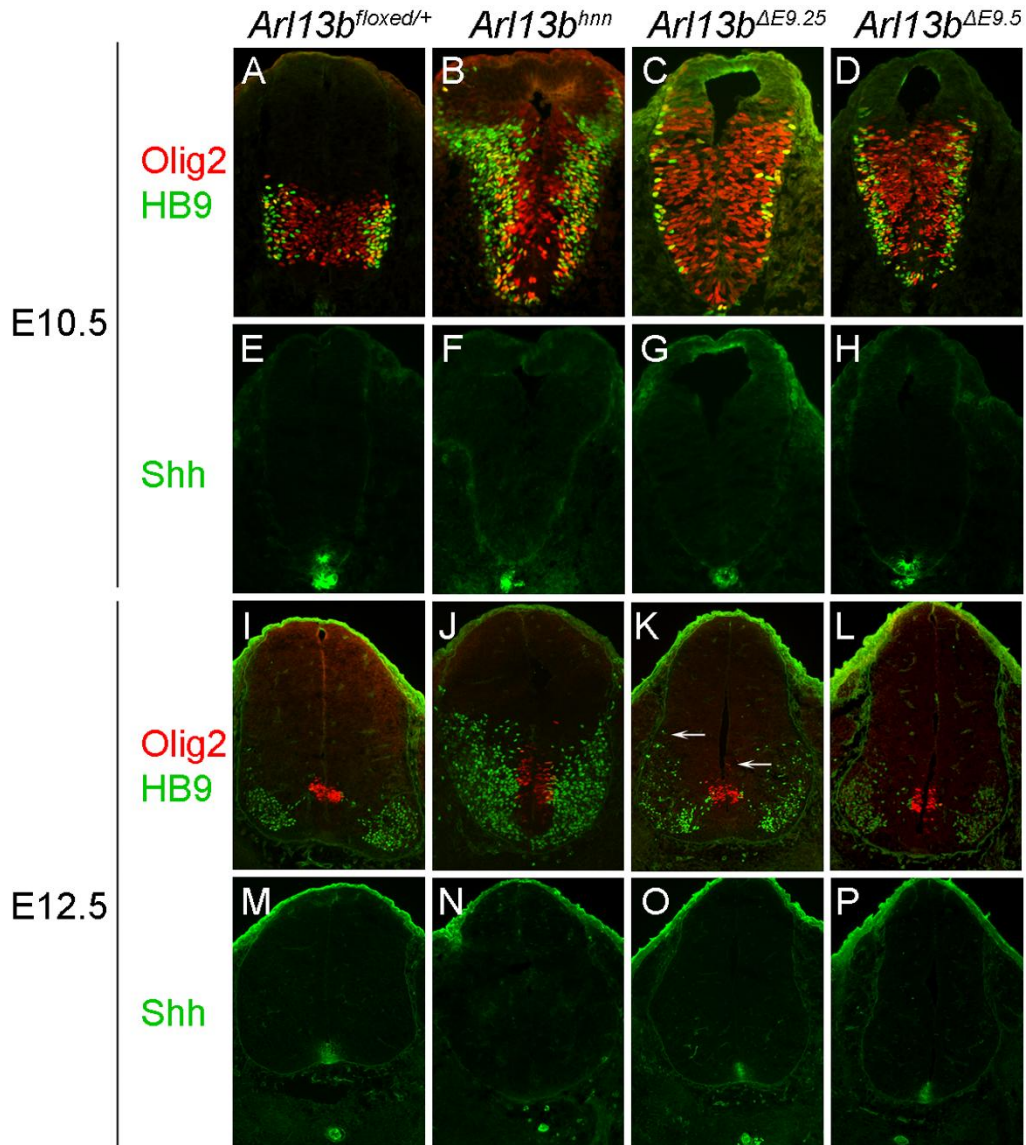


Figure 3.5 The localization of Smo in MEFs. **(A-H)** Confocal images of Smo (red) expression in the cilium that is marked by acetylated α -tubulin (green) in control *Ar113b*^{flxed/+} (A-D) or *Ar113b*^{ACAGG-Cre} (E and H) MEFs after cells have been treated with tamoxifen for 36 hours in the absence of Shh conditioned media (A,B, E, and F) or in the presence of Shh stimulation (C,D, G, and H). **(I)** A chart shows that Smo localization in *Ar113b*^{ACAGG-Cre} is similar to in *Ar113b*^{flxed/+}. **(J-Q)** After treating *Ar113b*^{flxed/+} MEFs with Shh conditioned media for 48 hours, Smo is no longer to respond thus there is no cilium localization of Smo (J-M). In contrast, Smo is localized in *Ar113b*^{ACAGG-Cre} cilia and enriched on the tip when Ar113b is deleted even without Shh stimulation (N and O). Smo is even enriched in the cilia upon Shh stimulation in *Ar113b*^{ACAGG-Cre} at 48 hour time point (P and Q). **(R)** A graph displays various Smo locations in *Ar113b*^{ACAGG-Cre} cilia.



Q E12.5 caudal neural tube

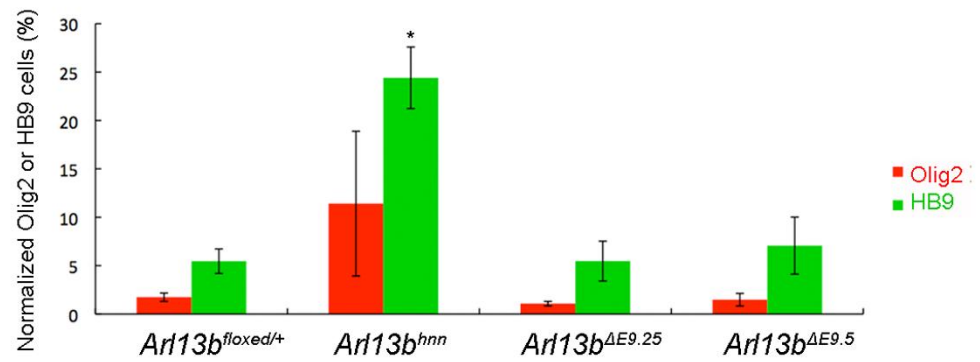


Figure 3.6 The pMN expansion is restored over time when *Arl13b* is deleted by E9.25 and E9.5. **(A-D)** Olig2 (red) and HB9 (green) cells are expressed in the pMN domain of *Arl13b^{floxexd/+}* at E10.5 (A), but are expanded in *Arl13b^{hmn}* (B), *Arl13b^{AE9.25}* (C), and *Arl13b^{AE9.5}* (D). **(E-H)** Shh (green) is expressed in the notochord and the floor plate in E10.5 *Arl13b^{floxexd/+}* (E) and *Arl13b^{AE9.5}* (H), but only in the notochord of *Arl13b^{hmn}* (F) and *Arl13b^{AE9.25}* (G). **(I-L)** At E12.5, there is normal Olig2 (red) and HB9 (green) expression in *Arl13b^{floxexd/+}* (I) and *Arl13b^{AE9.5}* (L), while there is an expansion in *Arl13b^{hmn}* caudal neural tube (J). Olig2 and HB9 cells are mainly in their correct domains in *Arl13b^{AE9.25}*, except there are some dorsally expressed Olig2 and HB9 cells (K and white arrows). **(M-P)** In *Arl13b^{floxexd/+}* (M), *Arl13b^{AE9.25}* (O), and *Arl13b^{AE9.5}* (P) caudal neural tube, Shh is expressed in the notochord and floor plate at E12.5, while it is only expressed in the notochord of *Arl13b^{hmn}* neural tube (N). **(Q)** Quantitative result shows that there is no increase of Olig2 (red) and HB9 (green) cells in E12.5 *Arl13b^{AE9.25}* and *Arl13b^{AE9.5}* caudal neural tube compared to *Arl13b^{floxexd/+}*. Both Olig2 and HB9 cells are still expressed excessively in E12.5 *Arl13b^{hmn}*.

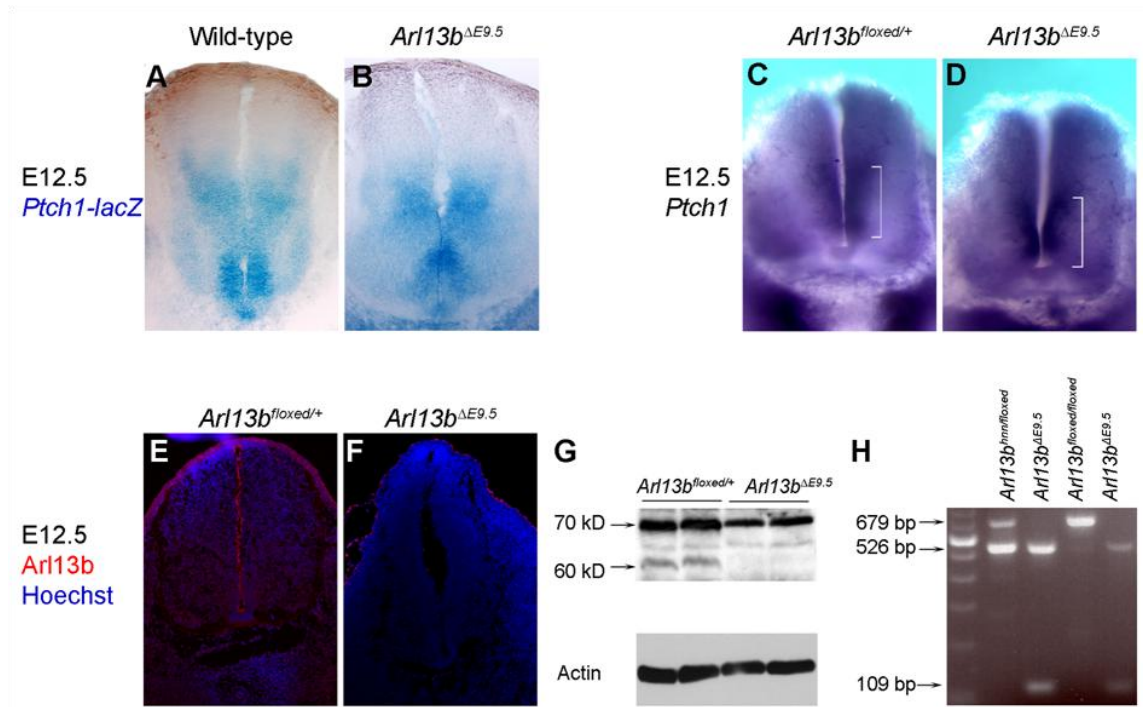


Figure 3.7 Rescue of patterning at E12.5 is not due to reactivation of Shh activity or incomplete deletion of *Arl13b*. (A, B) *Ptch1-lacZ* is uniformly expressed in E12.5 wild-type (A) and *Arl13b*^{ΔE9.5} (B) ventral neural tube. (C, D) *Ptch1* mRNA is expressed along the ventricular zone of E12.5 *Arl13b*^{flxed/+} (C) and *Arl13b*^{ΔE9.5} (D) ventral neural tubes. White bracket indicates a strong expression of *Ptch1*. (E, F) *Arl13b* (red) is expressed in cilia of *Arl13b*^{flxed/+} (F), but is absent from *Arl13b*^{ΔE9.5} (E) at E12.5. Hoechst (blue) stains nuclei. (G) Western blot shows the absence of a 60-kD *Arl13b* band in *Arl13b*^{ΔE9.5}. (H) PCR shows there is no conditional *Arl13b* allele DNA (679 bp), while a deleted band (109 bp) can be detected in *Arl13b*^{ΔE9.5}. A 526-bp band indicates the endogenous *Arl13b*^{hnn} allele.

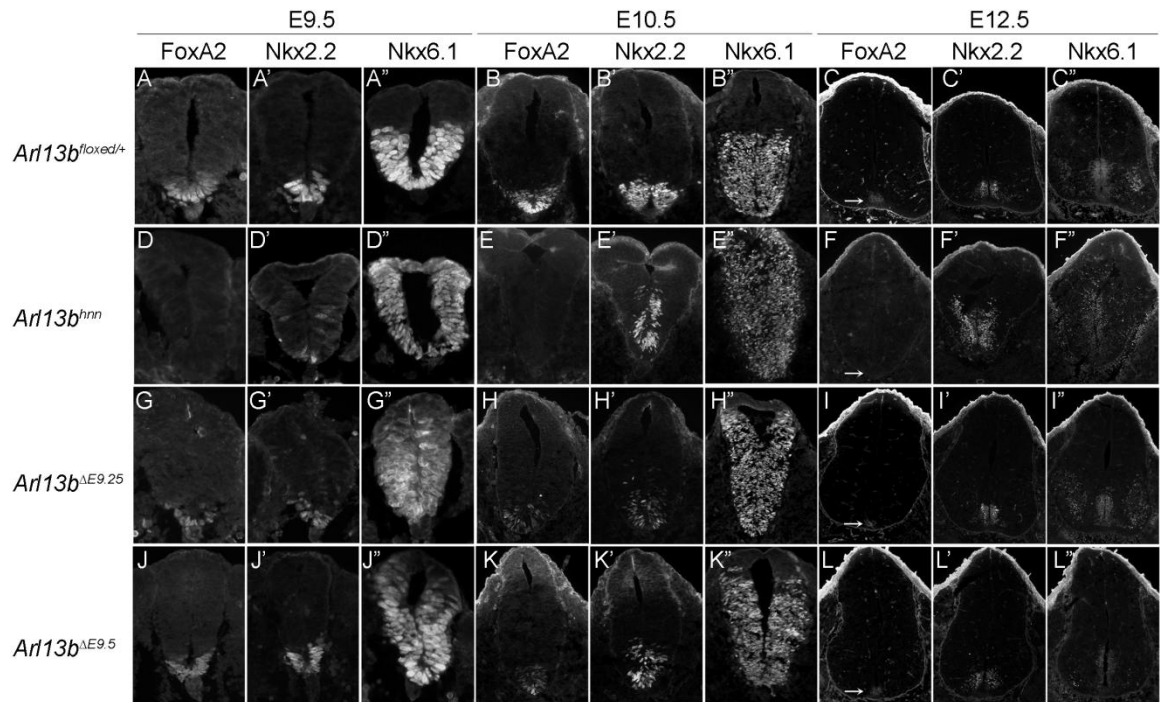


Figure 3.8 The expression of the floor plate and p3 progenitors in different conditional *Arl13b* knockout caudal neural tubes. **(A-C, A'-C', and A''-C'')** FoxA2 is expressed in the floor plate, Nkx2.2 is specified in the p3 domain while Nkx6.1 is restricted in the whole ventral neural tube in *Arl13b^{floxed/+}* at E9.5 (A, A', A''), E10.5 (B, B', B''), and E12.5 (C, C', C''). White arrow in C indicates FoxA2-expressing cells. **(D-F, D'-F', D''-F'')** FoxA2 is absent in *Arl13b^{hmn}* at E9.5 (D), E10.5 (E), and E12.5 (F), while Nkx2.2 is expanded dorsally in all three developmental stages (D'-F'). Nkx6.1 is specified in the whole neural tube at E9.5 (D'') and E10.5 (E''), and specified in the whole ventricular zone at E12.5 (F''). White arrow in F indicates the region that should be the floor plate. **(G-L, G'-L', G''-L'')** Both FoxA2 and Nkx2.2 cells are expanded dorsally in *Arl13b^{AE9.25}* and *Arl13b^{AE9.5}* at E9.5 (G, J, G', and J') and E10.5 (H, K, H', and K'). FoxA2 is restored at E12.5 in *Arl13b^{AE9.25}* and *Arl13b^{AE9.5}* at E12.5 (I and L). Nkx2.2 is expressed normally in both *Arl13b^{AE9.25}* and *Arl13b^{AE9.5}* (I' and L'). Nkx6.1 is expanded to the dorsal quarter of neural tube at E9.5 and E10.5 (G'', J'', H'', and K''), but restricted in the ventral ventricular zone at E12.5 (I'' and L''). Nkx6.1 expression in motor neurons is similar to control in E12.5 *Arl13b^{AE9.25}* (I'') while fewer motor neurons express Nkx6.1 in *Arl13b^{AE9.5}* (L''). White arrows in I and L shows FoxA2-expressing cells.

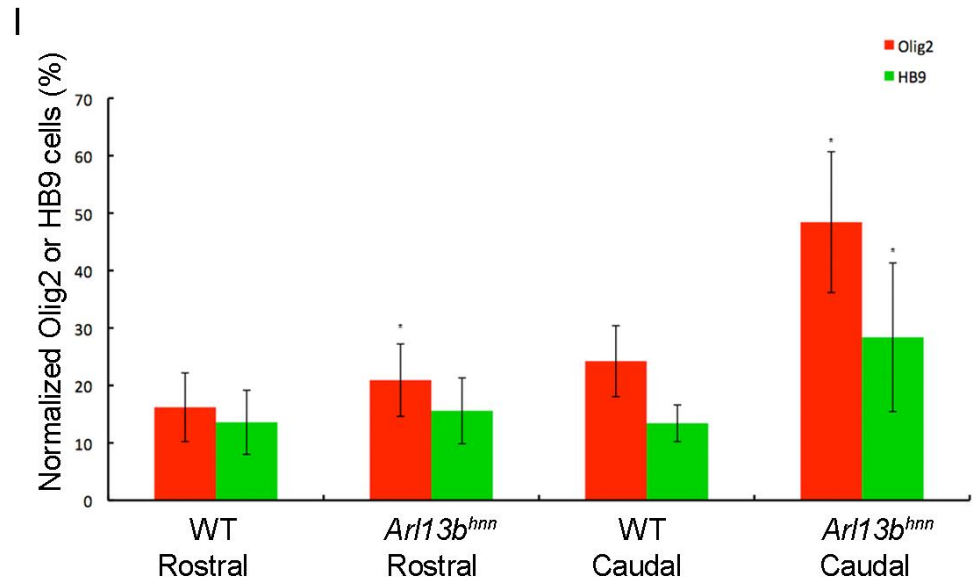
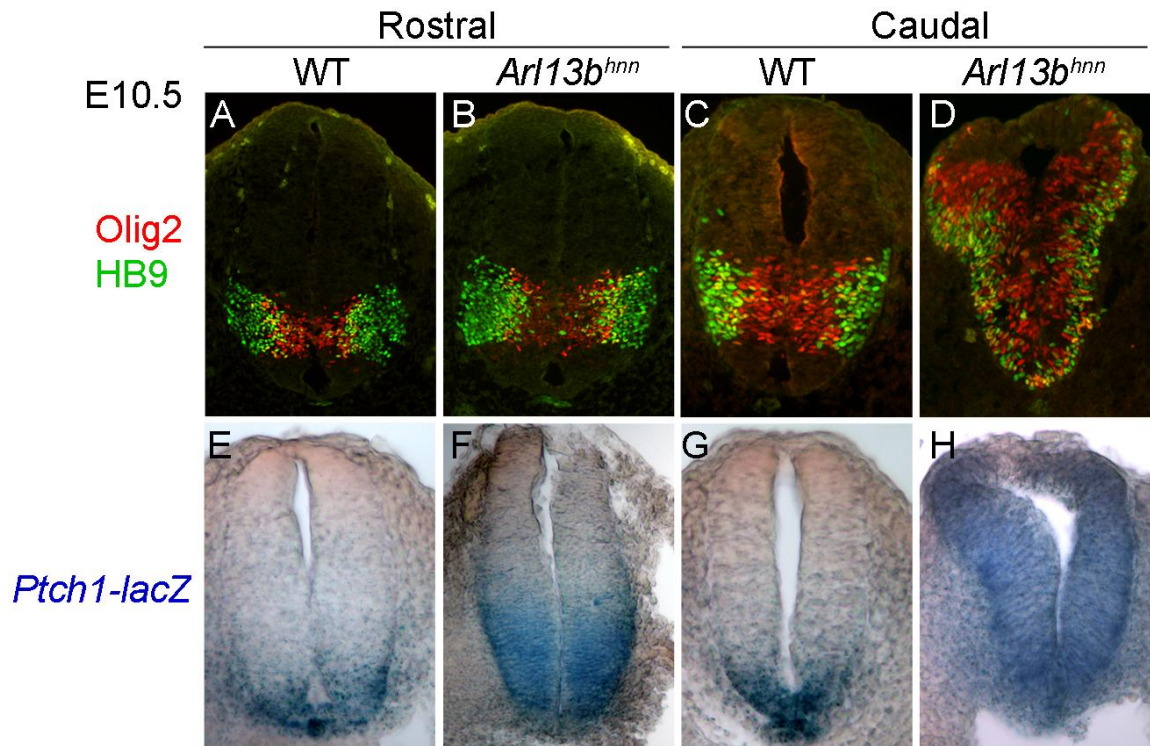


Figure 3.9 Abnormal Shh activity gradient results in distinct patterning in the *Ar13b^{hmn}* rostral and caudal neural tube. **(A, C, E, G)** E10.5 wild-type rostral (A and E) and caudal (C and G) neural tube shows Olig2 (red) and HB9 (green) cells in the pMN domain (A and C). Expression of *Ptch1-lacZ* displays a ventral-to-dorsal gradient of β -galactosidase activity (E and G). **(B, D, F, H)** E10.5 *Ar13b^{hmn}* rostral (B and F) and caudal (D and H) neural tube displays a uniform intermediate level of *Ptch1-lacZ* expression (F and H). *Ar13b^{hmn}* rostral neural tube shows a slight expansion of Olig2 but not HB9 (B), while there is a dramatic expansion of Olig2 and HB9 cells caudally (D). **(I)** A quantitative result shows normalized Olig2 (red) and HB9 (green) cells in wild-type and *Ar13b^{hmn}* along the rostral-caudal axis. The normalized result of *Ar13b^{hmn}* is compared to wild-type at the same axial level, and * indicates a significant difference when $p < 0.05$.

Figure 3.10 Rostral neural tube displays normal patterning in all conditional *Arl13b* knockout mutants. **(A, D, and G)** Olig2 (red) cells are specified in the pMN domain in *Arl13b^{flxed/+}* (A), *Arl13b^{ΔE9.25}* (D), and *Arl13b^{ΔE9.5}* (G) rostral neural tube at E9.5. **(B-C, E-F, H-I, and J-K)** Both Olig2 (red) and HB9 (green) cells are expressed normally at E10.5 or E12.5 in *Arl13b^{flxed/+}* (B and C), *Arl13b^{ΔE9.25}* (E and F), *Arl13b^{ΔE9.5}* (H and I), and *Arl13b^{ΔE10.5}* (J and K) rostral neural tube. **(L and M)** Quantitative analysis indicates that the percentage of Olig2 or HB9 cells in the rostral neural tube of *Arl13b^{ΔE9.25}*, *Arl13b^{ΔE9.5}*, and *Arl13b^{ΔE10.5}* is similar to it in control *Arl13b^{flxed/+}* at E10.5 (L) and at E12.5 (M).

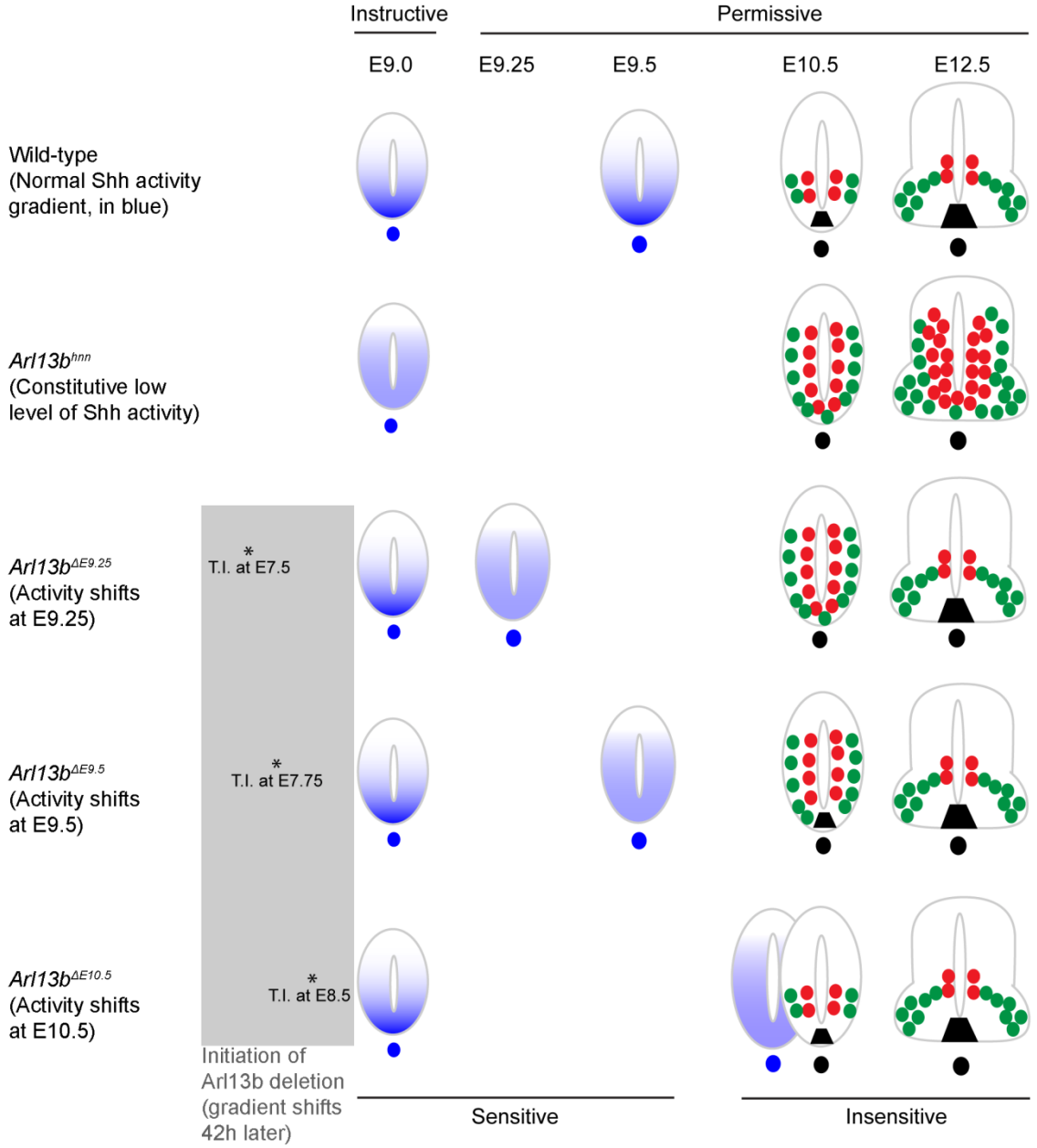


Figure 3.11 Summary of phenotypic analyses. In wild-type neural tube, Shh activity gradient is established normally at E9.0 and normal patterning is observed at E10.5 and E12.5. In *Arll3b^{hmn}*, there is a constitutive low level of Shh activity resulting in an expansion of pMN cells and motor neurons that persist to E12.5. In *Arll3b^{ΔE9.25}* and *Arll3b^{ΔE9.5}*, normal Shh activity gradient is established initially but disrupted at E9.25 and E9.5, respectively. An expansion of pMN cells and motor neurons is detected in E10.5 *Arll3b^{ΔE9.25}* and *Arll3b^{ΔE9.5}*, but both pMN cells and motor neurons are expressed normally at E12.5. In *Arll3b^{ΔE10.5}*, Shh activity gradient is disrupted at E10.5 but patterning is normal suggesting that cells are no longer sensitive to changes in Shh activity after E10.5. Lines on the top indicate Shh plays an instructive role at E9.0, and switches to become a permissive signal after E9.25. Asterisk represents the time point when tamoxifen is injected to pregnant females. Blue shading demonstrates Shh activity. In E10.5 and E12.5 neural tube, red and green circles represent cell fates that are resulting from Shh activity. Red circles are pMN cells, green circles are motor neurons, and black trapezoid is the floor plate. T.I., tamoxifen injection.

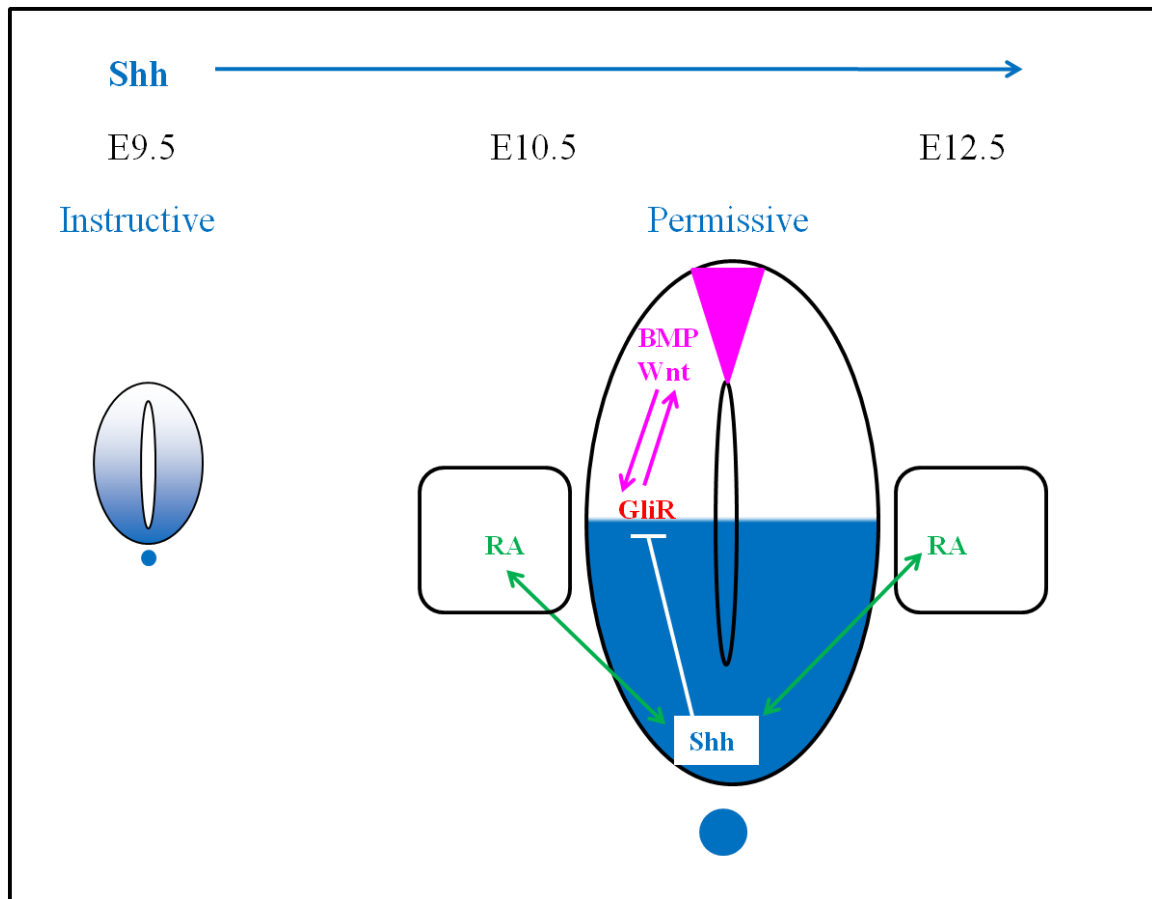


Figure 3.12 The timeframe for the role of Shh in neural tube patterning. There is a Shh activity gradient (blue shading) at E9.5, and cells are specified into distinct progenitors depending on concentration and duration of Shh signaling they receive. Shh then switches to become a permissive signal, and interact with BMP, Wnt, and RA signaling for maintaining a proper neural pattern. Therefore, the gradient of Shh activity does not need to be maintained but Shh needs to be present (blue arrow on the top) once Shh is a permissive signal.

CHAPTER 4

THE ROLE OF ARL13B IN OLIGODENDROCYTE DEVELOPMENT

4.1 Summary

In *Arl13b^{hmn}* embryos, there is no specification of oligodendrocyte precursors (OLPs) before the embryos die. Both motor neurons and OLPs are derived from pMN cells, and we observed an expansion of pMN cells in *Arl13b^{hmn}* during neurogenesis (Casparly et al., 2007; Rowitch, 2004) (chapter 3 of this dissertation). In the simplest model, an expansion of pMN cells should result in an expansion of OLPs so their absence in *Arl13b^{hmn}* is surprising. Both Shh and PDGFR α signaling are required for OLP specification, and cilia have been implicated to be important for both signaling pathways (Fruttiger et al., 1999; Huangfu et al., 2003; Lu et al., 2000; Orentas et al., 1999; Schneider et al., 2005). Thus the absence of OLPs may be due to mis-regulation of signaling pathways resulting from defective cilia in *Arl13b^{hmn}*.

To circumvent the embryonic lethality and investigate the role of Arl13b in oligodendrocyte development, we used our conditional *Arl13b* allele and deleted Arl13b at two time points: at E8.5 with *Olig1-Cre* (*Arl13b^{AOlig1-Cre}*), and at E10.5 with *Brn4-Cre* (*Arl13b^{ABrn4-Cre}*). We found that the initial specification of OLPs was normal in both *Arl13b^{AOlig1-Cre}* and *Arl13b^{ABrn4-Cre}* embryos. However, we saw a delay in a mature oligodendrocyte marker at E16.5 in *Arl13b^{ABrn4-Cre}*. Subsequently, these mice displayed problems in moving that is consistent with defects in myelination, suggesting that Arl13b is needed for both oligodendrocyte differentiation and myelination.

4.2 Introduction

In the developing central nervous system (CNS), motor neurons (MNs) and oligodendrocytes are essential for establishing neural circuits. MNs project their axons to

connect muscles and glands to the CNS, and oligodendrocytes myelinate the axons in the CNS (Schwartz, 1991). MNs and oligodendrocytes are distinct morphologically and functionally, but they are both derived from common progenitors – pMN cells during development (Lu et al., 2002; Zhou and Anderson, 2002). In mouse, pMN cells are specified at E8.5 and differentiate as MNs starting at E9.5. At E12.5, pMN cells switch to become oligodendrocyte precursors (OLPs) that differentiate as oligodendrocytes (Rowitch, 2004). The establishment of Shh activity gradient is needed for inducing different transcriptional factors to specify distinct ventral progenitors, and a low level of Shh activity is required for specifying pMN cells that are determined by two basic helix-loop-helix (bHLH) transcriptional factors, Olig1 and Olig2 (Briscoe et al., 2000; Dessaud et al., 2007; Ericson et al., 1997b; Lu et al., 2002; Takebayashi et al., 2002; Zhou and Anderson, 2002). Olig1/2 are the earliest markers for OLPs followed by PDGFR α (Lu et al., 2000; Pringle and Richardson, 1993; Zhou et al., 2000). In *Shh* null mutants, Olig1 and Olig2 are absent and there is no oligodendrocytes indicating that Shh is necessary for oligodendrocyte development (Lu et al., 2000; Orentas et al., 1999).

Primary cilia have been implicated in many cell signaling pathways, including Shh and PDGFR α signaling (Huangfu et al., 2003; Schneider et al., 2005). Many components of Shh signaling are localized to cilia, and cilium mouse mutants disrupt Shh activity resulting in defects in ventral neural tube patterning (Corbit et al., 2005; Haycraft et al., 2005; Houde et al., 2006; Huangfu et al., 2003; Liu et al., 2005; Rohatgi et al., 2007). We have shown that mouse mutants lacking the ciliary protein, Arl13b (called *Arl13b^{hmn}*), have defects in cilium architecture resulting in a constitutive low level of Shh activation in the developing caudal neural tube (Casparly et al., 2007). An expansion of

pMN cells and MNs are observed from E9.5 to E12.5 in response to the abnormal Shh activity in *Arl13b^{hmn}*, but there are no PDGFR α -expressing OLPs present at E13.5, right before the embryos die. PDGFR α is localized to cilia, and PDGFR α signaling is important for OLP specification (Calver et al., 1998; Schneider et al., 2005). Thus it is possible that defective cilia in *Arl13b^{hmn}* results in mis-regulation of PDGFR α and failure of OLP specification.

To investigate how Arl13b plays a role in oligodendrocyte development, we deleted Arl13b at two time points: at E8.5 with *Olig1-Cre* to specifically delete Arl13b in the pMN cells thus we can examine whether the loss of Arl13b has effect on oligodendrocyte development; at E10.5, right before OLP specification with *Brn4-Cre* in the whole neural tube, thus we can specifically target Arl13b deletion on progenitors as they become OLPs. In order to compare results of these two conditional deletions better, I will present the results according to different stages of oligodendrocyte development: specification, differentiation, and movement observation in animals.

4.3 Results

Arl13b is not needed for OLP specification

The *Arl13b^{hmn}* embryos die at E14.5, and we found no PDGFR α expression at E13.5 (Figure 4.1C and D). Normally PDGFR α marks OLPs at this stage (Figure 4.1A and B), but the lack of PDGFR α expression represented a specification defect since *Arl13b^{hmn}* embryos die at E14.5. In order to explore the role of Arl13b in the oligodendrocyte lineage, we examined *Arl13b ^{Δ Olig1-Cre}* when Arl13b was deleted

specifically in pMN cells that become OLPs at E12.5. At E14.5, we found normal *Olig2* and *PDGFR α* expression (Figure 4.2A-D).

We then used *Brn4-Cre* to delete *Arl13b* in the whole neural tube at E10.5, after motor neuron differentiation but prior to OLP specification. When we examined OLP specification at E14.5, *PDGFR α* expression in *Arl13b ^{Δ Brn4-Cre}* was similar to control as well as at E16.5 (Figure 4.3A-D). No matter *Arl13b* is deleted specifically in oligodendrocyte lineage or ubiquitously prior to specification of OLPs, we observed normal OLP expression suggesting that *Arl13b* is not needed for specifying OLPs.

The absence of *Arl13b* in the CNS affects oligodendrocyte differentiation

We next tested whether oligodendrocyte differentiation was affected in *Arl13b ^{Δ Olig1-Cre}* embryos, and we used myelin basic protein (MBP) as a marker for mature oligodendrocytes. We could observe MBP near ventricular zone at E16.5, and more MBP expression in both ventral and lateral neural tube at E18.5 in *Arl13b^{flxed/+}* (Figure 4.3G and K). In *Arl13b ^{Δ Olig1-Cre}* embryos, MBP expression was normal at E18.5 suggesting that deleting *Arl13b* in oligodendrocyte lineage does not affect oligodendrocyte differentiation (Figure 4.2E and F).

We then examined whether oligodendrocyte differentiation is affected when *Arl13b* is deleted in the whole neural tube, and found that there was no MBP expression in E16.5 *Arl13b ^{Δ Brn4-Cre}* embryos (Figure 4.3G and H). By E18.5, MBP could be detected suggesting there is a delay in oligodendrocyte differentiation when *Arl13b* is deleted in the CNS at E10.5 (Figure 4.3K and L).

Mice show defects in movement when *Arl13b* is deleted in CNS

We found both *Arl13b* ^{Δ Olig1-Cre} and *Arl13b* ^{Δ Brn4-Cre} mice survived after birth.

Arl13b ^{Δ Olig1-Cre} animals were indistinguishable from their littermates. On the other hand, *Arl13b* ^{Δ Brn4-Cre} mice were small compared to their control littermates. *Arl13b* ^{Δ Brn4-Cre} mice also showed defects in movement, and died between postnatal day 20 and 42. These phenotypes were not completely penetrant as only about half (8/15) the animals had them. Movement problems could be consistent with defects in myelination, thus myelination in *Arl13b* ^{Δ Brn4-Cre} animals might be affected. It is also possible that there are defects in the process of oligodendrocyte differentiation, thus defected oligodendrocytes cannot myelinate axons properly.

In order to investigate this possibility in *Arl13b* ^{Δ Brn4-Cre}, we examined the expression of LINGO-1, a known negative regulator in oligodendrocyte differentiation and myelination (Mi et al., 2005). We detected normal LINGO-1 expression in E16.5 *Arl13b* ^{Δ Brn4-Cre} compared to *Arl13b*^{flxed/+} (Figure 4.3I and J). However by E18.5, LINGO-1 expression was not downregulated in *Arl13b* ^{Δ Brn4-Cre} as it in control *Arl13b*^{flxed/+} (Figure 4.3M and N). We observed MBP-expressing oligodendrocyte at E18.5 in *Arl13b* ^{Δ Brn4-Cre} but movement defects after birth suggesting that abnormal LINGO-1 expression in E18.5 *Arl13b* ^{Δ Brn4-Cre} embryos is more likely to result in defects in myelination.

4.4 Discussion

It is very surprising to observe normal OLP specification in both *Arl13b*^{AOlig1-Cre} and *Arl13b*^{ABrm4-Cre} when cilia have been implicated to be important for PDGFR α signaling. Although PDGFR α has been shown to localize in the cilium *in vitro*, it is unclear how cilia are required for PDGFR α signaling in OLP specification *in vivo* (Schneider et al., 2005). It is possible that other signaling pathways are required for OLP specification since mouse mutants lacking PDGF-A, the ligand for PDGFR α , can still specify OLPs normally (Fruttiger et al., 1999).

In *Arl13b*^{ABrm4-Cre} animals, we observed some animals display severe defects in movements. Animals that have defects in myelination often show ataxia or shivering, such as *shiverer* mice lacks four isoforms of MBP and their axon displays severe demyelination (Chernoff, 1981). *Shiverer* mice start to show severe tremor at postnatal day 10, and then develop hindlimb ataxia later on, and they can only survive for few months (Readhead et al., 1987). Although *Arl13b*^{ABrm4-Cre} mice did not have tremor when they were young, they developed hindlimb ataxia after they were weaned and could not survive long consistent with defects in myelination.

We discovered the expression of LINGO-1, one of negative regulators of oligodendrocyte differentiation and myelination, is affected in *Arl13b*^{ABrm4-Cre} (Lee et al., 2007; Mi et al., 2005). It provides us a potential mechanism that *Arl13b* may normally promote oligodendrocyte development by inhibiting LINGO-1. LINGO-1 is a transmembrane receptor, and it is expressed in both neurons and oligodendrocytes (Mi et al., 2004; Park et al., 2005; Shao et al., 2005). In neurons, LINGO-1 inhibits neurite growth of axon in responsive to myelin inhibitors (Mi et al., 2004). The interaction

between axon and oligodendrocytes is critical for neurons to recruit immature oligodendrocytes and for promoting myelination (Nave and Trapp, 2008). LINGO-1 expression may be increased in both neurons and OLPs when Arl13b is ubiquitously deleted in the CNS (*Arl13b^{ΔBrn4-Cre}*). Thus axon shortens neurite outgrowth due to over-expression of LINGO-1, and abnormal axon is unable to stimulate differentiation of oligodendrocytes resulting in a improper myelination so *Arl13b^{ΔBrn4-Cre}* animals display defects in movement. To determine whether Arl13b plays a role in myelination, future study can focus on deleting Arl13b specifically in differentiated oligodendrocytes.

Interestingly, we did not observe defects in oligodendrocyte differentiation and myelination in *Arl13b^{ΔOlig1-Cre}* when Arl13b is deleted in OLP lineage. If Arl13b does interact with LINGO-1 to promote oligodendrocyte development, we should also observe some mild defects in *Arl13b^{ΔOlig1-Cre}*. Since LINGO-1 is expressed in both neurons and oligodendrocytes, LINGO-1 expression may only be abnormal in oligodendrocytes of *Arl13b^{ΔOlig1-Cre}*. Therefore, normal neurons can still attract OLPs to stimulate differentiation. Furthermore, *Arl13b^{ΔOlig1-Cre}* animals can move normally suggesting myelination might be normal or at least sufficient for gross movement, thus performing challenges of difficult movement tasks may provide important information about whether myelination in *Arl13b^{ΔOlig1-Cre}* is indeed functioned.

In summary, our results show that oligodendrocyte specification is unaffected by deleting the ciliary protein specifically in the pMN cells or in the whole neural tube. By deleting Arl13b in the CNS, our data display that Arl13b has effect on oligodendrocyte differentiation and myelination.

4.5 In the course of analysis of the *Arl13b* ^{Δ Olig1-Cre}, we found minority of mutants is identical to the null

When we examined the role of Arl13b in oligodendrocyte development by deleting Arl13b in the pMN cells, we found a subset of *Arl13b* ^{Δ Olig1-Cre} embryos (minority of *Arl13b* ^{Δ Olig1-Cre}) recapitulating the null phenotype. At E10.5, the minority of *Arl13b* ^{Δ Olig1-Cre} embryos showed exencephaly and an expansion of Olig2 and HB9 cells that were identical to *Arl13b*^{hmn} (Figure 4.4E-I). The chance of obtaining these embryos was about 5%. It suggests that Arl13b might be deleted prior to pMN specification in the minority of *Arl13b* ^{Δ Olig1-Cre}, thus we investigated whether *Olig1-Cre* expression was leaky.

We crossed a *Cre* reporter line, *R26R*, with *Olig1-Cre* thus a floxed stop codon in *R26R* can be excised upon *Cre*-mediated recombination and *Cre* activity can be detected by β -galactosidase (X-gal). In most cases, *Olig1-Cre* reporter expression was not observed at E8.5 but was in the pMN domain at E9.5 (Figure 4.5A and E). This is consistent with *Olig1-Cre* expression initially at E8.5 and taking a day to be detected by the *Cre* reporter. However, in a subset of embryos, we observed mosaic X-gal reporter expression at E8.5 (Figure 4.5B). Second, we examined Olig1-Cre protein expression directly by using Cre antibody. In the majority of cases, we found Cre protein in a specific cervical domain of the E8.5 embryo, consistent with the established Olig1 expression pattern (Figure 4.5C). However, we again found a subset of embryos in which Cre was expressed randomly in all parts of the embryos. These data show that Olig1-Cre expression is leaky (Figure 4.5D).

Finally, we stained the minority of *Arl13b*^{Δ*Olig1-Cre*} embryos for Arl13b. Arl13b is localized to cilia, and normally can be seen clearly along the ventricular zone. In minority of *Arl13b*^{Δ*Olig1-Cre*}, Arl13b was nearly gone at E9.5 (Figure 4.5F). We also observed an expansion of Olig2 and Olig1 (Cre-expressing cells) at E9.5 in these embryos (Figure 4.5 G), suggesting that an expansion of pMN cells is caused by earlier deletion of Arl13b and only occurs when Olig1-Cre expression is leaky. The fact that we observed Arl13b was not deleted in the same cells when we compared each mutant suggesting Arl13b deletion is random in the minority of *Arl13b*^{Δ*Olig1-Cre*}.

If excessive pMN cells and MNs in the minority of *Arl13b*^{Δ*Olig1-Cre*} embryos is caused by an early and random expression of *Olig1-Cre*, our next question becomes in what cells does *Arl13b* deletion lead to this phenotype. The deletion must occur prior to pMN specification, so *Arl13b* must be deleted in the precursors of pMN cells. There are two major models for how pMN cells can become MNs and OLPs: Model 1 hypothesizes that there are two populations of pMN cells, one differentiates as MNs and the other one becomes OLPs; Model 2 suggests that there is a stem cell population that continuously gives rise to pMN cells: neuroepithelial stem cells (NSCs). In model 1, random deletions of *Arl13b* in the neuroepithelium should result in distinct neural patterning phenotypes or at least variability in the phenotype (Figure 4.6A). In model 2, we would observe the same expansion of pMN cells if Arl13b was deleted in some of NSCs resulting NSCs precociously differentiation (Figure 4.6B).

We then used a tamoxifen-inducible *CAGG-CreER*TM to induce mosaic and full deletion of Arl13b (Hayashi and McMahon, 2002). When a high dose of tamoxifen was injected (*Arl13b*^{Δ*CAGG-Cre*}, 2 mg), we observed exencephaly and an expansion of pMN

cells as well as a complete absence of Arl13b that were distinct from control embryos (Figure 4.7A-F). When a low dose of tamoxifen was injected (*Arl13b*^{ΔCAGG-Cre}, 0.5 mg), we detected normal morphology of embryos and partial expression of Arl13b protein suggesting the deletion was mosaic (Figure 4.7G and H). However, we still observed an expansion of pMN cells that was identical to the full deletion (Figure 4.7I). We always see pMN expansion in *Arl13b*^{ΔCAGG-Cre} regardless of the amount of Arl13b deletion suggesting that our results are more consistent with model 2. Therefore, deletion of Arl13b in NSCs could lead to their precocious differentiation and expansion resulting in the expanded pMN domain (Figure 4.8).

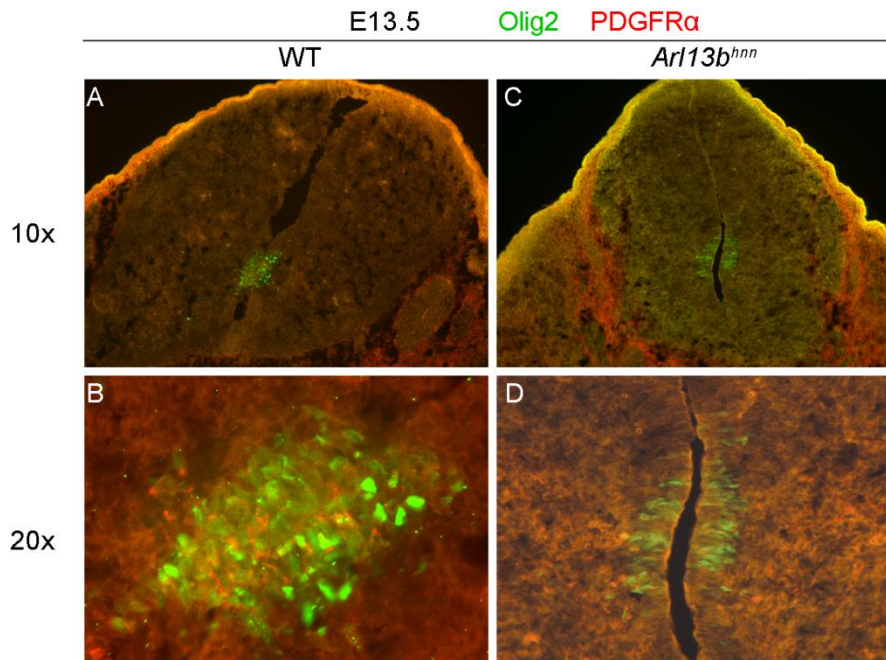


Figure 4.1 There are no OLPs in *Arl13b*^{hnn} at E13.5. (A-D) Olig2 cells (green) are in an expanded domain near the ventricular zone in E13.5 wild-type (WT) neural tube, and PDGFR α cells (red) can be seen near Olig2 cells (A and B). In *Arl13b*^{hnn}, Olig2 cells are in a similar expanded domain but fewer Olig2 cells are there and there are no PDGFR α cells (C and D).

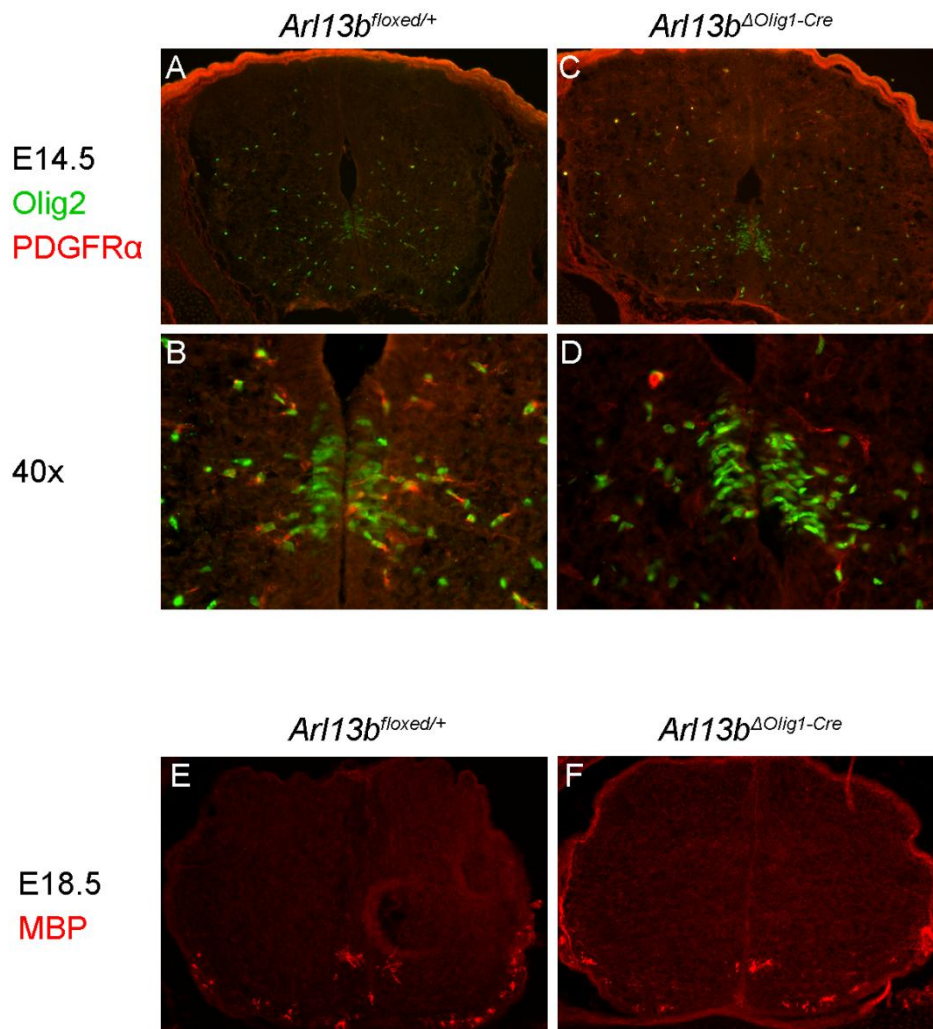


Figure 4.2 Oligodendrocyte specification and differentiation is normal when *Arl13b* is deleted in the pMN lineage. (A-D) The expression of Olig2 (green) and PDGFRα (red) in *Arl13b*^{flxed/+} at E14.5 is similar with it at E13.5, except both cells are more spread out (A), and the same expression is observed in *Arl13b*^{ΔOlig1-Cre} (C). A higher magnification of the region near the ventricular zone is shown in B and D. (E-F) MBP expression is similar in both *Arl13b*^{flxed/+} (E) and *Arl13b*^{ΔOlig1-Cre} (F) at E18.5.

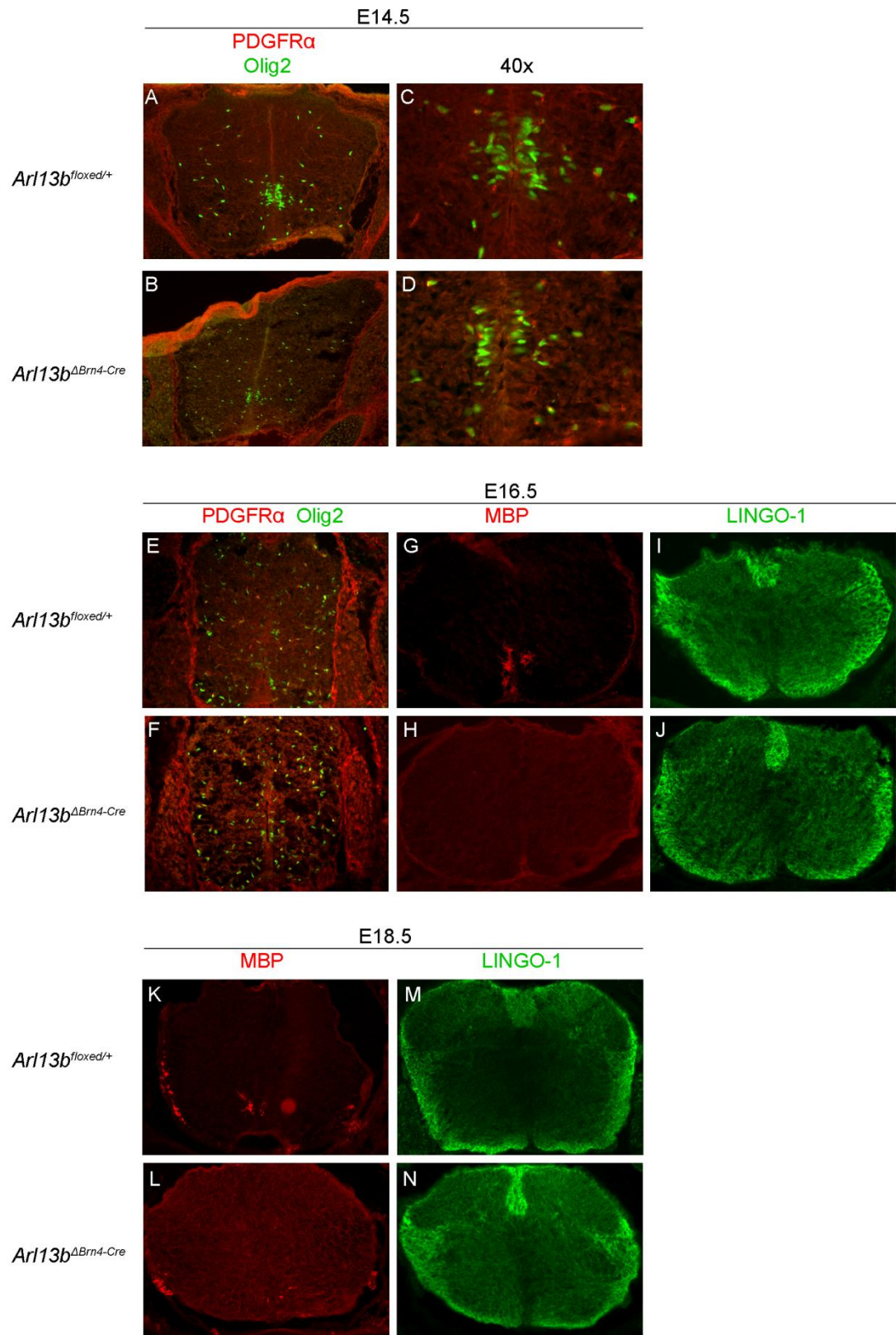


Figure 4.3 MBP and LINGO-1 expression is abnormal in *Arl13b* ^{Δ Brm4-Cre}. **(A-F)** At E14.5 and E16.5, both Olig2 (green) and PDGFR α (red) expression is normal in *Arl13b*^{floxed/+} (A and E) and *Arl13b* ^{Δ Brm4-Cre} (B and F). A higher magnification is shown in C and D. **(G-H; K-L)** MBP is normally expressed close to the ventricular zone in E16.5 *Arl13b*^{floxed/+} (G) and lateral neural tube at E18.5 (K), but it is absent in *Arl13b* ^{Δ Brm4-Cre} at E16.5(H) and it can be detected at E18.5 (L). **(I-J; M-N)** LINGO-1 expression is similar between *Arl13b*^{floxed/+} and *Arl13b* ^{Δ Brm4-Cre} at E16.5 (I and J), but it is only down-regulated in E18.5 *Arl13b*^{floxed/+} (M) not in *Arl13b* ^{Δ Brm4-Cre} (N).

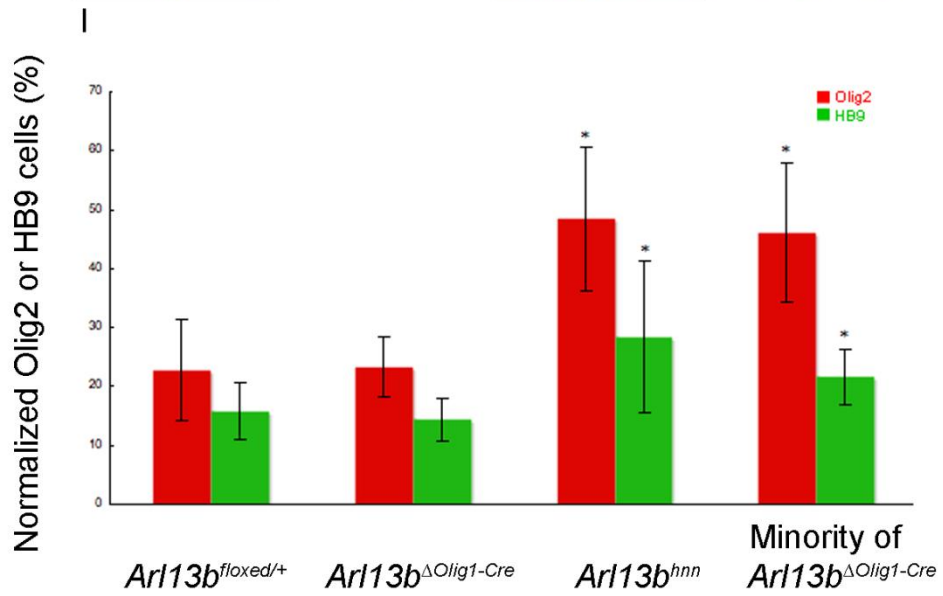
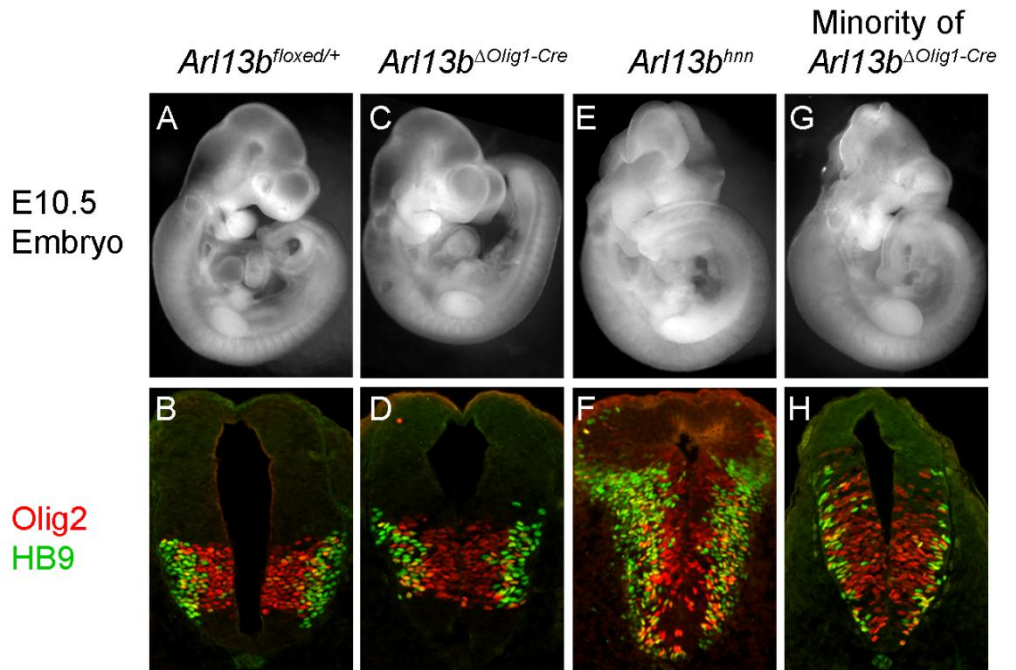


Figure 4.4 An expansion of pMN cells and MNs in the minority of *Arl13b*^{ΔOlig1-Cre}. **(A, C, E, G)** E10.5 embryo morphology is identical between *Arl13b*^{floxed/+} and *Arl13b*^{ΔOlig1-Cre} (A and C), but there is exencephaly in *Arl13b*^{hmn} and the minority of *Arl13b*^{ΔOlig1-Cre} (E and G). **(B, D, F, H)** Olig2 (red) and HB9 (green) cells are normally in their restricted domain in *Arl13b*^{floxed/+} and *Arl13b*^{ΔOlig1-Cre} neural tube (B and D), but they are expanded in *Arl13b*^{hmn} and the minority of *Arl13b*^{ΔOlig1-Cre} (F and H). **(I)** Normalized Olig2 (red) and HB9 (green) cells are presented as the mean ± SD from 3 sections of 5 embryos. The percentage of Olig2 cells increases from 22.8 ± 8.6% (*Arl13b*^{floxed/+}) or 23.4 ± 5.1% (*Arl13b*^{ΔOlig1-Cre}) to 48.4 ± 12.3% (*Arl13b*^{hmn}) or 46.1 ± 11.7% (the minority of *Arl13b*^{ΔOlig1-Cre}), and asterisk shows significant differences when p < 0.05. The percentage of HB9 cells is from 15.8 ± 4.8% (*Arl13b*^{floxed/+}) or 14.4 ± 3.6% (*Arl13b*^{ΔOlig1-Cre}) to 28.4 ± 12.9% (*Arl13b*^{hmn}) or 21.6 ± 4.8% (the minority of *Arl13b*^{ΔOlig1-Cre}).

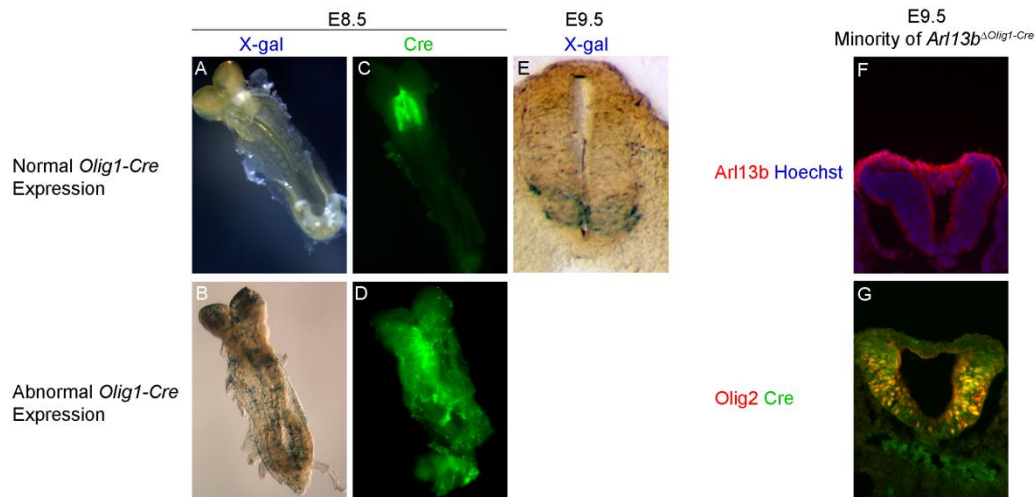


Figure 4.5 Leaky *Olig1-Cre* expression. Abnormal expression of *Olig1-Cre* causes earlier deletion of *Arl13b* and results in an expansion of pMN cells. (A-B, E) X-gal staining shows that normally *Olig1-Cre* reporter expression is not detected at E8.5 (A), and in the pMN domain at E9.5 (E) while it expresses in a mosaic manner in a subset of embryos (B). (C-D) *Olig1-Cre* is expressed in the cervical region when staining with Cre antibody (C), but random expression of *Olig1-Cre* can be detected sometimes at E8.5 (D). (F-G) *Arl13b* (red) is nearly gone in the minority of *Arl13b^{ΔOlig1-Cre}* (F). Hoechst stains nuclei in blue. Cre (green) antibody is used for detecting *Olig1* expression, and both *Olig1* and *Olig2* (red) are co-expressed but they are expanded dorsally and ventrally when *Olig1-Cre* expression is leaky (G).

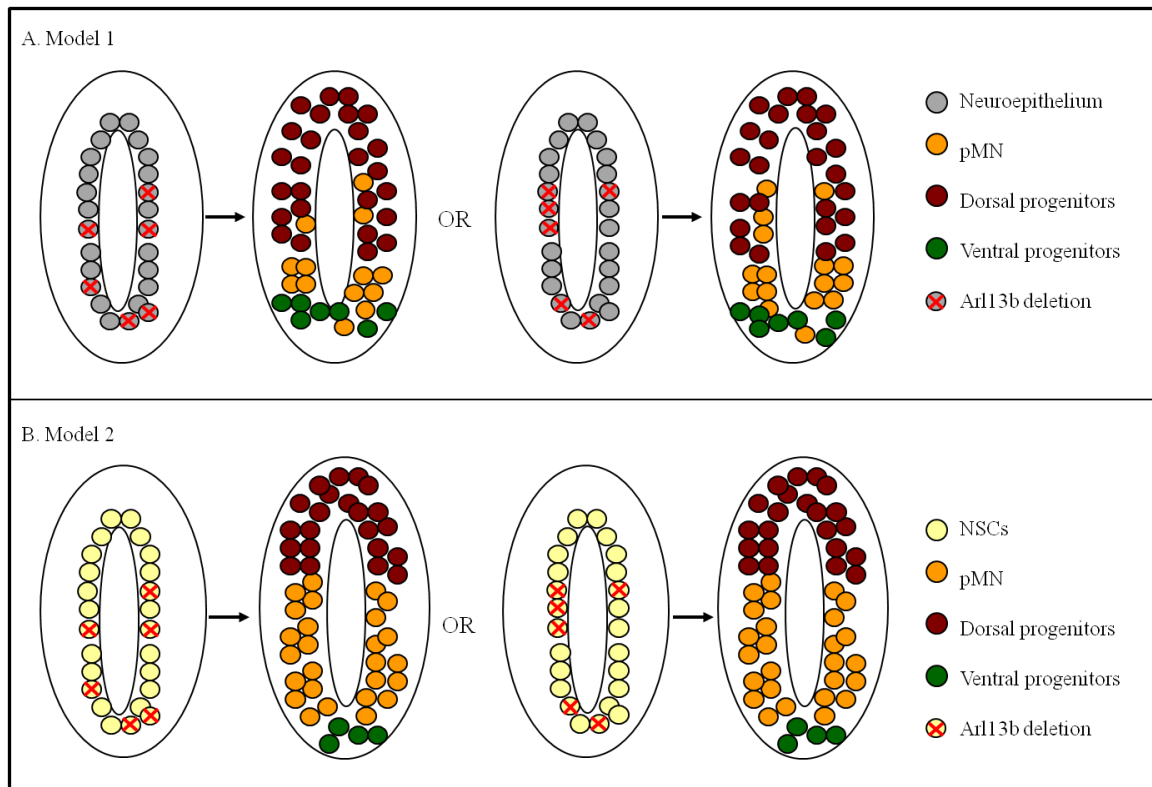


Figure 4.6 Predictions of two models. **(A)** When Arl13b is deleted in cells of the neuroepithelium, only cells that lack Arl13b will become pMN cells. Thus each embryo will show different patterning defects depending on where Arl13b is deleted. **(B)** When Arl13b is deleted in neuroepithelial stem cells (NSCs), each NSC will become two pMN cells in the absence of Arl13b. Therefore, there is always an expansion of pMN cells regardless of how many cells lack Arl13b.

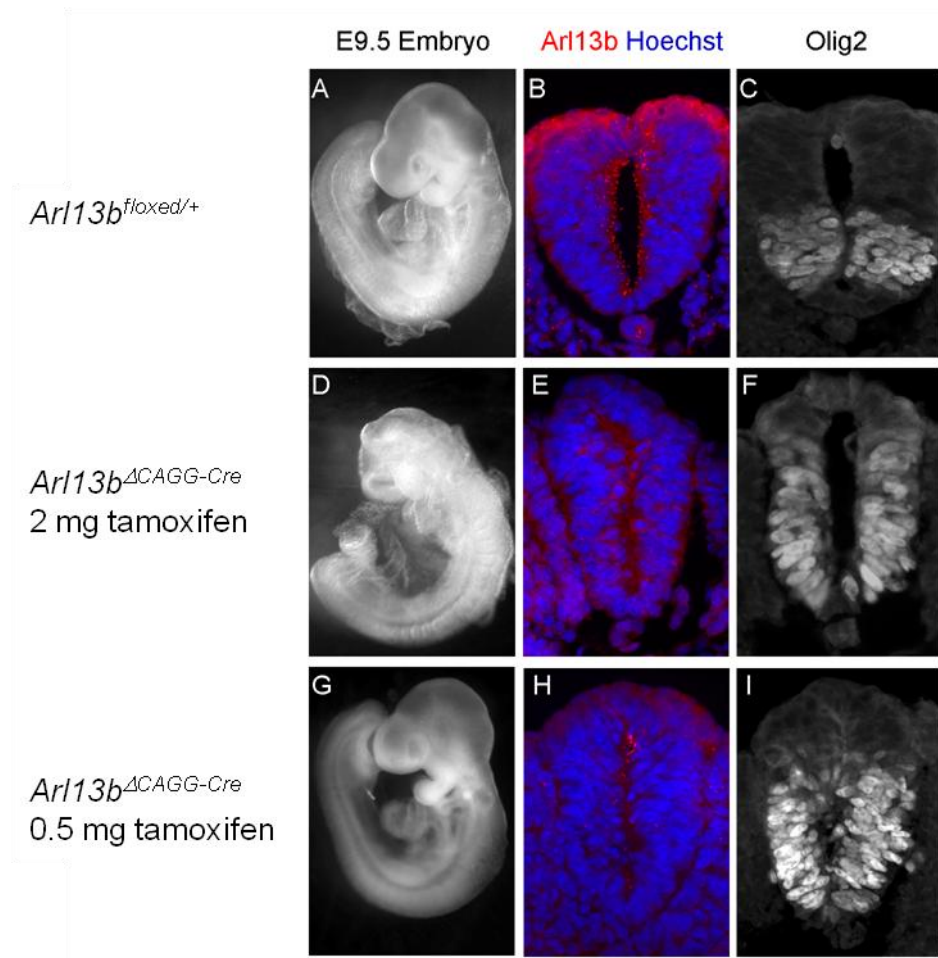


Figure 4.7 The expansion of pMN cells is resulted from *Arl13b* deletion regardless of the numbers of *Arl13b*-lacking cells. **(A-C)** E9.5 *Arl13b^{flxed/+}* embryo shows normal morphology (A). *Arl13b* can be observed along the ventricular zone of neural tube (B), and Olig2-expressing pMN cells are restricted in the pMN domain (C). **(D-F)** When *Arl13b* is deleted ubiquitously (D), *Arl13b^{ΔCAGG-Cre}* embryo shows exencephaly as well as an expansion of Olig2 cells (E and F). **(G-I)** When a low dose of tamoxifen (0.5 mg) is injected, only subsets of cells lack *Arl13b* (H). However, those embryos demonstrate exencephaly and an expansion of Olig2 cells that are identical to the full deletion (G and I).

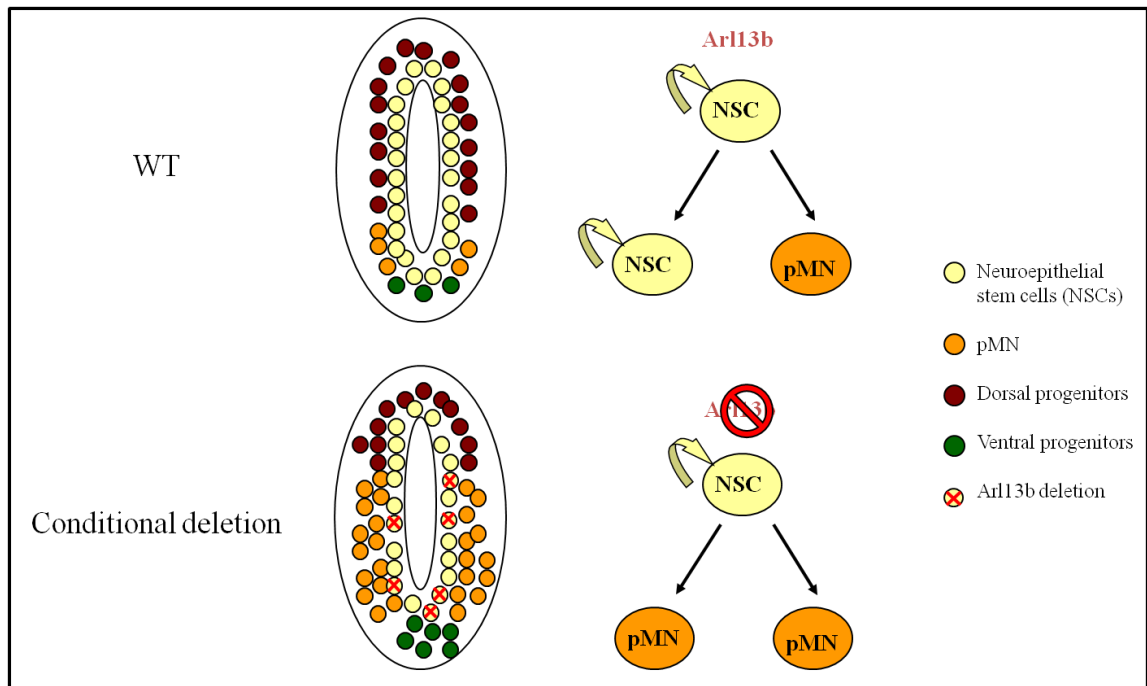


Figure 4.8 Working model for the specification of distinct progenitors in the neural tube.

In wild-type, one neuroepithelial stem cell (NSC) can become one pMN cell and the other one still maintains as a NSC. When Arl13b is deleted, NSCs cannot maintain their undifferentiated state thus both daughter cells precociously become pMN cells although only few NSCs lack Arl13b.

CHAPTER 5

THE PROSPECTIVE VIEWS OF ARL13B IN NEURAL TUBE DEVELOPMENT

AND THE SIGNIFICANCE OF SHH BEING A PERMISSIVE ROLE

5.1 Summary of chapter 3

In chapter 3 of this dissertation, we defined a specific period during when cells are sensitive to changes in levels of Shh activity. Cells that change their cell fate upon a constitutive low level of Shh activation are restored to normal over time suggesting that Shh activity gradient is not needed for maintaining neural tube patterning. Instead, Shh becomes a permissive signal so other signaling pathways can also act on patterning. Moreover, our data suggest that Shh is mainly a permissive role in rostral neural tube while Shh switches from an instructive to a permissive signal in caudal neural tube. Our results raise a question of why Shh plays two roles in neural tube patterning.

5.2 The significance of Shh being an instructive and a permissive signal

After we found that Shh activity gradient is not needed for maintaining neural tube patterning over time, we initiated collaboration with Sara Peyot in John Wallingford's lab. Sara found that ventral progenitors can still be specified when Shh is over-expressed or reduced in *Xenopus* embryos suggesting that Shh is not critical for specifying cells in neural tube (Peyot et al., unpublished). Blocking Shh signaling inhibits ventral neural tube patterning in zebrafish after somitogenesis (Chen et al., 2001; Guner and Karlstrom, 2007; Varga et al., 2001). However, Shh is only required for the floor plate during gastrulation and early somitogenesis in zebrafish suggesting that Shh is an instructive role for the floor plate during a specific period (Ribes et al., 2010). In both chick and mouse, Shh has been shown to play an instructive role to specify cells in the neural tube initially (Ericson et al., 1995; Wijgerde et al., 2002). Although Shh signaling is evolutionally conserved in neural tube specification of vertebrates, an instructive role

of Shh, however, is not. Our and Sara's data suggest that the basal role of Shh is a permissive signal, and Shh is evolved to become an instructive role. Perhaps in higher vertebrates, the central nervous system is more complex thus requires more precise specification of neural progenitors. Not only Shh signaling is required, but different levels of Shh activity are also needed for specifying distinct progenitors.

Ultimately, Shh needs to switch to its basal role, a permissive signal, in the maintenance of normal neural tube patterning. As embryos are developing, cell proliferation, tissue growth, and morphogenesis are involved. Shh can promote proliferation, as well as the survival of neural progenitors (Charrier et al., 2001; Chiang et al., 1996; Litingtung and Chiang, 2000; Rowitch et al., 1999). If Shh still remains as a morphogen, it cannot explain how the neural tube can continue to develop uniformly because progenitors receive higher Shh would proliferate more and survive better than those receive lower Shh. Therefore, it is critical for Shh to maintain as a permissive role so there is a balance between the maintenance of neural tube patterning, progenitor proliferation, and survival.

It has been shown that aberrant Shh activation can cause tumorigenesis, either through loss mutations in *Ptch1* or constitutive active of Smo (Goodrich et al., 1997; Hallahan et al., 2004; Mao et al., 2006; Oliver et al., 2005; Oro et al., 1997; Reifenberger et al., 1998; Schuller et al., 2008; Wolter et al., 1997; Xie et al., 1998; Yang et al., 2008). Current therapies focus on investigating Smo antagonists in order to block Shh signaling (Borzillo and Lippa, 2005; Chen et al., 2002; Frank-Kamenetsky et al., 2002; Garber, 2008; Taipale et al., 2000). Our results, however, suggest that blocking Shh signaling might not be an efficient way to suppress tumors. Indeed, several other pathways have

been implicated to alter Gli activity resulting in tumor formations (Dennler et al., 2007; Nolan-Stevaux et al., 2009; Riobo et al., 2006). Therefore, future studies can focus on examining the interactions among Shh, Wnt, BMP, and RA signaling in the absence of graded Shh activity in the maintenance of neural tube patterning to help us better understanding the potential mechanisms of how the balance between patterning, cell growth, and survival is achieved.

5.3 Summary of chapter 4

In chapter 4 of this dissertation, we found that Arl13b is not required for specification of oligodendrocytes when Arl13b is deleted specifically in oligodendrocyte lineage (*Arl13b^{AOlig1-Cre}*) and in the whole neural tube (*Arl13b^{ABrn4-Cre}*). We also observed that movement defects in *Arl13b^{ABrn4-Cre}* suggesting that Arl13b is involved in later stages of oligodendrocyte development. Finally, we discovered LINGO-1 is not down-regulated providing a potential mechanism in which Arl13b normally inhibits LINGO-1 to promote oligodendrocyte development. The questions of why disrupting cilia does not affect OLP specification, and why normal specification of oligodendrocytes still result in a delay in oligodendrocyte differentiation in *Arl13b^{ABrn4-Cre}* still remain unanswered.

5.4 The potential roles of Arl13b in oligodendrocyte development

PDGFR α is the first marker for OLPs, and PDGFR α signaling is also important for oligodendrocyte specification (Klinghoffer et al., 2002; Zhou et al., 2000). Because PDGFR α has shown to be localized in cilia (Schneider et al., 2005), it is surprising to observe disrupting cilia by deleting Arl13b has does not affect OLP specification.

PDGFR α signaling is activated by dimerizing receptors when the ligand PDGF-A is present, and then activate downstream of Akt and Mek1/2-Erk1/2 cascade (Araki et al., 2003). Although phosphorylation of Mek1/2 has also been shown to occur within the cilium, there is no evidence proving that shifts of localization of PDGFR α signaling component are required for proper transduction (Schneider et al., 2005). It is possible that OLPs can be specified as long as PDGFR α localizes in the cilia, and the length or the axoneme structure of cilia is not critical. In Arl13b-lacking cells, cilia are still present despite of defects in axoneme architecture. Therefore, oligodendrocyte specification is normal in *Arl13b*^{AOlig1-Cre} and *Arl13b*^{ABrm4-Cre} embryos. To understand whether cilia are required for PDGFR α signaling and oligodendrocyte specification, future study can focus on deleting cilia specifically in oligodendrocyte lineage.

After OLPs are specified, they undergo massive proliferation while migrating throughout the spinal cord and brain. A delay of MBP expression in *Arl13b*^{ABrm4-Cre} may result from three possibilities: first, OLPs proliferate slower in the absence of Arl13b; second, there are defects in migration; third, Arl13b may regulate MBP expression directly or indirectly. The first possibility is unlikely, as we did not observe proliferation defects in *Arl13b*^{hmm} embryos (Caspary et al., 2007; Horner and Caspary, under revision). Secondly, primary cilia have been shown to re-orientate themselves in the direction of migration (Schneider et al., 2010). In the absence of cilia, cell migration is impaired by wound healing approach suggesting that cilia can facilitate migration (Jones et al., 2011; Schneider et al., 2010; Schneider et al., 2009). It is possible that Arl13b-lacking OLPs cannot migrate to their destination at the full speed, thus we observed a delay in differentiated oligodendrocyte expression. It will be interesting in examining whether

defective cilia result in impaired migration, and it will be easier to investigate this by knocking down Arl13b in oligodendrocytes in culture. Finally, Arl13b may regulate MBP expression. Although Arl13b is known to be associated to the cilium, our lab has preliminary data suggest that Arl13b can localize to the nucleus (Larkins and Caspary, unpublished). It is possible that Arl13b can directly regulate MBP expression at the transcriptional level resulting in a delay of MBP protein expression. As we have identified LINGO-1 as a potential Arl13b-interacting partner, it is also possible that Arl13b can interact with other proteins that regulate MBP expression. Taken together, the loss of Arl13b may affect multiple steps in oligodendrocyte development. Therefore, determining in which steps Arl13b is involved will help us to understand better how Arl13b plays a role in oligodendrocyte development.

5.5 The potential role of Arl13b in neuroepithelial stem cells (NSCs)

Surprisingly by investigating *Arl13b* ^{Δ Olig1-Cre}, we found that deleting Arl13b prior to pMN specification results in the null phenotype suggesting that Arl13b is deleted in the precursors of pMN cells: neuroepithelial stem cells (NSCs). When a cell divides, one daughter cell receives the mother centriole forms a primary cilium prior to the other one. The one grows a cilium first can respond to cell signaling, such as Shh signaling (Anderson and Stearns, 2009). This asynchronous formation of the cilium can apply to how NSCs give rise to pMN cells while they still remain undifferentiated. Normally, one daughter cell forms a cilium when a NSC divides thus that cell can respond to Shh signaling and become pMN cell (Figure 5.1A). In the absence of Arl13b, there is a constitutive low level of Shh activation and both daughter cells become pMN cells

regardless which one forms a cilium first. Therefore, NSCs differentiate precociously and result in an expansion of pMN cells when *Arl13b* is deleted prior to pMN specification (Figure 5.1B).

Many human diseases are caused by mis-functioned motor neurons or oligodendrocytes. Motor neuron disease is characterized by progressive degeneration of motor neurons, and affects almost two adults per 100,000 (Shaw, 1999). Demyelinating diseases are involved in failure to restore myelin sheaths which require oligodendrocytes (Franklin, 2002). The potential treatments for regenerating motor neurons or oligodendrocytes are focused on cellular therapies, including the use of stem cells or genetically engineered neuronal progenitors. Thus our NSC model provides a potential method to derived pMN cells from neural stem cells, and future studies can focus on understanding the relationships among neuroepithelial stem cell division, cilium formation, Shh signaling responses, and pMN cell specification.

5.6 Perspective and conclusion

From the results of chapter 3 and our NSC model, the question then becomes whether *Arl13b* is only dedicated to Shh signaling. *Arl13b* is a ciliary protein, and it is localized in both motile and primary cilia. Therefore, *Arl13b* is involved in many developmental pathways in which motile and primary cilia play essential roles. For instance, *Arl13b^{hnn}* mutant embryos display defects in left-right axis establishment suggesting that *Arl13b* plays a role in Nodal signaling (Larkins et al., unpublished). From the results of chapter 4, we now start to reveal the role of *Arl13b* in LINGO-1 signaling that is important for oligodendrocyte development. Thus by using our conditional *Arl13b*

allele, we can discover the significances of Arl13b in specific developmental processes that we are interested in.

This dissertation provides the specific timeframe when Shh shifts from an instructive to a permissive signal *in vivo*, and reveals the fundamental mechanism in which how neural tube patterning is maintained over time. This work additionally provides a potential model that neural progenitors are derived from neuroepithelial stem cells. This dissertation also adds new knowledge about the role of the ciliary protein, Arl13b, in oligodendrocyte development.

BIBLIOGRAPHY:

Alcedo, J., Ayzenzon, M., Von Ohlen, T., Noll, M. and Hooper, J. E. (1996). The *Drosophila* smoothed gene encodes a seven-pass membrane protein, a putative receptor for the hedgehog signal. *Cell* **86**, 221-32.

Alvarez-Medina, R., Cayuso, J., Okubo, T., Takada, S. and Marti, E. (2008). Wnt canonical pathway restricts graded Shh/Gli patterning activity through the regulation of Gli3 expression. *Development* **135**, 237-47.

Anderson, C. T. and Stearns, T. (2009). Centriole age underlies asynchronous primary cilium growth in mammalian cells. *Curr Biol* **19**, 1498-502.

Anitei, M., Ifrim, M., Ewart, M. A., Cowan, A. E., Carson, J. H., Bansal, R. and Pfeiffer, S. E. (2006). A role for Sec8 in oligodendrocyte morphological differentiation. *J Cell Sci* **119**, 807-18.

Araki, T., Nawa, H. and Neel, B. G. (2003). Tyrosyl phosphorylation of Shp2 is required for normal ERK activation in response to some, but not all, growth factors. *J Biol Chem* **278**, 41677-84.

Aza-Blanc, P., Lin, H. Y., Ruiz i Altaba, A. and Kornberg, T. B. (2000). Expression of the vertebrate Gli proteins in *Drosophila* reveals a distribution of activator and repressor activities. *Development* **127**, 4293-301.

Bai, C. B., Stephen, D. and Joyner, A. L. (2004). All mouse ventral spinal cord patterning by hedgehog is Gli dependent and involves an activator function of Gli3. *Dev Cell* **6**, 103-15.

Barbarese, E., Brumwell, C., Kwon, S., Cui, H. and Carson, J. H. (1999). RNA on the road to myelin. *J Neurocytol* **28**, 263-70.

- Bogler, O., Wren, D., Barnett, S. C., Land, H. and Noble, M.** (1990). Cooperation between two growth factors promotes extended self-renewal and inhibits differentiation of oligodendrocyte-type-2 astrocyte (O-2A) progenitor cells. *Proc Natl Acad Sci U S A* **87**, 6368-72.
- Borzillo, G. V. and Lippa, B.** (2005). The Hedgehog signaling pathway as a target for anticancer drug discovery. *Curr Top Med Chem* **5**, 147-57.
- Briscoe, J., Chen, Y., Jessell, T. M. and Struhl, G.** (2001). A hedgehog-insensitive form of patched provides evidence for direct long-range morphogen activity of sonic hedgehog in the neural tube. *Mol Cell* **7**, 1279-91.
- Briscoe, J., Pierani, A., Jessell, T. M. and Ericson, J.** (2000). A homeodomain protein code specifies progenitor cell identity and neuronal fate in the ventral neural tube. *Cell* **101**, 435-45.
- Briscoe, J., Sussel, L., Serup, P., Hartigan-O'Connor, D., Jessell, T. M., Rubenstein, J. L. and Ericson, J.** (1999). Homeobox gene Nkx2.2 and specification of neuronal identity by graded Sonic hedgehog signalling. *Nature* **398**, 622-7.
- Calver, A. R., Hall, A. C., Yu, W. P., Walsh, F. S., Heath, J. K., Betsholtz, C. and Richardson, W. D.** (1998). Oligodendrocyte population dynamics and the role of PDGF in vivo. *Neuron* **20**, 869-82.
- Campagnoni, A. T.** (1988). Molecular biology of myelin proteins from the central nervous system. *J Neurochem* **51**, 1-14.
- Caspary, T., Larkins, C. E. and Anderson, K. V.** (2007). The graded response to Sonic Hedgehog depends on cilia architecture. *Dev Cell* **12**, 767-78.

- Charrier, J. B., Lapointe, F., Le Douarin, N. M. and Teillet, M. A.** (2001). Anti-apoptotic role of Sonic hedgehog protein at the early stages of nervous system organogenesis. *Development* **128**, 4011-20.
- Chen, J. K., Taipale, J., Young, K. E., Maiti, T. and Beachy, P. A.** (2002). Small molecule modulation of Smoothed activity. *Proc Natl Acad Sci U S A* **99**, 14071-6.
- Chen, M. H., Wilson, C. W., Li, Y. J., Law, K. K., Lu, C. S., Gacayan, R., Zhang, X., Hui, C. C. and Chuang, P. T.** (2009). Cilium-independent regulation of Gli protein function by Sufu in Hedgehog signaling is evolutionarily conserved. *Genes Dev* **23**, 1910-28.
- Chen, W., Burgess, S. and Hopkins, N.** (2001). Analysis of the zebrafish smoothed mutant reveals conserved and divergent functions of hedgehog activity. *Development* **128**, 2385-96.
- Chen, Y. and Struhl, G.** (1996). Dual roles for patched in sequestering and transducing Hedgehog. *Cell* **87**, 553-63.
- Chernoff, G. F.** (1981). Shiverer: an autosomal recessive mutant mouse with myelin deficiency. *J Hered* **72**, 128.
- Chesnutt, C., Burrus, L. W., Brown, A. M. and Niswander, L.** (2004). Coordinate regulation of neural tube patterning and proliferation by TGFbeta and WNT activity. *Dev Biol* **274**, 334-47.
- Chiang, C., Litingtung, Y., Lee, E., Young, K. E., Corden, J. L., Westphal, H. and Beachy, P. A.** (1996). Cyclopia and defective axial patterning in mice lacking Sonic hedgehog gene function. *Nature* **383**, 407-13.

- Corbit, K. C., Aanstad, P., Singla, V., Norman, A. R., Stainier, D. Y. and Reiter, J. F.** (2005). Vertebrate Smoothed functions at the primary cilium. *Nature* **437**, 1018-21.
- Cortellino, S., Wang, C., Wang, B., Bassi, M. R., Caretti, E., Champeval, D., Calmont, A., Jarnik, M., Burch, J., Zaret, K. S. et al.** (2009). Defective ciliogenesis, embryonic lethality and severe impairment of the Sonic Hedgehog pathway caused by inactivation of the mouse complex A intraflagellar transport gene *Ift122/Wdr10*, partially overlapping with the DNA repair gene *Med1/Mbd4*. *Dev Biol* **325**, 225-37.
- D'Souza-Schorey, C. and Chavrier, P.** (2006). ARF proteins: roles in membrane traffic and beyond. *Nat Rev Mol Cell Biol* **7**, 347-58.
- Dai, P., Akimaru, H., Tanaka, Y., Maekawa, T., Nakafuku, M. and Ishii, S.** (1999). Sonic Hedgehog-induced activation of the *Gli1* promoter is mediated by *GLI3*. *J Biol Chem* **274**, 8143-52.
- Denef, N., Neubuser, D., Perez, L. and Cohen, S. M.** (2000). Hedgehog induces opposite changes in turnover and subcellular localization of patched and smoothed. *Cell* **102**, 521-31.
- Dennler, S., Andre, J., Alexaki, I., Li, A., Magnaldo, T., ten Dijke, P., Wang, X. J., Verrecchia, F. and Mauviel, A.** (2007). Induction of sonic hedgehog mediators by transforming growth factor-beta: Smad3-dependent activation of *Gli2* and *Gli1* expression in vitro and in vivo. *Cancer Res* **67**, 6981-6.
- Dessaud, E., Ribes, V., Balaskas, N., Yang, L. L., Pierani, A., Kicheva, A., Novitch, B. G., Briscoe, J. and Sasai, N.** (2010). Dynamic assignment and maintenance of positional identity in the ventral neural tube by the morphogen sonic hedgehog. *PLoS Biol* **8**, e1000382.

Dessaud, E., Yang, L. L., Hill, K., Cox, B., Ulloa, F., Ribeiro, A., Mynett, A., Novitch, B. G. and Briscoe, J. (2007). Interpretation of the sonic hedgehog morphogen gradient by a temporal adaptation mechanism. *Nature* **450**, 717-20.

Diez del Corral, R., Olivera-Martinez, I., Goriely, A., Gale, E., Maden, M. and Storey, K. (2003). Opposing FGF and retinoid pathways control ventral neural pattern, neuronal differentiation, and segmentation during body axis extension. *Neuron* **40**, 65-79.

Eggenschwiler, J. T., Bulgakov, O. V., Qin, J., Li, T. and Anderson, K. V. (2006). Mouse Rab23 regulates hedgehog signaling from smoothed to Gli proteins. *Dev Biol* **290**, 1-12.

Eggenschwiler, J. T., Espinoza, E. and Anderson, K. V. (2001). Rab23 is an essential negative regulator of the mouse Sonic hedgehog signalling pathway. *Nature* **412**, 194-8.

Endoh-Yamagami, S., Evangelista, M., Wilson, D., Wen, X., Theunissen, J. W., Phamluong, K., Davis, M., Scales, S. J., Solloway, M. J., de Sauvage, F. J. et al. (2009). The mammalian Cos2 homolog Kif7 plays an essential role in modulating Hh signal transduction during development. *Curr Biol* **19**, 1320-6.

Ericson, J., Briscoe, J., Rashbass, P., van Heyningen, V. and Jessell, T. M. (1997a). Graded sonic hedgehog signaling and the specification of cell fate in the ventral neural tube. *Cold Spring Harb Symp Quant Biol* **62**, 451-66.

Ericson, J., Morton, S., Kawakami, A., Roelink, H. and Jessell, T. M. (1996). Two critical periods of Sonic Hedgehog signaling required for the specification of motor neuron identity. *Cell* **87**, 661-73.

Ericson, J., Muhr, J., Placzek, M., Lints, T., Jessell, T. M. and Edlund, T. (1995).

Sonic hedgehog induces the differentiation of ventral forebrain neurons: a common signal for ventral patterning within the neural tube. *Cell* **81**, 747-56.

Ericson, J., Rashbass, P., Schedl, A., Brenner-Morton, S., Kawakami, A., van

Heyningen, V., Jessell, T. M. and Briscoe, J. (1997b). Pax6 controls progenitor cell identity and neuronal fate in response to graded Shh signaling. *Cell* **90**, 169-80.

Frank-Kamenetsky, M., Zhang, X. M., Bottega, S., Guicherit, O., Wichterle, H.,

Dudek, H., Bumcrot, D., Wang, F. Y., Jones, S., Shulok, J. et al. (2002). Small-molecule modulators of Hedgehog signaling: identification and characterization of Smoothed agonists and antagonists. *J Biol* **1**, 10.

Franklin, R. J. (2002). Why does remyelination fail in multiple sclerosis? *Nat Rev Neurosci* **3**, 705-14.

Fruttiger, M., Karlsson, L., Hall, A. C., Abramsson, A., Calver, A. R., Bostrom, H.,

Willets, K., Bertold, C. H., Heath, J. K., Betsholtz, C. et al. (1999). Defective oligodendrocyte development and severe hypomyelination in PDGF-A knockout mice. *Development* **126**, 457-67.

Garber, K. (2008). Hedgehog drugs begin to show results. *J Natl Cancer Inst* **100**, 692-7.

Garcia-Garcia, M. J., Eggenschwiler, J. T., Caspary, T., Alcorn, H. L., Wyler, M. R.,

Huangfu, D., Rakeman, A. S., Lee, J. D., Feinberg, E. H., Timmer, J. R. et al. (2005). Analysis of mouse embryonic patterning and morphogenesis by forward genetics. *Proc Natl Acad Sci U S A* **102**, 5913-9.

Genoud, S., Lappe-Siefke, C., Goebbels, S., Radtke, F., Aguet, M., Scherer, S. S., Suter, U., Nave, K. A. and Mantei, N. (2002). Notch1 control of oligodendrocyte differentiation in the spinal cord. *J Cell Biol* **158**, 709-18.

Goodrich, L. V., Johnson, R. L., Milenkovic, L., McMahon, J. A. and Scott, M. P. (1996). Conservation of the hedgehog/patched signaling pathway from flies to mice: induction of a mouse patched gene by Hedgehog. *Genes Dev* **10**, 301-12.

Goodrich, L. V., Milenkovic, L., Higgins, K. M. and Scott, M. P. (1997). Altered neural cell fates and medulloblastoma in mouse patched mutants. *Science* **277**, 1109-13.

Grindstaff, K. K., Yeaman, C., Anandasabapathy, N., Hsu, S. C., Rodriguez-Boulan, E., Scheller, R. H. and Nelson, W. J. (1998). Sec6/8 complex is recruited to cell-cell contacts and specifies transport vesicle delivery to the basal-lateral membrane in epithelial cells. *Cell* **93**, 731-40.

Gudis, D. A. and Cohen, N. A. (2010). Cilia dysfunction. *Otolaryngol Clin North Am* **43**, 461-72, vii.

Guner, B. and Karlstrom, R. O. (2007). Cloning of zebrafish nkx6.2 and a comprehensive analysis of the conserved transcriptional response to Hedgehog/Gli signaling in the zebrafish neural tube. *Gene Expr Patterns* **7**, 596-605.

Hallahan, A. R., Pritchard, J. I., Hansen, S., Benson, M., Stoeck, J., Hatton, B. A., Russell, T. L., Ellenbogen, R. G., Bernstein, I. D., Beachy, P. A. et al. (2004). The SmoA1 mouse model reveals that notch signaling is critical for the growth and survival of sonic hedgehog-induced medulloblastomas. *Cancer Res* **64**, 7794-800.

- Hayashi, S. and McMahon, A. P.** (2002). Efficient recombination in diverse tissues by a tamoxifen-inducible form of Cre: a tool for temporally regulated gene activation/inactivation in the mouse. *Dev Biol* **244**, 305-18.
- Haycraft, C. J., Banizs, B., Aydin-Son, Y., Zhang, Q., Michaud, E. J. and Yoder, B. K.** (2005). Gli2 and Gli3 localize to cilia and require the intraflagellar transport protein polaris for processing and function. *PLoS Genet* **1**, e53.
- Hazuka, C. D., Foletti, D. L., Hsu, S. C., Kee, Y., Hopf, F. W. and Scheller, R. H.** (1999). The sec6/8 complex is located at neurite outgrowth and axonal synapse-assembly domains. *J Neurosci* **19**, 1324-34.
- Horner, V. L. and Caspary, T.** (under revision). Disrupted dorsal neural tube BMP signaling in the cilia mutant *Arl13b^{hmn}* stems from abnormal Shh signaling. *Dev Biol*.
- Houde, C., Dickinson, R. J., Houtzager, V. M., Cullum, R., Montpetit, R., Metzler, M., Simpson, E. M., Roy, S., Hayden, M. R., Hoodless, P. A. et al.** (2006). Hippo is essential for node cilia assembly and Sonic hedgehog signaling. *Dev Biol* **300**, 523-33.
- Hsu, S. C., Hazuka, C. D., Foletti, D. L. and Scheller, R. H.** (1999). Targeting vesicles to specific sites on the plasma membrane: the role of the sec6/8 complex. *Trends Cell Biol* **9**, 150-3.
- Huangfu, D. and Anderson, K. V.** (2005). Cilia and Hedgehog responsiveness in the mouse. *Proc Natl Acad Sci U S A* **102**, 11325-30.
- Huangfu, D., Liu, A., Rakeman, A. S., Murcia, N. S., Niswander, L. and Anderson, K. V.** (2003). Hedgehog signalling in the mouse requires intraflagellar transport proteins. *Nature* **426**, 83-7.

Hui, C. C., Slusarski, D., Platt, K. A., Holmgren, R. and Joyner, A. L. (1994).

Expression of three mouse homologs of the *Drosophila* segment polarity gene *cubitus interruptus*, *Gli*, *Gli-2*, and *Gli-3*, in ectoderm- and mesoderm-derived tissues suggests multiple roles during postimplantation development. *Dev Biol* **162**, 402-13.

Hynes, M., Stone, D. M., Dowd, M., Pitts-Meek, S., Goddard, A., Gurney, A. and Rosenthal, A. (1997). Control of cell pattern in the neural tube by the zinc finger transcription factor and oncogene *Gli-1*. *Neuron* **19**, 15-26.

Jeong, J. and McMahon, A. P. (2005). Growth and pattern of the mammalian neural tube are governed by partially overlapping feedback activities of the hedgehog antagonists *patched 1* and *Hhip1*. *Development* **132**, 143-54.

Jia, J., Kolterud, A., Zeng, H., Hoover, A., Teglund, S., Toftgard, R. and Liu, A. (2009). *Suppressor of Fused* inhibits mammalian Hedgehog signaling in the absence of cilia. *Dev Biol* **330**, 452-60.

Jones, T. J., Adapala, R. K., Geldenhuys, W. J., Bursley, C., AbouAlaiwi, W. A., Nauli, S. M. and Thodeti, C. K. (2011). Primary cilia regulates the directional migration and barrier integrity of endothelial cells through the modulation of *hsp27* dependent actin cytoskeletal organization. *Journal of Cellular Physiology*.

Kahn, R. A., Volpicelli-Daley, L., Bowzard, B., Shrivastava-Ranjan, P., Li, Y., Zhou, C. and Cunningham, L. (2005). Arf family GTPases: roles in membrane traffic and microtubule dynamics. *Biochem Soc Trans* **33**, 1269-72.

Kim, H. J., DiBernardo, A. B., Sloane, J. A., Rasband, M. N., Solomon, D., Kosaras, B., Kwak, S. P. and Vartanian, T. K. (2006). *WAVE1* is required for oligodendrocyte morphogenesis and normal CNS myelination. *J Neurosci* **26**, 5849-59.

- Kippert, A., Trajkovic, K., Rajendran, L., Ries, J. and Simons, M.** (2007). Rho regulates membrane transport in the endocytic pathway to control plasma membrane specialization in oligodendroglial cells. *J Neurosci* **27**, 3560-70.
- Klein, C., Kramer, E. M., Cardine, A. M., Schraven, B., Brandt, R. and Trotter, J.** (2002). Process outgrowth of oligodendrocytes is promoted by interaction of fyn kinase with the cytoskeletal protein tau. *J Neurosci* **22**, 698-707.
- Klinghoffer, R. A., Hamilton, T. G., Hoch, R. and Soriano, P.** (2002). An allelic series at the PDGFalphaR locus indicates unequal contributions of distinct signaling pathways during development. *Dev Cell* **2**, 103-13.
- Larkins, C. E., Gonzalez Aviles, G. D., East, M. P., Kahn, R. A. and Caspary, T.** (under revision). Arl13b Regulates Ciliogenesis and the Dynamic Localization of Shh Signaling Proteins. *Molecular Biology of the cell*.
- Lee, J., Platt, K. A., Censullo, P. and Ruiz i Altaba, A.** (1997). Gli1 is a target of Sonic hedgehog that induces ventral neural tube development. *Development* **124**, 2537-52.
- Lee, K. J., Dietrich, P. and Jessell, T. M.** (2000). Genetic ablation reveals that the roof plate is essential for dorsal interneuron specification. *Nature* **403**, 734-40.
- Lee, K. J., Mendelsohn, M. and Jessell, T. M.** (1998). Neuronal patterning by BMPs: a requirement for GDF7 in the generation of a discrete class of commissural interneurons in the mouse spinal cord. *Genes Dev* **12**, 3394-407.
- Lee, S., Lee, B., Lee, J. W. and Lee, S. K.** (2009). Retinoid signaling and neurogenin2 function are coupled for the specification of spinal motor neurons through a chromatin modifier CBP. *Neuron* **62**, 641-54.

- Lee, X., Yang, Z., Shao, Z., Rosenberg, S. S., Levesque, M., Pepinsky, R. B., Qiu, M., Miller, R. H., Chan, J. R. and Mi, S.** (2007). NGF regulates the expression of axonal LINGO-1 to inhibit oligodendrocyte differentiation and myelination. *J Neurosci* **27**, 220-5.
- Lei, Q., Zelman, A. K., Kuang, E., Li, S. and Matisse, M. P.** (2004). Transduction of graded Hedgehog signaling by a combination of Gli2 and Gli3 activator functions in the developing spinal cord. *Development* **131**, 3593-604.
- Liang, X., Draghi, N. A. and Resh, M. D.** (2004). Signaling from integrins to Fyn to Rho family GTPases regulates morphologic differentiation of oligodendrocytes. *J Neurosci* **24**, 7140-9.
- Liem, K. F., Jr., Jessell, T. M. and Briscoe, J.** (2000). Regulation of the neural patterning activity of sonic hedgehog by secreted BMP inhibitors expressed by notochord and somites. *Development* **127**, 4855-66.
- Liem, K. F., Jr., Tremml, G. and Jessell, T. M.** (1997). A role for the roof plate and its resident TGFbeta-related proteins in neuronal patterning in the dorsal spinal cord. *Cell* **91**, 127-38.
- Liem, K. F., Jr., Tremml, G., Roelink, H. and Jessell, T. M.** (1995). Dorsal differentiation of neural plate cells induced by BMP-mediated signals from epidermal ectoderm. *Cell* **82**, 969-79.
- Litingtung, Y. and Chiang, C.** (2000). Specification of ventral neuron types is mediated by an antagonistic interaction between Shh and Gli3. *Nat Neurosci* **3**, 979-85.

Litingtung, Y., Dahn, R. D., Li, Y., Fallon, J. F. and Chiang, C. (2002). Shh and Gli3 are dispensable for limb skeleton formation but regulate digit number and identity.

Nature **418**, 979-83.

Liu, A., Wang, B. and Niswander, L. A. (2005). Mouse intraflagellar transport proteins regulate both the activator and repressor functions of Gli transcription factors.

Development **132**, 3103-11.

Liu, F., Massague, J. and Ruiz i Altaba, A. (1998). Carboxy-terminally truncated Gli3 proteins associate with Smads. *Nat Genet* **20**, 325-6.

Lu, Q. R., Sun, T., Zhu, Z., Ma, N., Garcia, M., Stiles, C. D. and Rowitch, D. H.

(2002). Common developmental requirement for Olig function indicates a motor neuron/oligodendrocyte connection. *Cell* **109**, 75-86.

Lu, Q. R., Yuk, D., Alberta, J. A., Zhu, Z., Pawlitzky, I., Chan, J., McMahon, A. P.,

Stiles, C. D. and Rowitch, D. H. (2000). Sonic hedgehog--regulated oligodendrocyte lineage genes encoding bHLH proteins in the mammalian central nervous system. *Neuron* **25**, 317-29.

Mao, J., Ligon, K. L., Rakhlin, E. Y., Thayer, S. P., Bronson, R. T., Rowitch, D. and

McMahon, A. P. (2006). A novel somatic mouse model to survey tumorigenic potential applied to the Hedgehog pathway. *Cancer Res* **66**, 10171-8.

Marigo, V., Davey, R. A., Zuo, Y., Cunningham, J. M. and Tabin, C. J. (1996).

Biochemical evidence that patched is the Hedgehog receptor. *Nature* **384**, 176-9.

Marigo, V. and Tabin, C. J. (1996). Regulation of patched by sonic hedgehog in the

developing neural tube. *Proc Natl Acad Sci U S A* **93**, 9346-51.

- May, S. R., Ashique, A. M., Karlen, M., Wang, B., Shen, Y., Zarbali, K., Reiter, J., Ericson, J. and Peterson, A. S.** (2005). Loss of the retrograde motor for IFT disrupts localization of Smo to cilia and prevents the expression of both activator and repressor functions of Gli. *Dev Biol* **287**, 378-89.
- McKinnon, R. D., Matsui, T., Aranda, M. and Dubois-Dalcq, M.** (1991). A role for fibroblast growth factor in oligodendrocyte development. *Ann N Y Acad Sci* **638**, 378-86.
- McKinnon, R. D., Matsui, T., Dubois-Dalcq, M. and Aaronson, S. A.** (1990). FGF modulates the PDGF-driven pathway of oligodendrocyte development. *Neuron* **5**, 603-14.
- McMahon, J. A., Takada, S., Zimmerman, L. B., Fan, C. M., Harland, R. M. and McMahon, A. P.** (1998). Noggin-mediated antagonism of BMP signaling is required for growth and patterning of the neural tube and somite. *Genes Dev* **12**, 1438-52.
- Meyer, N. P. and Roelink, H.** (2003). The amino-terminal region of Gli3 antagonizes the Shh response and acts in dorsoventral fate specification in the developing spinal cord. *Dev Biol* **257**, 343-55.
- Mi, S., Lee, X., Shao, Z., Thill, G., Ji, B., Relton, J., Levesque, M., Allaire, N., Perrin, S., Sands, B. et al.** (2004). LINGO-1 is a component of the Nogo-66 receptor/p75 signaling complex. *Nat Neurosci* **7**, 221-8.
- Mi, S., Miller, R. H., Lee, X., Scott, M. L., Shulag-Morskaya, S., Shao, Z., Chang, J., Thill, G., Levesque, M., Zhang, M. et al.** (2005). LINGO-1 negatively regulates myelination by oligodendrocytes. *Nat Neurosci* **8**, 745-51.
- Mizutani, C. M., Meyer, N., Roelink, H. and Bier, E.** (2006). Threshold-dependent BMP-mediated repression: a model for a conserved mechanism that patterns the neuroectoderm. *PLoS Biol* **4**, e313.

Motoyama, J., Milenkovic, L., Iwama, M., Shikata, Y., Scott, M. P. and Hui, C. C.

(2003). Differential requirement for Gli2 and Gli3 in ventral neural cell fate specification.

Dev Biol **259**, 150-61.

Muller, T., Anlag, K., Wildner, H., Britsch, S., Treier, M. and Birchmeier, C. (2005).

The bHLH factor Olig3 coordinates the specification of dorsal neurons in the spinal cord.

Genes Dev **19**, 733-43.

Muroyama, Y., Fujihara, M., Ikeya, M., Kondoh, H. and Takada, S. (2002). Wnt

signaling plays an essential role in neuronal specification of the dorsal spinal cord. *Genes*

Dev **16**, 548-53.

Nave, K. A. and Trapp, B. D. (2008). Axon-glia signaling and the glial support of axon

function. *Annu Rev Neurosci* **31**, 535-61.

Nishi, Y., Ji, H., Wong, W. H., McMahon, A. P. and Vokes, S. A. (2009). Modeling

the spatio-temporal network that drives patterning in the vertebrate central nervous

system. *Biochim Biophys Acta* **1789**, 299-305.

Nolan-Stevaux, O., Lau, J., Truitt, M. L., Chu, G. C., Hebrok, M., Fernandez-

Zapico, M. E. and Hanahan, D. (2009). GLI1 is regulated through Smoothened-

independent mechanisms in neoplastic pancreatic ducts and mediates PDAC cell survival

and transformation. *Genes Dev* **23**, 24-36.

Noll, E. and Miller, R. H. (1993). Oligodendrocyte precursors originate at the ventral

ventricular zone dorsal to the ventral midline region in the embryonic rat spinal cord.

Development **118**, 563-73.

Novitch, B. G., Chen, A. I. and Jessell, T. M. (2001). Coordinate regulation of motor neuron subtype identity and pan-neuronal properties by the bHLH repressor Olig2.

Neuron **31**, 773-89.

Novitch, B. G., Wichterle, H., Jessell, T. M. and Sockanathan, S. (2003). A requirement for retinoic acid-mediated transcriptional activation in ventral neural patterning and motor neuron specification. *Neuron* **40**, 81-95.

Oliver, T. G., Read, T. A., Kessler, J. D., Mehmeti, A., Wells, J. F., Huynh, T. T., Lin, S. M. and Wechsler-Reya, R. J. (2005). Loss of patched and disruption of granule cell development in a pre-neoplastic stage of medulloblastoma. *Development* **132**, 2425-39.

Orentas, D. M., Hayes, J. E., Dyer, K. L. and Miller, R. H. (1999). Sonic hedgehog signaling is required during the appearance of spinal cord oligodendrocyte precursors.

Development **126**, 2419-29.

Oro, A. E., Higgins, K. M., Hu, Z., Bonifas, J. M., Epstein, E. H., Jr. and Scott, M. P. (1997). Basal cell carcinomas in mice overexpressing sonic hedgehog. *Science* **276**, 817-21.

Osterhout, D. J., Wolven, A., Wolf, R. M., Resh, M. D. and Chao, M. V. (1999). Morphological differentiation of oligodendrocytes requires activation of Fyn tyrosine kinase. *J Cell Biol* **145**, 1209-18.

Park, J. B., Yiu, G., Kaneko, S., Wang, J., Chang, J., He, X. L., Garcia, K. C. and He, Z. (2005). A TNF receptor family member, TROY, is a coreceptor with Nogo receptor in mediating the inhibitory activity of myelin inhibitors. *Neuron* **45**, 345-51.

- Parr, B. A., Shea, M. J., Vassileva, G. and McMahon, A. P.** (1993). Mouse Wnt genes exhibit discrete domains of expression in the early embryonic CNS and limb buds. *Development* **119**, 247-61.
- Patten, I. and Placzek, M.** (2002). Opponent activities of Shh and BMP signaling during floor plate induction in vivo. *Curr Biol* **12**, 47-52.
- Persson, M., Stamatakis, D., te Welscher, P., Andersson, E., Bose, J., Ruther, U., Ericson, J. and Briscoe, J.** (2002). Dorsal-ventral patterning of the spinal cord requires Gli3 transcriptional repressor activity. *Genes Dev* **16**, 2865-78.
- Pierani, A., Brenner-Morton, S., Chiang, C. and Jessell, T. M.** (1999). A sonic hedgehog-independent, retinoid-activated pathway of neurogenesis in the ventral spinal cord. *Cell* **97**, 903-15.
- Praetorius, H. A. and Spring, K. R.** (2003). The renal cell primary cilium functions as a flow sensor. *Curr Opin Nephrol Hypertens* **12**, 517-20.
- Pringle, N. P. and Richardson, W. D.** (1993). A singularity of PDGF alpha-receptor expression in the dorsoventral axis of the neural tube may define the origin of the oligodendrocyte lineage. *Development* **117**, 525-33.
- Qin, J., Lin, Y., Norman, R. X., Ko, H. W. and Eggenschwiler, J. T.** (2011). Intraflagellar transport protein 122 antagonizes Sonic Hedgehog signaling and controls ciliary localization of pathway components. *Proc Natl Acad Sci U S A* **108**, 1456-61.
- Readhead, C., Popko, B., Takahashi, N., Shine, H. D., Saavedra, R. A., Sidman, R. L. and Hood, L.** (1987). Expression of a myelin basic protein gene in transgenic shiverer mice: correction of the dysmyelinating phenotype. *Cell* **48**, 703-12.

Reifenberger, J., Wolter, M., Weber, R. G., Megahed, M., Ruzicka, T., Lichter, P. and Reifenberger, G. (1998). Missense mutations in SMOH in sporadic basal cell carcinomas of the skin and primitive neuroectodermal tumors of the central nervous system. *Cancer Res* **58**, 1798-803.

Ribes, V., Balaskas, N., Sasai, N., Cruz, C., Dessaud, E., Cayuso, J., Tozer, S., Yang, L. L., Novitch, B., Marti, E. et al. (2010). Distinct Sonic Hedgehog signaling dynamics specify floor plate and ventral neuronal progenitors in the vertebrate neural tube. *Genes Dev* **24**, 1186-200.

Riobo, N. A., Lu, K., Ai, X., Haines, G. M. and Emerson, C. P., Jr. (2006). Phosphoinositide 3-kinase and Akt are essential for Sonic Hedgehog signaling. *Proc Natl Acad Sci U S A* **103**, 4505-10.

Rodriguez, C. I., Buchholz, F., Galloway, J., Sequerra, R., Kasper, J., Ayala, R., Stewart, A. F. and Dymecki, S. M. (2000). High-efficiency deleter mice show that FLP_e is an alternative to Cre-loxP. *Nat Genet* **25**, 139-40.

Rohatgi, R., Milenkovic, L. and Scott, M. P. (2007). Patched1 regulates hedgehog signaling at the primary cilium. *Science* **317**, 372-6.

Rowitch, D. H. (2004). Glial specification in the vertebrate neural tube. *Nat Rev Neurosci* **5**, 409-19.

Rowitch, D. H., B, S. J., Lee, S. M., Flax, J. D., Snyder, E. Y. and McMahon, A. P. (1999). Sonic hedgehog regulates proliferation and inhibits differentiation of CNS precursor cells. *J Neurosci* **19**, 8954-65.

Ruiz i Altaba, A. (1998). Combinatorial Gli gene function in floor plate and neuronal inductions by Sonic hedgehog. *Development* **125**, 2203-12.

Sander, M., Paydar, S., Ericson, J., Briscoe, J., Berber, E., German, M., Jessell, T. M. and Rubenstein, J. L. (2000). Ventral neural patterning by Nkx homeobox genes: Nkx6.1 controls somatic motor neuron and ventral interneuron fates. *Genes Dev* **14**, 2134-9.

Sasaki, H., Hui, C., Nakafuku, M. and Kondoh, H. (1997). A binding site for Gli proteins is essential for HNF-3beta floor plate enhancer activity in transgenics and can respond to Shh in vitro. *Development* **124**, 1313-22.

Sasaki, H., Nishizaki, Y., Hui, C., Nakafuku, M. and Kondoh, H. (1999). Regulation of Gli2 and Gli3 activities by an amino-terminal repression domain: implication of Gli2 and Gli3 as primary mediators of Shh signaling. *Development* **126**, 3915-24.

Schneider, L., Cammer, M., Lehman, J., Nielsen, S. K., Guerra, C. F., Veland, I. R., Stock, C., Hoffmann, E. K., Yoder, B. K., Schwab, A. et al. (2010). Directional cell migration and chemotaxis in wound healing response to PDGF-AA are coordinated by the primary cilium in fibroblasts. *Cell Physiol Biochem* **25**, 279-92.

Schneider, L., Clement, C. A., Teilmann, S. C., Pazour, G. J., Hoffmann, E. K., Satir, P. and Christensen, S. T. (2005). PDGFRalpha signaling is regulated through the primary cilium in fibroblasts. *Curr Biol* **15**, 1861-6.

Schneider, L., Stock, C. M., Dieterich, P., Jensen, B. H., Pedersen, L. B., Satir, P., Schwab, A., Christensen, S. T. and Pedersen, S. F. (2009). The Na⁺/H⁺ exchanger NHE1 is required for directional migration stimulated via PDGFR-alpha in the primary cilium. *J Cell Biol* **185**, 163-76.

Schuller, U., Heine, V. M., Mao, J., Kho, A. T., Dillon, A. K., Han, Y. G., Huillard, E., Sun, T., Ligon, A. H., Qian, Y. et al. (2008). Acquisition of granule neuron

precursor identity is a critical determinant of progenitor cell competence to form Shh-induced medulloblastoma. *Cancer Cell* **14**, 123-34.

Schwartz, J. H. (1991). The Cytology of neurons. In *Principles of neural science*, (ed. E. R. Kandel J. H. Schwartz and T. M. Jessell), pp. 37-48. New York: Elsevier.

See, J., Mamontov, P., Ahn, K., Wine-Lee, L., Crenshaw, E. B., 3rd and Grinspan, J. B. (2007). BMP signaling mutant mice exhibit glial cell maturation defects. *Mol Cell Neurosci* **35**, 171-82.

Shao, Z., Browning, J. L., Lee, X., Scott, M. L., Shulga-Morskaya, S., Allaire, N., Thill, G., Levesque, M., Sah, D., McCoy, J. M. et al. (2005). TAJ/TROY, an orphan TNF receptor family member, binds Nogo-66 receptor 1 and regulates axonal regeneration. *Neuron* **45**, 353-9.

Shaw, P. J. (1999). Motor neurone disease. *BMJ* **318**, 1118-21.

Taipale, J., Chen, J. K., Cooper, M. K., Wang, B., Mann, R. K., Milenkovic, L., Scott, M. P. and Beachy, P. A. (2000). Effects of oncogenic mutations in Smoothed and Patched can be reversed by cyclopamine. *Nature* **406**, 1005-9.

Takebayashi, H., Nabeshima, Y., Yoshida, S., Chisaka, O. and Ikenaka, K. (2002). The basic helix-loop-helix factor olig2 is essential for the development of motoneuron and oligodendrocyte lineages. *Curr Biol* **12**, 1157-63.

Takenawa, T. and Miki, H. (2001). WASP and WAVE family proteins: key molecules for rapid rearrangement of cortical actin filaments and cell movement. *J Cell Sci* **114**, 1801-9.

- Tan, M., Hu, X., Qi, Y., Park, J., Cai, J. and Qiu, M.** (2006). Gli3 mutation rescues the generation, but not the differentiation, of oligodendrocytes in Shh mutants. *Brain Res* **1067**, 158-63.
- TerBush, D. R., Maurice, T., Roth, D. and Novick, P.** (1996). The Exocyst is a multiprotein complex required for exocytosis in *Saccharomyces cerevisiae*. *EMBO J* **15**, 6483-94.
- Timmer, J. R., Wang, C. and Niswander, L.** (2002). BMP signaling patterns the dorsal and intermediate neural tube via regulation of homeobox and helix-loop-helix transcription factors. *Development* **129**, 2459-72.
- Ting, A. E., Hazuka, C. D., Hsu, S. C., Kirk, M. D., Bean, A. J. and Scheller, R. H.** (1995). rSec6 and rSec8, mammalian homologs of yeast proteins essential for secretion. *Proc Natl Acad Sci U S A* **92**, 9613-7.
- Tran, P. V., Haycraft, C. J., Besschetnova, T. Y., Turbe-Doan, A., Stottmann, R. W., Herron, B. J., Chesebro, A. L., Qiu, H., Scherz, P. J., Shah, J. V. et al.** (2008). THM1 negatively modulates mouse sonic hedgehog signal transduction and affects retrograde intraflagellar transport in cilia. *Nat Genet* **40**, 403-10.
- Tukachinsky, H., Lopez, L. V. and Salic, A.** (2010). A mechanism for vertebrate Hedgehog signaling: recruitment to cilia and dissociation of SuFu-Gli protein complexes. *J Cell Biol* **191**, 415-28.
- Ulloa, F., Itasaki, N. and Briscoe, J.** (2007). Inhibitory Gli3 activity negatively regulates Wnt/beta-catenin signaling. *Curr Biol* **17**, 545-50.
- Vallstedt, A., Muhr, J., Pattyn, A., Pierani, A., Mendelsohn, M., Sander, M., Jessell, T. M. and Ericson, J.** (2001). Different levels of repressor activity assign redundant and

specific roles to Nkx6 genes in motor neuron and interneuron specification. *Neuron* **31**, 743-55.

Varga, Z. M., Amores, A., Lewis, K. E., Yan, Y. L., Postlethwait, J. H., Eisen, J. S. and Westerfield, M. (2001). Zebrafish *smoothed* functions in ventral neural tube specification and axon tract formation. *Development* **128**, 3497-509.

Vartanian, T., Fischbach, G. and Miller, R. (1999). Failure of spinal cord oligodendrocyte development in mice lacking neuregulin. *Proc Natl Acad Sci U S A* **96**, 731-5.

Wang, B., Fallon, J. F. and Beachy, P. A. (2000). Hedgehog-regulated processing of Gli3 produces an anterior/posterior repressor gradient in the developing vertebrate limb. *Cell* **100**, 423-34.

Wichterle, H., Lieberam, I., Porter, J. A. and Jessell, T. M. (2002). Directed differentiation of embryonic stem cells into motor neurons. *Cell* **110**, 385-97.

Wijgerde, M., McMahon, J. A., Rule, M. and McMahon, A. P. (2002). A direct requirement for Hedgehog signaling for normal specification of all ventral progenitor domains in the presumptive mammalian spinal cord. *Genes Dev* **16**, 2849-64.

Wine-Lee, L., Ahn, K. J., Richardson, R. D., Mishina, Y., Lyons, K. M. and Crenshaw, E. B., 3rd. (2004). Signaling through BMP type 1 receptors is required for development of interneuron cell types in the dorsal spinal cord. *Development* **131**, 5393-403.

Wolter, M., Reifenberger, J., Sommer, C., Ruzicka, T. and Reifenberger, G. (1997). Mutations in the human homologue of the *Drosophila* segment polarity gene *patched*

(PTCH) in sporadic basal cell carcinomas of the skin and primitive neuroectodermal tumors of the central nervous system. *Cancer Res* **57**, 2581-5.

Wu, S., Wu, Y. and Capecchi, M. R. (2006). Motoneurons and oligodendrocytes are sequentially generated from neural stem cells but do not appear to share common lineage-restricted progenitors in vivo. *Development* **133**, 581-90.

Xie, J., Murone, M., Luoh, S. M., Ryan, A., Gu, Q., Zhang, C., Bonifas, J. M., Lam, C. W., Hynes, M., Goddard, A. et al. (1998). Activating Smoothed mutations in sporadic basal-cell carcinoma. *Nature* **391**, 90-2.

Yang, Z. J., Ellis, T., Markant, S. L., Read, T. A., Kessler, J. D., Bourbonoulas, M., Schuller, U., Machold, R., Fishell, G., Rowitch, D. H. et al. (2008). Medulloblastoma can be initiated by deletion of Patched in lineage-restricted progenitors or stem cells. *Cancer Cell* **14**, 135-45.

Yu, W., McDonnell, K., Taketo, M. M. and Bai, C. B. (2008). Wnt signaling determines ventral spinal cord cell fates in a time-dependent manner. *Development* **135**, 3687-96.

Zechner, D., Muller, T., Wende, H., Walther, I., Taketo, M. M., Crenshaw, E. B., 3rd, Treier, M., Birchmeier, W. and Birchmeier, C. (2007). Bmp and Wnt/beta-catenin signals control expression of the transcription factor Olig3 and the specification of spinal cord neurons. *Dev Biol* **303**, 181-90.

Zhang, X. M., Ramalho-Santos, M. and McMahon, A. P. (2001). Smoothed mutants reveal redundant roles for Shh and Ihh signaling including regulation of L/R symmetry by the mouse node. *Cell* **106**, 781-92.

Zhou, Q. and Anderson, D. J. (2002). The bHLH transcription factors OLIG2 and OLIG1 couple neuronal and glial subtype specification. *Cell* **109**, 61-73.

Zhou, Q., Wang, S. and Anderson, D. J. (2000). Identification of a novel family of oligodendrocyte lineage-specific basic helix-loop-helix transcription factors. *Neuron* **25**, 331-43.

Zhu, A. J., Zheng, L., Suyama, K. and Scott, M. P. (2003). Altered localization of Drosophila Smoothed protein activates Hedgehog signal transduction. *Genes Dev* **17**, 1240-52.